Reply to Anonymous Referee # 4 Comment on 'Dynamics of gaseous oxidized mercury at Villum Research Station during the High Arctic summer'

The authors present data from two summer measurement campaigns at a high Arctic station. The presentation and discussion of the data is focused on the origin of the gaseous oxidized mercury (GOM). They arrive at the conclusion that high GOM concentrations during all 5 events are due to the transport from the free troposphere. At a very remote site this is almost always the case and, as such, too unspecific. This is a pity because the observed events display different patterns which would enable more specific conclusions.

The data are valuable and worth of detailed analysis. Unfortunately, the manuscript is difficult to read because GEM, GOM, PHg, O_3, BC, H_2O, and N_{coarse} are all discussed in different chapters. A change of perspective in O_3 chapter from the analysis of individual events to the whole campaign analysis does not make the understanding easier. Ideally, the air mass of each event would be characterised by all of the available data, including backward trajectories (the consideration of the latter would probably result in splitting the event 1 into two events). This would be followed by detailed discussion of GOM origin in each of the characterised events separately before making final conclusions. I recommend the publication of the manuscript after a thorough reorganisation of the text along the lines proposed above. Some of the comments below are also to be considered:

We thank Referee # 4 for their careful review of our manuscript. Their comments and suggestions will improve the clarity, presentation, and discussion of the results. We have addressed the referee's concerns and corrected errors below with the author's responses in blue. The line numbers refer to the text in the clean version of the revised manuscript. New references are highlighted in yellow.

We regret the referee found the manuscript difficult to read and agree a detailed discussion of each event is warranted. Therefore, we have made substantial changes to the organization of the text, we have split the Results and Discussion section into two separate sections. In the new Results section, we present the results of each parameter for each campaign. We also agree that the criteria for defining an event should include considerations for specific air masses. We have also recalculated the trajectory length for 240 hours. Using these new trajectories and the new criteria, we have split Event 1 into Events 1a and 1b, per the referee's suggestion, this also made us re-evaluate other events, resulting in Event 5 being split into 5a and 5b. These two events occurred sequentially therefore the naming convention using the same number and different letters. In the new Discussion section, we discuss factors influencing event vs non-event periods and factors influencing individual events, per the referee's suggestion. We feel this is a compromise between addressing the referee's concerns and completely rewriting the manuscript.

Lines 12-13: „we performed measurements of ……air mass history"?

This is a good catch by the referee, we did not measure air mass history but utilized modeled air mass history. The text has been amended accordingly.

Lines 11-14: "Therefore, to further our understanding of the dynamics of gaseous oxidized mercury in the High Arctic during the late summer, we performed measurements of GEM and GOM along with meteorological parameters, atmospheric constituents, and utilized modeled air mass history during two summer campaigns in 2019 and 2020 at Villum Research Station (Villum) in Northeastern Greenland."

Line 24: Biomass burning is partly natural and partly man-made.

We have included 'biomass combustion' in the list of anthropogenic sources of mercury.

Lines 31-33: Wording: During depletion events… GOM and PHg can constitute large fractions of… In contrast,….. GOM and PHg can constitute large fractions of. ??

We have amended the text to delineate when the authors refer to the distribution of atmospheric mercury in the polar regions and the mid-latitudes.

Lines 41-44: "However, during depletion events in the spring, GOM and PHg can constitute large fractions of total atmospheric mercury (Steffen et al., 2014). In contrast to the polar regions, the mid-latitudes, and especially locations close to anthropogenic emission point sources, GOM and PHg can be emitted directly to the atmosphere and represent significant fractions of the atmospheric mercury burden (Muntean et al., 2018)"

Steffen, A., Bottenheim, J., Cole, A., Ebinghaus, R., Lawson, G., and Leaitch, W. R.: Atmospheric mercury speciation and mercury in snow over time at Alert, Canada, Atmos Chem Phys, 14, 2219-2231, 10.5194/acp-14-2219-2014, 2014.

Line 41: "oxidation" instead of "oxidization"

We have corrected this embarrassing spelling mistake.

Line 51: What does it mean "liable halogen reservoir species"?

We have corrected 'liable' to 'labile'.

Lines 56-57: Uptake by vegetation and soil in the high Arctic? Is there enough vegetation and soil not covered with snow for that in the high Arctic?

We have similar questions about how the results of these studies would translate to the High Arctic as indicated in the text, however, we thought this information relevant to the reader since it shows GEM dry deposition to be the main source of mercury input even though this has yet to be demonstrated in the High Arctic.

Line 65: "important" instead of "pertinent"?

We have made this change in the text.

Line 80: CA stands usually for California, not Canada.

The ISO 3166-1 alpha-2 code for Canada is CA. To avoid further confusion for the reader, we have specified, throughout the text, the full location for Alert as 'Alert, Nunavut, Canada'.

Section 2.2: Duration of GOM and PHg sampling time should be given. This is important because the usual 2h sampling at 10 L/min usually provides too small Hg amounts for analysis unbiased by the internal Tekran signal integration routine (Slemr et al., Atmos. Meas. Tech., 9, 2291-2302, 2016; Ambrose, Atmos. Meas. Tech., 10, 5063-5073, 2017). This artefact applies also for 5 min GEM sampling time which probably leads to a small underreporting of the GEM concentrations.

We acknowledge the internal integration routine may be biased low. We are aware of the problem at low mercury values since 2017, therefore we use 15 minutes average in

our monitoring program (Skov et al. 2020). Furthermore, we have taken the results into account in estimating the overall uncertainty. In the present study, GEM is always above 0.5 ng m^{-3} and thus the uncertainty is 20% (95% confidence interval). For measurements of mercury using the speciation monitors from Tekran, the use of 15 minutes time resolution for a single measurement cycle would result in too coarse of a time resolution (~6 hours), therefore we have opted for the 5 min cycles.

Skov, H., Hjorth, J., Nordstrøm, C., Jensen, B., Christoffersen, C., Bech Poulsen, M., Baldtzer Liisberg, J., Beddows, D., Dall'Osto, M., and Christensen, J. H.: Variability in gaseous elemental mercury at Villum Research Station, Station Nord, in North Greenland from 1999 to 2017, Atmos. Chem. Phys., 20, 13253-13265, 10.5194/acp-20-13253-2020, 2020.

The sampling times for the campaigns are listed on lines 141-142: "For the 2019 campaign, the sampling time was 80 minutes, while for the 2020 campaign the sampling time was 60 minutes.".

We have added the following sentence, commenting on the quality of the GOM measurements.

Lines 145-148: "With the KCl denuders being prone to unequal collection efficiencies for different GOM species and artifacts (Gustin et al., 2015) and the internal signal integration routine biasing the concentrations low (Slemr et al., 2016; Ambrose, 2017), the GEM and GOM concentrations are likely a lower limit (Huang and Gustin, 2015; Huang et al., 2017; Marusczak et al., 2017)."

Gustin, M. S., Amos, H. M., Huang, J., Miller, M. B., and Heidecorn, K.: Measuring and modeling mercury in the atmosphere: a critical review, Atmos. Chem. Phys., 15, 5697-5713, 10.5194/acp-15-5697-2015, 2015.

Slemr, F., Weigelt, A., Ebinghaus, R., Kock, H. H., Bödewadt, J., Brenninkmeijer, C. A. M., Rauthe-Schöch, A., Weber, S., Hermann, M., Becker, J., Zahn, A., and Martinsson, B.: Atmospheric mercury measurements onboard the CARIBIC passenger aircraft, Atmos. Meas. Tech., 9, 2291-2302, 10.5194/amt-9-2291-2016, 2016.

Ambrose, J. L.: Improved methods for signal processing in measurements of mercury by Tekran® 2537A and 2537B instruments, Atmos. Meas. Tech., 10, 5063-5073, 10.5194/amt-10-5063-2017, 2017.

Huang, J., and Gustin, M. S.: Uncertainties of Gaseous Oxidized Mercury Measurements Using KCl-Coated Denuders, Cation-Exchange Membranes, and Nylon Membranes: Humidity Influences, Environmental Science & Technology, 49, 6102-6108, 10.1021/acs.est.5b00098, 2015.

Huang, J., Miller, M. B., Edgerton, E., and Sexauer Gustin, M.: Deciphering potential chemical compounds of gaseous oxidized mercury in Florida, USA, Atmos. Chem. Phys., 17, 1689-1698, 10.5194/acp-17-1689-2017, 2017.

Marusczak, N., Sonke, J. E., Fu, X., and Jiskra, M.: Tropospheric GOM at the Pic du Midi Observatory—Correcting Bias in Denuder Based Observations, Environmental Science & Technology, 51, 863-869, 10.1021/acs.est.6b04999, 2017.

Line 181: RH at a given H$_2$O content of air is inversely related to temperature and as such provides a redundant information on temperature (as can be clearly seen in Figures 1 and 2). Consequently, it is not a suitable variable for the characterisation of the air mass. H$_2$O content of

air, as shown in Figure S5 and discussed elsewhere in the manuscript, should be used mostly through the paper. The use of RH makes sense only when discussing the GOM attachment to particles.

We agree with the referee and have calculated an H_2O mixing using ground-level measurements of temperature, RH, and pressure. We have included H_2O mixing ratios in Figures 1 and 2 and have discussed the results concerning this parameter.

Lines 151-152: "Ground-level H_2O mixing ratios were calculated using ambient temperature, RH, and pressure (Bolton, 1980; Weiss-Penzias et al., 2015).

Bolton, D.: The Computation of Equivalent Potential Temperature, Monthly Weather Review, 108, 1046-1053, 10.1175/1520-0493(1980)108<1046:Tcoept>2.0.Co;2, 1980.

Weiss-Penzias, P., Amos, H. M., Selin, N. E., Gustin, M. S., Jaffe, D. A., Obrist, D., Sheu, G. R., and Giang, A.: Use of a global model to understand speciated atmospheric mercury observations at five high-elevation sites, Atmos. Chem. Phys., 15, 1161-1173, 10.5194/acp-15-1161-2015, 2015.

Section 3.1: Figures S1 and S3 show that local meteorological parameters essentially do not matter. What matters are the times of the air mass exchanges, characterized more clearly by their specific chemical fingerprints, and the question where they come from. As already mentioned, RH should be replaced by H_2O content of the air.

We agree with the referee's suggestion and have re-evaluated our criteria for the event definition. We have also recalculated the trajectory length, which revealed a synoptic view of the air mass history this enabled us to define each event considering air mass history. This resulted in the splitting of Event 1 into Event 1a and 1b as well as the splitting of Event 5 into 5a and 5b. These two events occurred sequentially therefore the naming convention using the same number and different letters. We have examined each event based on all the parameters in the section 'Factors influencing individual events'. We have included the H_2O mixing ratio in our revised manuscript as indicated above.

Figures 1 and 2: I think that these figures should include all measured parameters, i.e. additionally O_3, BC and N_{coarse}. Measurements of BC and N_{coarse} shown in Figure 7 are especially important because these species are specific tracers for anthropogenic activities and biomass burning. GOM and PHg below detection limit are plotted as zero concentration which is misleading because "below detection limit" does not mean zero. As mentioned above, their concentrations are underreported due to the internal Tekran integration procedure. I would plot only the measured GOM and PHg concentrations above the detection limit.

We have remade Figures 1 and 2 to include all parameters and have added H_2O mixing ratios and accumulated precipitation along the trajectory path.

We have not plotted values <LOD as zero. All measurements as recorded by the instrument are plotted as is. Readings of zero GOM concentrations were included in the figures to reflect the inability to detect a GOM signal during the non-event periods.

We have excluded values <LOD in the revised versions of Figures 1 and 2.

Figure 3: RH in panel b provides hardly any additional information to T in panel a. Water content could be more useful because it would reveal the precipitation along the trajectory as discussed in the related text. A comparison of panel a (T) with panel d (altitude) shows an inverse relationship which is not mentioned in the text.

> We have also remade Figures 3 and 4 to include H$_2$O mixing ratios and precipitation. We have also commented on the relationship between altitude and temperature.
>
> Lines 465-466: "The temperature and altitude parameters are interconnected since with increasing altitude the temperature will decrease as the air becomes less dense."

Figures 1, 5a and S2 show that event 1 consists essentially of two events with different trajectories which should be perhaps treated separately.

> Following the referee's suggestion about evaluating events based on air mass characterization, we have split Event 1 and 5 into two events as described above.

Figure 5: The addition of trajectory altitudes, as in Figure S4, could provide support for the claim of GOM arriving from the free troposphere.

> We have remade Figure 5 with trajectories colored-coded by arrival date at Villum and added a boxplot showing the distribution of trajectories altitudes binned in increments of ten hours. This shows the temporal evolution of trajectories and the distribution of trajectories' altitudes.

Line 325: "Influence of the troposphere on mercury concentrations" sounds like "water has influence on fish". Please reword.

> We have reworded to:
>
> Line 480-481: "Previous studies have demonstrated the influence of the free troposphere on mercury concentrations within the boundary layer."

Lines 328-332: Measurements of GEM by Talbot et al. (2007) are subject to two experimental artefacts: a) with their specific inlet system they measured most likely GEM + GOM, not only GEM as they claim, and b) their reported concentrations are too low because they relied on internal Tekran signal integration procedure which was demonstrated to underreport Hg concentrations leading to numerous zero concentrations in the paper which are incorrect. With these problems, Talbot et al. does not provide any usable information about GOM. A reference to Lyman and Jaffe (Nature Geosci., 5, 114-117, 2012) and Slemr et al. (Atmos. Meas. Tech., 9, 2291-2302, 2016; Atmos. Chem. Phys., 18, 12329-12343, 2018) would be more appropriate.

> We have removed reference to Talbot et al., 2007 since they measure in altitudes that are outside of the range in this study. We appreciate the two references the referee suggested and will keep them for future reference.

Line 355: Do you mean O$_3$ median at Villum station?

> Yes, we have amended the text to reflect this.

Section 3.4: Elevated O$_3$ mixing ratios could be due to a transport from free troposphere but also due to O$_3$ formation in polluted air masses. The latter applies clearly due to anthropogenic pollution during the events 1 and 3 and to a smaller degree to event 2 as indicated by BC and N$_{coarse}$. A discussion of the elevated GOM concentrations during these events in terms of anthropogenic pollution would be more appropriate.

> We agree elevated ozone could arise from other sources such as pollution from either anthropogenic sources or biomass burning. We have updated our interpretations of the trajectories and discussed these sources of ozone accordingly.

Figure 6: Putting all data for 2019 and 2020 campaigns into each GEM vs O_3 and GOM vs O_3 diagrams is inconsistent with the discussion of individual events 1-5 in other chapters and obscures the origin of GEM instead of revealing it. What would be the GEM vs O_3 and GOM vs O_3 correlations for each of the individual events $1 - 5$?

> We agree with the referee's suggestion. We have removed Figure 6 in the previous version of the manuscript and replaced it with one including a scatter plot for important parameters for each event. We have included a discussion on the correlations between GOM and these parameters in the discussion section.

Section 3.5: This discussion is muddled. GOM correlates well with BC and N_{coarse} during the events 1, 2, and 3 but not during the events 4 and 5. Despite the different patterns, the authors conclude that emissions from biomass burning and combustion have little to no influence on GOM levels at Villum station. That may be true for events 4 and 5 but obviously not for events 1, 2, and 3. The discussion in lines $445 – 454$ may be used as an argument against biomass burning being the source of GOM in some of the events but not in all.

> We agree that grouping ozone during all the event periods can muddle the interpretation of individual events. We have replaced Fig. 6 in the previous version of the manuscript with a figure detailing the correlations between GOM and important parameters for individual events (Fig. 7 in the revised manuscript. With the new trajectory analysis, we have indicated which events could have been influenced by active fires.

Section 3.6: This section is highly speculative and confusing. As in the discussion of GOM vs O_3 the different pattern of each of the five events is not mentioned. Especially that of event 5 with no relation between GOM and N_{coarse} and BC, whatsoever. A weak correlation with of GOM with O_3 in this event could be interpreted as transport from the free troposphere. A general problem is that the authors attribute high GOM to free troposphere in all events while the halogens claimed for GEM oxidation are produced more likely in the boundary layer. I would skip this section.

> We agree with the referee that we should remove this section. We have made changes to the analysis methods and criteria for event classification and therefore changed our conclusions based on the new discussion.

Line 491: The statement about "the positive correlation between GOM and N_{coarse} observed in our study (Figure 7).." is valid only for events 1, 2, and 3, not for the events 4 and 5. The statement is thus wrong without a qualifier.

> We agree this statement is not valid for all events and have removed this sentence in the revised manuscript. We have recalculated the correlation between GOM and important parameters for individual events, see comment above. We have discussed these correlations for individual events in the revised manuscript.

Section 4: The conclusions are too unspecificl, they do not reflect on the different patterns of the individual events.

> We thank the referee for challenging us in this manner. Our new analysis reveals the unique origins of each event in the revised manuscript.

Figure S4: I could not find a reference to it in the manuscript.

> We reference Fig. S4a-c on Line 204 of the original manuscript.

Ambrose, J. L.: Improved methods for signal processing in measurements of mercury by Tekran® 2537A and 2537B instruments, Atmos. Meas. Tech., 10, 5063-5073, 10.5194/amt-10-5063-2017, 2017.

Bolton, D.: The Computation of Equivalent Potential Temperature, Monthly Weather Review, 108, 1046-1053, 10.1175/1520-0493(1980)108<1046:Tcoept>2.0.Co;2, 1980.

Gustin, M. S., Amos, H. M., Huang, J., Miller, M. B., and Heidecorn, K.: Measuring and modeling mercury in the atmosphere: a critical review, Atmos. Chem. Phys., 15, 5697-5713, 10.5194/acp-15-5697-2015, 2015.

Huang, J., and Gustin, M. S.: Uncertainties of Gaseous Oxidized Mercury Measurements Using KCl-Coated Denuders, Cation-Exchange Membranes, and Nylon Membranes: Humidity Influences, Environmental Science & Technology, 49, 6102-6108, 10.1021/acs.est.5b00098, 2015.

Huang, J., Miller, M. B., Edgerton, E., and Sexauer Gustin, M.: Deciphering potential chemical compounds of gaseous oxidized mercury in Florida, USA, Atmos. Chem. Phys., 17, 1689-1698, 10.5194/acp-17-1689-2017, 2017.

Marusczak, N., Sonke, J. E., Fu, X., and Jiskra, M.: Tropospheric GOM at the Pic du Midi Observatory—Correcting Bias in Denuder Based Observations, Environmental Science & Technology, 51, 863-869, 10.1021/acs.est.6b04999, 2017.

Slemr, F., Weigelt, A., Ebinghaus, R., Kock, H. H., Bödewadt, J., Brenninkmeijer, C. A. M., Rauthe-Schöch, A., Weber, S., Hermann, M., Becker, J., Zahn, A., and Martinsson, B.: Atmospheric mercury measurements onboard the CARIBIC passenger aircraft, Atmos. Meas. Tech., 9, 2291-2302, 10.5194/amt-9-2291-2016, 2016.

Steffen, A., Bottenheim, J., Cole, A., Ebinghaus, R., Lawson, G., and Leaitch, W. R.: Atmospheric mercury speciation and mercury in snow over time at Alert, Canada, Atmos Chem Phys, 14, 2219-2231, 10.5194/acp-14-2219-2014, 2014.

Weiss-Penzias, P., Amos, H. M., Selin, N. E., Gustin, M. S., Jaffe, D. A., Obrist, D., Sheu, G. R., and Giang, A.: Use of a global model to understand speciated atmospheric mercury observations at five high-elevation sites, Atmos. Chem. Phys., 15, 1161-1173, 10.5194/acp-15-1161-2015, 2015.

Review of Dynamics of gaseous oxidized mercury at Villum Research Station during the High Arctic summer by Jakob Boyd Pernov et al.

This manuscript presents original data regarding atmospheric Hg species during summertime in the high Arctic. The authors suggest that the GOM peaks (so called " events") that are measured are explained by the influence of free tropospheric production of GOM and transport to the sea-level site.

The scientific reasoning that is conducted here is presented in backwards order. The authors conclude on the influence of air masses from the free troposphere on GOM measurements. To my opinion, the supplementary data are not robust enough to support this very original but debatable hypothesis. Then the authors examine additional data to further explore the GOM origin including other GOM sources. From the data they show, it appears to me that the hypothesis of alternative GOM sources remain still valid awhile the authors clearly reject these sources since they do not support their initial idea. I think this is a biased way of discussing their data set, and that their initial hypothesis is not supported by clear evidence and data.

Demonstrating the direct influence of the free troposphere at an ocean-front site requires solid multiparameter measurements, on-site knowledge of the vertical structure of the atmosphere and probably vertical concentration profiles (aircraft). Although the hypothesis is attractive, there are many other possibilities to explain these peaks of GOM , which have been only partially studied in this manuscript, including local pollution sources (ships, airplanes), biomass fires, anthropogenic influence of European pollution, and transport of GOM species from the Greenland ice cap. The back-trajectory analysis is not deep enough and the statistics are not convincing.

Moreover, the introductory part contains too many approximations and requires an obvious reformulation work.

For these reasons, this work cannot be published in ACP . It could at least be requalified as a "measurement report" with however an important work on the formulation of the different hypotheses.

> We would like to thank Referee # 1 for their review of our manuscript. Some of their comments and suggestions will improve the clarity, presentation, and discussion of the work. We will have to respectfully disagree with the main conclusion of the review. We acknowledge the reviewer's viewpoint that we focused on the parameters first and then analyzed the events from the viewpoint of these parameters and that might lead to confusion. Therefore, we have redone the structure of the article as suggested by another review so we now focus on the general pattern observed during event vs non-event periods as well as each individual event. In this way, we make clear what conclusions can be extracted from all event and non-event periods and which events deviate from this general pattern. Thus, we will offer our rebuttal on the overall conclusion of Referee 1. We have addressed the referee's concerns and corrected errors in the manuscript below with the author's responses in blue. Due to the large amounts of changes in the manuscript, line numbers refer to the clean version of the manuscript which has no track changes present. New references are highlighted in yellow.

They state that our hypothesis is very original but debatable, however, this process has been repeatedly demonstrated to occur throughout the global atmosphere both through in situ measurements and modeling studies as we indicate in the text. While we are the first to propose this process is occurring in the High Arctic, it has been widely demonstrated at lower latitudes, and so the hypothesis is not unreasonable nor is it a far stretch beyond current scientific understanding. They go on to state that we reject alternative sources of GOM. While we explore possible sources of GOM oxidation, at no point in the manuscript do we use such language as reject. We assessed the data, weighed the likelihood of all possibilities, and adjusted our hypothesis accordingly. We respectfully, yet firmly, disagree with their assessment that we discuss our data set in a biased way and that our initial hypothesis is not supported by clear evidence and data.

The referee argues that the demonstration of our hypothesis at an oceanfront site (while Villum is located near the coast the surrounding waters are ice-covered throughout the year making it a cryosphere station and not an oceanfront site) requires solid multiparameter measurements (which we have attempted to provide although we are limited by the instrumentation available), on-site knowledge of the vertical structure of the atmosphere, and probably vertical concentration profiles (aircraft). We have attempted to address the verticality issue by using back trajectory modeling. Adding vertical measurements would require a completely different project, which is outside of the scope of the current project.

The referee concludes by stating many other possibilities that explain the GOM events, such as local anthropogenic pollution (ships and airplanes), biomass burning, anthropogenic influence of European pollution, and transport of GOM species from the Greenland ice cap. To counter their alternative possibilities, we offer the following response. All datasets have been extensively quality controlled to remove the influence of local pollution from the Station Nord military base including all airplane activity and ship traffic is minimal in this part of the Arctic (due to ice-covered sea surfaces in the surrounding waters) and would not produce the long, gradual increases in GOM over several days. We have recalculated the trajectories for a length of 240 hours as suggested by the referee and indicated where necessary if active fires are influencing individual events. Finally, the transport of GOM species from aloft the Greenland ice cap is shown in Event 5b, the two studies cited by the referee concerning this matter both deal with boundary layer processes involving the snowpack and not air mass arriving from aloft. We fail to see how these alternative possibilities could explain our observations given the supporting evidence. In our reorganization of the text, we have indicated where alternative processes could in influencing GOM concentrations.

Details comments.

Line 9: « GOM, once introduced into the ecosystem, »- GOM are not really introduced in ecosystems, these species are deposited. The link with « threat to human and wildlife » is exaggerated since there is no proven direct link between GOM and wildlife contamination. This need to be rephrased

While it has been shown that mercury in the snow is bioavailable at Station Nord (Moller et al. 2011), we have rephrased the sentence to remove any exaggeration.

Lines 9-11: "GOM, once deposited and incorporated into the ecosystem, can pose a threat to human and wildlife health, though there remain large uncertainties regarding the transformation, deposition, and assimilation of mercury into the food web."

Moller, A. K., T. Barkay, W. Abu Al-Soud, S. J. Sorensen, H. Skov and N. Kroer (2011). "Diversity and characterization of mercury-resistant bacteria in snow, freshwater and sea-ice brine from the High Arctic." Fems Microbiology Ecology **75**(3): 390-401.

Line 11 : « the ecosystem » is not appropriate.

We have replaced 'ecosystem' with 'food web'

Line 21 « an »

While ubiquitous starts with a vowel, the spoken word starts with a 'y' sound which is a consonant sound therefore not warranting the preceding 'an'.

Line 21 : what is « relaxation time » ?

The relaxation time of GEM is the time delay between emission reductions and the effect on actual concentrations (Skov et al., 2020), this term is frequently used for CO_2. We have included this definition in the text to aid the reader.

Line 31: "relaxation time refers to the time delay between emission reductions and effect on ambient concentrations".

Skov, H., Hjorth, J., Nordstrøm, C., Jensen, B., Christoffersen, C., Bech Poulsen, M., Baldtzer Liisberg, J., Beddows, D., Dall 'Osto, M., and Christensen, J. H.: Variability in gaseous elemental mercury at Villum Research Station, Station Nord, in North Greenland from 1999 to 2017, Atmos. Chem. Phys., 20, 13253-13265, 10.5194/acp-20-13253-2020, 2020.

Line 24 : artisanal small-scale gold mining

We have amended the text to read "artisanal small-scale gold mining".

Line 28 : atmospheric particles or aerosol, not a combination of both

From Table 2.18 in Seinfeld and Pandis (2016), an aerosol is defined as "tiny particles dispersed in gases" and a particle is defined as "an aerosol particle may consist of a single continuous unit of solid or liquid containing many molecules held together by intermolecular forces and primarily larger than molecular dimensions (> 0.001 μm); a particle may also consist of two or more such unit structures held together by interparticle adhesive forces such that it behaves as a single unit in suspension or on deposit".

This is a common term used widely in the atmospheric community, for example, see Kulmala et al. (2012).

Seinfeld, J. H., and Pandis, S. N.: Atmospheric Chemistry and Physics: From Air Pollution to Climate Change, 3 ed., John Wiley & Sons, 1152 pp., 2016.

Kulmala, M., Petaja, T., Nieminen, T., Sipila, M., Manninen, H. E., Lehtipalo, K., Dal Maso, M., Aalto, P. P., Junninen, H., Paasonen, P., Riipinen, I., Lehtinen, K. E., Laaksonen, A., and Kerminen, V. M.: Measurement of the nucleation of atmospheric aerosol particles, Nat Protoc, 7, 1651-1667, 10.1038/nprot.2012.091, 2012.

Line 31. A reference is missing for « depletion events », at least you should cite Schroeder et al 1998.

We have added the references Steffen et a. (2014) and Steen et al. (2011) since these studies specifically deal with Hg speciation. Schroeder et al. (1998) only measures TGM and not GOM nor PHg. When we discuss AMDEs we cite Schroeder et al. (1998).

Steffen, A., Bottenheim, J., Cole, A., Ebinghaus, R., Lawson, G., and Leaitch, W. R.: Atmospheric mercury speciation and mercury in snow over time at Alert, Canada, Atmos Chem Phys, 14, 2219-2231, 10.5194/acp-14-2219-2014, 2014.

Steen, A. O., Berg, T., Dastoor, A. P., Durnford, D. A., Engelsen, O., Hole, L. R., and Pfaffhuber, K. A.: Natural and anthropogenic atmospheric mercury in the European Arctic: a fractionation study, Atmos Chem Phys, 11, 6273-6284, 10.5194/acp-11-6273-2011, 2011.

Line 31 PHg is not a fraction of total gaseous mercury.

We have replaced 'gaseous' with 'atmospheric'; we thank the referee for this good catch.

Line 32. The link with the previous sentence is not straightforward. « in contrast » is not appropriate here.

We have revised the text to connect these two sentences.

Lines 42-44: "In contrast to the polar regions, the mid-latitudes, and especially locations close to anthropogenic emission point sources, GOM and PHg can be emitted directly to the atmosphere and represent significant fractions of the atmospheric mercury burden (Muntean et al., 2018).

Line 34 – reactive halogens would be better. And especially bromine radicals. There is no real evidence for other halogens reactivity. Why coastal regions? There are many coastal sites where no reactivity is observed (e.g Mace Head in Ireland).

We have modified the text to reflect the presence of elevated reactive halogen concentrations and especially bromine radicals and replaced "coastal regions" with "the marine boundary layer" to be more precise. We thank the referee for pointing out this necessary distinction.

Lines 45-47: "In locations with elevated reactive halogen concentrations (e.g., polar environments, the marine boundary layer, volcanic plumes, and salt lakes) and especially bromine radicals, GEM is quickly transformed into GOM (Obrist et al., 2010; von Glasow, 2010; Angot et al., 2016; Ye et al., 2016; Wang et al., 2019)."

von Glasow, R.: Atmospheric chemistry in volcanic plumes, Proceedings of the National Academy of Sciences, 107, 6594-6599, 10.1073/pnas.0913164107, 2010.

Obrist, D., Tas, E., Peleg, M., Matveev, V., Faïn, X., Asaf, D., and Luria, M.: Bromine-induced oxidation of mercury in the mid-latitude atmosphere, Nature Geoscience, 4, 22-26, 10.1038/ngeo1018, 2010.

Ye, Z., Mao, H., Lin, C. J., and Kim, S. Y.: Investigation of processes controlling summertime gaseous elemental mercury oxidation at midlatitudinal marine, coastal, and inland sites, Atmos. Chem. Phys., 16, 8461-8478, 10.5194/acp-16-8461-2016, 2016.

Wang, S. Y., S. M. McNamara, C. W. Moore, D. Obrist, A. Steffen, P. B. Shepson, R. M. Staebler, A. R. W. Raso and K. A. Pratt (2019). "Direct detection of atmospheric atomic bromine leading to mercury and ozone depletion." Proceedings of the National Academy of Sciences of the United States of America 116(29): 14479-14484.

Line 38-39 : This statement is only valid for Alert in Canada. Has it been observed elsewhere?

The referee is correct that this only applies to Alert, NU, which is the only site where long-term Hg speciation is available. Although, the Arctic Haze phenomenon and AMDEs are observed at locations across the Arctic (Steffen et al., 2008; Freud et al., 2017) so this is not an unreasonable assumption.

Steffen, A., Douglas, T., Amyot, M., Ariya, P., Aspmo, K., Berg, T., Bottenheim, J., Brooks, S., Cobbett, F., Dastoor, A., Dommergue, A., Ebinghaus, R., Ferrari, C., Gardfeldt, K., Goodsite, M. E., Lean, D., Poulain, A. J., Scherz, C., Skov, H., Sommar, J., and Temme, C.: A synthesis of atmospheric mercury depletion event chemistry in the atmosphere and snow, Atmos Chem Phys, 8, 1445-1482, 10.5194/acp-8-1445-2008, 2008.

To be concise, we have amended the text to reflect that this has only been demonstrated at Alert, NU.

Lines 50-53: "In the early spring at Alert, Nunavut, Canada, it has been demonstrated that GOM is converted to PHg (through condensational processes due to the cold temperatures and high aerosol surface area concentration (Freud et al., 2017)) while in the late spring oxidized mercury is mainly present as GOM (due to reduced surface area and increased temperatures) (Steffen et al., 2014)."

Freud, E., Krejci, R., Tunved, P., Leaitch, R., Nguyen, Q. T., Massling, A., Skov, H., and Barrie, L.: Pan-Arctic aerosol number size distributions: seasonality and transport patterns, Atmos Chem Phys, 17, 8101-8128, 10.5194/acp-17-8101-2017, 2017.

Line 40 : the peak of Hg in snow – This should be clarified. What kind of peak ? is it totalHg in surface snow ? « GOM is the main deposition pathway » does not mean anything.

We have specified that this is the peak of total Hg in surface snow and amended the text to specify that dry deposition is a major pathway of mercury into the ecosystem.

Lines 53-55: "Late spring is also the peak of total Hg in surface snow at Alert, Nunavut, Canada and Utqiagvik, Alaska, USA (formerly Barrow), indicating that dry deposition of GOM is a major pathway of mercury into the ecosystem (Lu et al., 2001; Lindberg et al., 2002; Steffen et al., 2002; Steffen et al., 2014)."

Steffen, A., Schroeder, W., Bottenheim, J., Narayan, J., and Fuentes, J. D.: Atmospheric mercury concentrations: measurements and profiles near snow and ice surfaces in the Canadian Arctic during Alert 2000, Atmospheric Environment, 36, 2653-2661, https://doi.org/10.1016/S1352-2310(02)00112-7, 2002.

Lindberg, S. E., Brooks, S., Lin, C. J., Scott, K. J., Landis, M. S., Stevens, R. K., Goodsite, M., and Richter, A.: Dynamic oxidation of gaseous mercury in the Arctic troposphere at polar sunrise, Environmental Science & Technology, 36, 1245-1256, 10.1021/es0111941, 2002.

Line 60 : Do Ariya et al really mention a ionic pulse ? there are better references for this .

Aryia et al. (2004) does not specifically mention an ionic pulse, but it does give the reader more context into the removal processes and the fate of atmospheric and deposited mercury in the Arctic. We have included more references that deal with the ionic pulse.

Lines 74-76: "The snowpack will retain a fraction of this mercury and release it with the ionic pulse during the melt season, introducing mercury into the ecosystem (Lu et al., 2001; Ariya et al., 2004; Durnford and Dastoor, 2011; Douglas et al., 2017)."

Lu, J. Y., Schroeder, W. H., Barrie, L. A., Steffen, A., Welch, H. E., Martin, K., Lockhart, L., Hunt, R. V., Boila, G., and Richter, A.: Magnification of atmospheric mercury deposition to polar regions in springtime: The link to tropospheric ozone depletion chemistry, Geophysical Research Letters, 28, 3219-3222, 10.1029/2000gl012603, 2001.

Douglas, T. A., Sturm, M., Blum, J. D., Polashenski, C., Stuefer, S., Hiemstra, C., Steffen, A., Filhol, S., and Prevost, R.: A Pulse of Mercury and Major Ions in Snowmelt Runoff from a Small Arctic Alaska Watershed, Environmental Science & Technology, 51, 11145-11155, 10.1021/acs.est.7b03683, 2017.

Line 61. Are you sure that GEM can be directly methylated ? PHG ? Methylation does not occur at the « earth's surface, this should be better explained.

We have removed 'onto the Earth's surface', 'GEM', and 'PHg' to be more concise.

Lines 79-80: "After deposition, GOM can be methylated through biotic and abiotic processes to organic mercury (methyl- and dimethylmercury) (Macdonald and Loseto, 2010; Møller et al., 2011)."

Line 65. I do not understand why « it is pertinent to understand mercury oxidation in response to a changing climate » . There is no link with the preceding sentences.

In this paragraph, we describe how mercury, once methylated, can be detrimental to human and ecosystem health and why it is important to research this pollutant at high latitudes. We have amended the text to make this link clearer.

Lines 82-84: "Therefore, as the Arctic becomes more populated and continues to change it is important to understand mercury oxidation in response to a changing climate, especially in high latitude regions (AMAP, 2011; Durnford and Dastoor, 2011; Stern et al., 2012)."

AMAP: AMAP Assessment 2011: Mercury in the Arctic, Arctic Monitoring and Assessment Programme (AMAP), Oslo, Norway, xiv + 193 pp., 2011.

Line 71 : GOM deposition does exist outside of AMDE since this is a major removal pathway for Hg on a global scale

We have added 'in the Arctic' at the end of this sentence to indicate that we are specifically referring to the Arctic here.

Line 88-89: "This study revealed a pattern of GOM previously unknown to the Arctic, with elevated GOM concentrations during the summer, which postulates GOM deposition occurs outside of AMDEs in the Arctic."

Line 82-83 : I do not agree with this conclusion. Most of the studies report low GOM/PHG values.

Studies utilizing short shipborne campaigns found relatively low levels of GOM/PHg, although a year-long campaign found high levels of GOM during the Arctic summer (Steen et al., 2011). We have rephrased the last sentence in the paragraph to indicate that while the levels are relatively low, they do show mercury oxidation and deposition is occurring.

Lines 101-102: "While these latter studies found relatively low levels of GOM, the presence of GOM at all indicates that mercury oxidation and deposition are occurring outside of AMDEs in the Arctic."

Line 84-86 : this sentence is difficult to understand.

We have rewritten the beginning of this paragraph and made additions to the paragraph above to increase the readability and flow of this part of the introduction.

Lines 103-105: "With only limited measurements of GOM performed in the High Arctic summertime, there are many questions still unanswered. The dynamics of GOM in the Arctic are extremely complex; uncertainties in its spatiotemporal variability, annual cycle, and formation mechanisms emphasize the need for further examination."

Line 87 – I don't understand what « will help to infer the response of mercury in the context of a changing climate » mean

Climate change in the Arctic is proceeding at a rapid rate, twice the global average, a term called 'Arctic Amplification'. This change is manifesting as changes in temperature, RH, precipitation, and sea ice extent/concentration/age. All of which can affect mercury dynamics, which is poorly understood during the Arctic summer. Therefore, resolving these dynamics can provide knowledge that will help predict mercury oxidation in a changing climate. We have rephrased the sentence to convey this.

Lines 105-108: "The Arctic region is undergoing rapid changes due to anthropogenic climate change and the dynamics of mercury oxidation are poorly resolved, especially in summer. Understanding these dynamics can offer insight into the general chemistry during Arctic summer and atmospheric mercury will respond to future changes in the Arctic climate."

Line 88 : It does not make sense "is also important to understand the dynamics of mercury to assess the effects of abatement strategies on atmospheric concentrations in the framework of the Minamata Convention (UNEP, 2013) »

What is the link between abatement strategy and Hg dynamic in the Arctic ?

Due to the complex nature of mercury cycling in the environment, it is important to have spatiotemporal measurements of mercury speciation from around the globe to assess any changes in concentrations levels. We have rephrased the sentence to make this link clearer.

Lines 108-109: "It is also important to understand the changes of mercury concentrations in the Arctic to assess the effects of abatement strategies of the Minamata Convention (UNEP, 2013) globally."

Line 125. You should be consistent with the numbers.

We have added the trailing zero for 0.180 on Line 145 so the number of significant figures is consistent between the two LOD values. We thank the referee for this good catch.

Line 128 : How is snow depth measured ?

Snow depth is measured with one Campbell SR50A sonic sensor. The sensor is placed at 3 m in height. The sensor is based on a 50 kHz (Ultrasonic) electrostatic transducer. The SR50A determines the distance to a target by sending out ultrasonic pulses. The time from transmissions to the return of an echo is the basis for obtaining the distance measurement. Since the speed of sound in air varies with temperature, an independent

temperature measurement is required to compensate for the distance reading for the SR50A. A simple calculation is applied to initial readings for this purpose. The SR50A projects an ultrasonic beam that can pick up objects in its field of view that is 30° or less. The closest object to the sensor will be detected if it is within this field of view.

Line 129 : What does « averaged to 30 - minute means » mean?

We have amended the text to indicate that we refer to arithmetic mean here.

Line 151-153: "Ozone (O_3) was measured at Villum using a photometric O_3 analyzer (API M400) at 1 Hz, averaged to a 30-minute arithmetic mean."

GOM data

Is the use of the GOM detection limit appropriate? Why not using the Quantification limit since we all know that these speciation instruments are quite difficult to manage? Event 2 is very closed to the detection limit and the first days of Event 1 and may be excluded.

We have opted to use the limit of detection and not the limit of quantification since we are investigating events of GOM enhancements. These events involve the presence of GOM in elevated concentrations over background levels. Therefore, we choose the limit of detection as a lower analytical limit since we are largely interested in distinguishing the presence of GOM from the noise of blank measurements. For the sake of argument, we calculated the limit of quantification (LOQ) as 10 times the standard deviation of blank measurements. This resulted in LOQs of 0.300 and 2.28 for the 2019 and 2020 campaigns, respectively. For the 2019 campaign, there were no non-zero values <LOD or <LOQ. For the 2020 campaign, the number of GOM measurements <LOD or <LOQ was 17 and 80, respectively, although none of the measurements <LOQ occurred during the GOM enhancement events. The use of LOQ would not affect the timing of the events nor our interpretation of them since no event measurements were <LOQ.

There is no discussion on the quality of GOM data obtained with denuders while the authors may know that Tekran speciation unit underestimate GOM value as shown in recent studies (Marusczak et al 2017 – Gustin et al 2015 – Huang et al 2015, 2017)

We have added the following sentences to comment on the quality of the data.

Lines 145-148: "With the KCl denuders being prone to unequal collection efficiencies for different GOM species and artifacts (Gustin et al., 2015) and the internal signal integration routine biasing the concentrations low (Slemr et al., 2016; Ambrose, 2017), the GEM and GOM concentrations are likely a lower limit (Huang and Gustin, 2015; Huang et al., 2017; Marusczak et al., 2017)."

Gustin, M. S., Amos, H. M., Huang, J., Miller, M. B., and Heidecorn, K.: Measuring and modeling mercury in the atmosphere: a critical review, Atmos. Chem. Phys., 15, 5697-5713, 10.5194/acp-15-5697-2015, 2015.

Slemr, F., Weigelt, A., Ebinghaus, R., Kock, H. H., Bödewadt, J., Brenninkmeijer, C. A. M., Rauthe-Schöch, A., Weber, S., Hermann, M., Becker, J., Zahn, A., and

Martinsson, B.: Atmospheric mercury measurements onboard the CARIBIC passenger aircraft, Atmos. Meas. Tech., 9, 2291-2302, 10.5194/amt-9-2291-2016, 2016.

Ambrose, J. L.: Improved methods for signal processing in measurements of mercury by Tekran® 2537A and 2537B instruments, Atmos. Meas. Tech., 10, 5063-5073, 10.5194/amt-10-5063-2017, 2017.

Huang, J., and Gustin, M. S.: Uncertainties of Gaseous Oxidized Mercury Measurements Using KCl-Coated Denuders, Cation-Exchange Membranes, and Nylon Membranes: Humidity Influences, Environmental Science & Technology, 49, 6102-6108, 10.1021/acs.est.5b00098, 2015.

Huang, J., Miller, M. B., Edgerton, E., and Sexauer Gustin, M.: Deciphering potential chemical compounds of gaseous oxidized mercury in Florida, USA, Atmos. Chem. Phys., 17, 1689-1698, 10.5194/acp-17-1689-2017, 2017.

Marusczak, N., Sonke, J. E., Fu, X., and Jiskra, M.: Tropospheric GOM at the Pic du Midi Observatory—Correcting Bias in Denuder Based Observations, Environmental Science & Technology, 51, 863-869, 10.1021/acs.est.6b04999, 2017.

Are the raw data available for all these events ? This is critical to make sure that all the blanks where correctly made.

All data required to reproduce this study, in its fully processed and quality-controlled form, will be made available before publication.

Blanks were calculated according strictly to Model 1130/1135 Mercury Speciation Unit User Manuals. We are confident all measurements included in this manuscript were calculated correctly.

Line 204 : yes but there is no evidence that there are open leads on the way ?

The sentence indicates that the elevated GEM concentrations *could* be the result of oceanic evasion as previously observed by the references given. To further support this statement, we have added a link to satellite images of sea ice in the surrounding areas of Villum. While these images only show the sea ice conditions on a scale of 100s of kilometers and not over the central Arctic Ocean, they give an idea of the conditions that *could* lead to oceanic evasion of mercury.

Line 244-247: "These elevated concentrations could be the result of oceanic evasion through open leads and fissures in the consolidated pack ice (Aspmo et al., 2006; DiMento et al., 2019), as air masses experienced extensive surface contact with sea ice on July 19–21 (Fig. S4a–c). Satellite images, which show fractured sea ice surrounding Villum are available at http://ocean.dmi.dk/arctic/nord.uk.php."

Line 218 : snow cover is not displayed in figure S2

> We thank the referee for catching this error, this sentence has been corrected to refer to Fig. S3.

By the way the color scale for the contour is quite difficult to read.

> Contour plots are always rather difficult to read, especially when values cover a wide range. We have tested the figures on people with unimpaired vision and with colorblind people and found this color scheme to be an appropriate compromise between clarity and detail.

Line 230 : What is considered as high radiation and low RH ? How are those thresholds defined ? Event 1 had some low radiation too (<200). Was there a snow/rain fall ? on august 21st ?

> We have amended the text to make these thresholds relative when compared to the non-event periods.

What is the dynamic of the boundary layer ? This is an important factor that can explain some variation in your concentrations.

> We have added a short statistical description of the modeled mixed layer depth from HYSPLIT during each campaign in the Methods and Materials sections. Our analysis revealed no connection between the modeled mixed layer height and GOM concentrations.

Line 230 : your suggestion that cold temperatures are associated to mercury oxidation is not valid in volcanic plumes or in salt lake regions. To me, the temperatures are not a solid argument to reject in situ production. Halogen measurements could give a major evidence to demonstrate this -although I do not believe that this is likely to happen at this time of the year.

> The state of the knowledge indicates that the oxidation of GEM is temperature-dependent and dominated by Br initiated oxidation. In volcanic plumes and salt lake regions, the Br concentration is orders of magnitude higher than in the Arctic and is not representatively for the air masses at Villum. We have indicated that the observations were performed in the Arctic to clarify this. Preliminary measurements of BrO show a U-shaped concentration profile with peaks in the spring and autumn and minima during the summer (personal communication Alfonso Saiz-Lopez). Therefore, the statement is correct, and too high temperatures is a logical argument.

Line 249-253 : How are calculated those averages ? on the whole trajectory duration ?

Given the uncertainties of all these measurements and of the average, are these air masses statistically different ? Given the shown interval, I do not see any evidence of a robust difference. The Wicoxon test is used for comparing independant populations. Here you have an overlap on « event » and « non-event » trajectorie : for example the 28/08 -120h trajectories overlap and are supposed to be included with the one from the 26/08.

Where the test conducted on each separate observation? (ie RH in « event » with RH in « non event »). Btw, water mixing ratio if a function of temperature and RH ?

The Wilcoxon rank sum test is a nonparametric test for two independent populations. The distribution of the trajectory-derived meteorological parameters is non-normal and the high sample size adds confidence to the power of the test statistic. For our research, we have assumed independent populations given the variability of the geographic location (latitude, longitude, and altitude) for each step along the trajectory path. Using meteorological data at each step of each trajectory for event vs. non-event periods, which covers a range of altitudes and geographic locations, is the likely cause for the slight differences. Our goal was to test for statistically significant differences, not the absolute differences, between these periods which the Wilcoxon rank sum test has accomplished. Given the new analysis of the revised manuscript, we have opted to remove the use of this test since we focus more on the general pattern observed during event periods relative to non-event periods as well as individual events.

Line 276 : The meaning of this sentence is not clear. What does « these air masses » refer to ?

'These air masses' refers to event period air masses. Although we have removed this sentence from the revised manuscript.

Line 280 : Figure 3d and 4d With this figure the author suggest that GOM event air masses spent more time at high altitude. The overall picture is not that clear. Event 3 and 4 are not very different from the non-event period (27/07-31/07). Regarding the strongest event in 2020 (on the 23/07) these air masses are not different from the day before and the altitude is close to what one can expect as a marine boundary layer. In summer time it can be several hundreds of meters thick, even more when passing over turbulent and convective areas.

The exact wording used in the text is 'aloft' and not 'high altitude', in this context aloft is referring to above the mixed layer. As indicated in Table S2, air masses that arrived during event periods were consistently above the mixed layer height compared to air masses that arrived during non-event periods. This demonstrates numerically what the figure is displaying and supports our statement.

Air masses spending time above the mixed layer is not the only condition conducive for GOM formation but also cold temperatures, low RH, low H_2O mixing ratios, and intense radiation along the trajectory path. So, while these altitudes might be similar, favorable conditions for GOM formation (cold and dry air masses from aloft with intense radiation) were only present during the event periods as shown in Fig. 4.

Line 282 : for the 2019 campaign : what is the value show with the median height ? 1sigma ? min-max ? For this campaign, there are important overlap between « event » and « non event » periods.

The variance stated after the median altitude is the median absolute deviation (m.a.d.), for an overview of the trajectory derived parameters see Table S2.

Line 285 : how is retrieved the mixed layer height ? How robust is it in Hysplit ? Why is it no plotted on your figures ?

Overall with the presented data, I do not come to the same conclusion (line 286-289).

The HYSPLIT model uses the mixed layer depth value from the meteorological model, in this case, Global Data Assimilation System (GDAS) meteorological data on a 1° spatial resolution and 3-hour time resolution. We have updated Fig. S5 to include the mixed layer height for the 2019 and 2020 campaigns. We have systematically analyzed the altitudes and trajectory-derived meteorological parameters for event vs. non-event periods and this is our interpretation of the general pattern observed in the data.

Line 295 : you mentioned earlier than cold temperature below -15°C are likely needed.

Looking at temperature along the BT ways, it is not the case here ?

In the free troposphere what could cause the formation of GOM is mainly the supposed abundance of Br concentrations ?

We gave this value as a literature example of field observations that indicates cold temperature are required for the oxidation of mercury to proceed in the Arctic region. In one of the campaigns presented in Brooks et al. (2011), the temperature exceeded their threshold during observations of oxidized mercury, indicating this is not an absolute threshold. We have updated the text to indicate this as well as including other references which show a frozen heterogeneous surface is required for halogen propagation. The trajectory-derived temperatures were frequently below 0°C.

Lines 436-442: "Lower temperatures aid in the formation of GOM from HgBr, for example, Skov et al. (2004) and Christensen et al. (2004) modeled a surface temperature below -4 °C for mercury depletion to occur in the Arctic, while Brooks et al. (2011) observed a temperature threshold of -15 °C for mercury oxidation to occur at Summit Station, atop the Greenlandic ice sheet. It should be noted that Brooks et al. (2011) detected oxidized mercury at temperatures above this threshold but not above 0 °C. Tarasick and Bottenheim (2002) analyzed ozonesonde records and observed surface temperatures below -20 °C were required for the occurrence of ozone depletion events. Furthermore, Halfacre et al. (2019) and Burd et al. (2017) demonstrated that a frozen heterogeneous surface is required for the propagation of halogen explosion events."

Halfacre, J. W., Shepson, P. B., and Pratt, K. A.: pH-dependent production of molecular chlorine, bromine, and iodine from frozen saline surfaces, Atmos. Chem. Phys., 19, 4917-4931, 10.5194/acp-19-4917-2019, 2019.

Burd, J. A., Peterson, P. K., Nghiem, S. V., Perovich, D. K., and Simpson, W. R.: Snowmelt onset hinders bromine monoxide heterogeneous recycling in the Arctic, Journal of Geophysical Research: Atmospheres, 122, 8297-8309, 10.1002/2017jd026906, 2017.

Tarasick, D. W., and Bottenheim, J. W.: Surface ozone depletion episodes in the Arctic and Antarctic from historical ozonesonde records, Atmos. Chem. Phys., 2, 197-205, 10.5194/acp-2-197-2002, 2002.

Line 298 what is the low surface resistance ?

The surface resistant is commonly used in description of fluxes F

F = vC where v = $(r_a + r_b + r_c)^{-1}$, where C is the concentration, v is the flux velocity and r_a and r_b are atmospheric resistances and r_c is aerodynamic resistance, see Seinfeld and Pandis, 2016.

Seinfeld, J. H., and Pandis, S. N.: Atmospheric Chemistry and Physics: From Air Pollution to Climate Change, 3 ed., John Wiley & Sons, 1152 pp., 2016.

We have amended the text to give the estimate of the surface resistance of GOM given by Skov et al. (2006).

Lines 469-472: "Additionally, given the low surface resistance of GOM over snowpack (Skov et al. (2006) estimated a surface resistance of GOM close to zero), the occurrence of dry (and possibly wet) deposition will increase when air masses come in close contact with the surface layer (i.e., below the mixed layer), resulting in decreased concentrations."

Line 299 There are two verbs in the sentence.

Please see the amended text in our reply to the comment above. We thank the referee for catching this error.

Line 301 : survival is not appropriate for a chemical species

In this context, we feel survival is appropriate as it explains the ability of GOM to overcome removal by deposition, although this sentence was removed in the revised manuscript.

Line 31 – 5 days backtrajectories are clearly not long enough. For BC studies or aerosols 10 days are usually used (see Thomas et al 2017 in GRL). The life time of GOM is poorly known and could be of several days to weeks in dry conditions?

This approach is not relevant. CO data and BC may be a more straightforward approach to track fires. This whole paragraph does not bring any relevant information and fires may contribute to these GOM events, and/or GEM.

The original length of back trajectories was chosen as a compromise between information gained and associated uncertainty, which is estimated to be around 20 % of the distance traveled by the trajectory (Stohl, 1998). We decided for a limited length of 120 hours as uncertainties rise with the distance back in time and this is especially the case where meteorological fields are based on a limited number of meteorological measurements, as in the Arctic. Therefore, we have erred on the side of caution with our original analysis.

We acknowledge 120 hours might have been too short, therefore, we doubled the length of the trajectories and thus doubled our criteria for intersections between trajectories and active fires to account for any added uncertainty in the locations of the trajectory endpoints and active fires. We have incorporated our interpretation of the new air mass history analysis and interactions with active fires in the revised manuscript.

Our analysis indicates interaction between active fires and air mass trajectories. We, therefore, disagree with the referee's statement that this approach is not relevant. The section of air mass history details the geospatial extent of air masses during each event period, which highlights how they are heterogeneously distributed, which we find highly relevant. While back trajectory modeling is not a perfect representation and has its document uncertainties/drawbacks, we feel its use in this study is warranted and appropriate.

Stohl, A.: Computation, accuracy and applications of trajectories - A review and bibliography, Atmospheric Environment, 32, 947-966, 10.1016/s1352-2310(97)00457-3, 1998.

Line 325 : this first sentence has no meaning in atmospheric chemistry.

We have amended the text to make the meaning of this sentence clearer.

Lines 480-481: "Previous studies have demonstrated the influence of the free troposphere on mercury concentrations within the boundary layer."

The Shah and Jaeglé study point sub-tropical areas and this is an important difference from mid-latitudes.

We have removed 'in the mid-latitudes' from this sentence to indicate this is occurring over the entire Northern Hemisphere and not just the mid-latitudes.

Line 340 : Why not using aerosols (check Uge et al in GRL 2017). The paragraph 3.3 is only a short review of FT measurements and is of no interest for the discussion.

In their initial assessment of the manuscript, the referee states that our hypothesis is very original but debatable. While this paragraph is a short review, it details how the free troposphere has been repeatedly demonstrated to be a source of GOM throughout the global atmosphere both through in situ measurements and modeling studies. While we are the first to propose this process is occurring in the High Arctic, it has been widely and repeatedly demonstrated at lower latitudes, and so the hypothesis is not unreasonable nor is it a far stretch beyond current scientific understanding.

The authors were unable to find Uge et al. in GRL 2017. The authors will kindly ask the referee to at least give a digital object identifier (DOI) when referencing articles, this will ensure unambiguous identification and save time in the future.

In our reorganization of the text, we have moved this text to a location where it supports our findings.

Line 390 – and after. The authors make a confusion between the influence of free troposphere and a stratosphere intrusion Stratospheric intrusion would bring very dry air masses and very high ozone. It is likely that the Biomass burning may have an influence on ozone.

We agree the text could be confusing. While we observe a correlation between ozone, GOM, and hydrological-related parameters during event periods, they are not to the extreme that would be representative of stratospheric air masses. We have removed

parts of this text in the revised manuscript to avoid any confusion. We have also acknowledged the influence of active fires on ozone levels during the event periods, due to the new analysis of air mass history.

There is not ozone data presented in Jacob et al 2010. I don't understand what do the authors find in Monks et al 2015 to support their statements. Monks et al suggest that European anthropogenic emissions may be important for lower tropospheric summertime ozone and that PAN reactivity may be a source of ozone.

The Jacob et al. (2010) reference is in relation to the ARCTAS campaigns and the Monks et al. (2015) reference was incorrectly inserted as Monks et al published another article in the same year which was mistaken for the article listed below. Figure 7 in Monks et al. (2015) shows increasing ozone mixing ratios with increasing altitude. We thank the referee for this good catch and have corrected the mistake in the bibliography.

Monks, S. A., Arnold, S. R., Emmons, L. K., Law, K. S., Turquety, S., Duncan, B. N., Flemming, J., Huijnen, V., Tilmes, S., Langner, J., Mao, J., Long, Y., Thomas, J. L., Steenrod, S. D., Raut, J. C., Wilson, C., Chipperfield, M. P., Diskin, G. S., Weinheimer, A., Schlager, H., and Ancellet, G.: Multi-model study of chemical and physical controls on transport of anthropogenic and biomass burning pollution to the Arctic, Atmos. Chem. Phys., 15, 3575-3603, 10.5194/acp-15-3575-2015, 2015.

In the reorganization of the text, we have however removed these references.

Paragraph 435 – 444 . The correlation of GOM and BC looks very interesting in 2019 so I do not understand why the conclusion is that combustion sources has no influence – As said earlier the 5 days trajectories are too short to reach this conclusion. For year 2020, event 3 and 4 may be as well related to combustion sources (the scale is different on figure 7a and b). Event 5 could be due to production of GOM over the Greenland ice cap (as mentioned in Brooks et al 2011 – although earlier in the season), or as proposed in Angot et al 2016 10.5194/acp-16-8265-201. This hypothesis would also lead to low BC.

Then I do not agree that this airmasses comes from the upper troposphere. The GOM peak on August 1st show trajectories around 1000-2000 m ? This could only be air masses leaching the Greenland icecap before arriving to VRS.

Given our previous length of the trajectories, no influence of active fires and trajectories could be observed. We have recalculated the length of the trajectories and expanded the criteria for intersections between trajectories and active fires, as mentioned above. We have updated the manuscript to reflect this new analysis and our interpretation of the results, in which we found active fires to likely be contributing the coarse mode aerosol needed for halogen propagation. For Event 3, the new trajectory length revealed only one intersection between trajectories and active fires, and none for Event 4 (Fig. 5). We have recharacterized the events, as suggested by another referee, in which we have split Event 5 into 5a and 5b. Event 5a appears to be the results of emissions in Northern Scandinavia, either from active fires or anthropogenic sources. For Event 5b, we observe air masses arriving from over the Greenland Ice Sheet. We have offered

hypotheses in the revised manuscript about the similarities in the levels of BC for these two events, however, a definitive conclusion is unavailable.

Brooks et al. (2011) detected GOM during Arctic springtime depletion events at Summit, their analysis showed that during periods of large GOM concentrations air masses had largely resided near the surface, void of marine and upper troposphere influence, and the GOM formation likely occurred because of surface-related processes (Thomas et al., 2012). This is contrary to Event 5b, from which air masses arrived over the Greenland Ice Sheet from high altitudes under cold, dry, and sunlit conditions (Fig. 4 and 5).

Thomas, J. L., Dibb, J. E., Huey, L. G., Liao, J., Tanner, D., Lefer, B., von Glasow, R., and Stutz, J.: Modeling chemistry in and above snow at Summit, Greenland – Part 2: Impact of snowpack chemistry on the oxidation capacity of the boundary layer, Atmos. Chem. Phys., 12, 6537-6554, 10.5194/acp-12-6537-2012, 2012.

453-454 – This is not because a high BC is observed without GOM for a single event that biomass burning cannot influence artic GOM concentration. This is too speculative.

We acknowledge this is speculation. Given the new trajectory analysis, we have added to our interpretation of the interaction between event periods and active fire emissions.

508-511 – This is a very vague speculation.

We have re-evaluated our interpretations and conclusions based on new knowledge and removed this section in the revised manuscript.

Angot, H., Dastoor, A., De Simone, F., Gårdfeldt, K., Gencarelli, C. N., Hedgecock, I. M., Langer, S., Magand, O., Mastromonaco, M. N., Nordstrøm, C., Pfaffhuber, K. A., Pirrone, N., Ryjkov, A., Selin, N. E., Skov, H., Song, S., Sprovieri, F., Steffen, A., Toyota, K., Travnikov, O., Yang, X., and Dommergue, A.: Chemical cycling and deposition of atmospheric mercury in polar regions: review of recent measurements and comparison with models, Atmos Chem Phys, 16, 10735-10763, 10.5194/acp-16-10735-2016, 2016.

Ariya, P. A., Dastroor, A. P., Amyot, M., Schroeder, W. H., Barrie, L., Anlauf, K., Raofie, F., Ryzhkov, A., Davignon, D., Lalonde, J., and Steffen, A.: The Arctic: a sink for mercury, Tellus B: Chemical and Physical Meteorology, 56, 397-403, 10.3402/tellusb.v56i5.16458, 2004.

Brooks, S., Moore, C., Lew, D., Lefer, B., Huey, G., and Tanner, D.: Temperature and sunlight controls of mercury oxidation and deposition atop the Greenland ice sheet, Atmos Chem Phys, 11, 8295-8306, 10.5194/acp-11-8295-2011, 2011.

Burd, J. A., Peterson, P. K., Nghiem, S. V., Perovich, D. K., and Simpson, W. R.: Snowmelt onset hinders bromine monoxide heterogeneous recycling in the Arctic, Journal of Geophysical Research: Atmospheres, 122, 8297-8309, 10.1002/2017jd026906, 2017.

Christensen, J. H., Brandt, J., Frohn, L. M., and Skov, H.: Modelling of Mercury in the Arctic with the Danish Eulerian Hemispheric Model, Atmos. Chem. Phys., 4, 2251-2257, 10.5194/acp-4-2251-2004, 2004.

Douglas, T. A., Sturm, M., Blum, J. D., Polashenski, C., Stuefer, S., Hiemstra, C., Steffen, A., Filhol, S., and Prevost, R.: A Pulse of Mercury and Major Ions in Snowmelt Runoff from a Small Arctic Alaska Watershed, Environmental Science & Technology, 51, 11145-11155, 10.1021/acs.est.7b03683, 2017.

Durnford, D., and Dastoor, A.: The behavior of mercury in the cryosphere: A review of what we know from observations, Journal of Geophysical Research, 116, 10.1029/2010jd014809, 2011.

Freud, E., Krejci, R., Tunved, P., Leaitch, R., Nguyen, Q. T., Massling, A., Skov, H., and Barrie, L.: Pan-Arctic aerosol number size distributions: seasonality and transport patterns, Atmos Chem Phys, 17, 8101-8128, 10.5194/acp-17-8101-2017, 2017.

Halfacre, J. W., Shepson, P. B., and Pratt, K. A.: pH-dependent production of molecular chlorine, bromine, and iodine from frozen saline surfaces, Atmos. Chem. Phys., 19, 4917-4931, 10.5194/acp-19-4917-2019, 2019.

Lindberg, S. E., Brooks, S., Lin, C. J., Scott, K. J., Landis, M. S., Stevens, R. K., Goodsite, M., and Richter, A.: Dynamic oxidation of gaseous mercury in the Arctic troposphere at polar sunrise, Environmental Science & Technology, 36, 1245-1256, 10.1021/es0111941, 2002.

Lu, J. Y., Schroeder, W. H., Barrie, L. A., Steffen, A., Welch, H. E., Martin, K., Lockhart, L., Hunt, R. V., Boila, G., and Richter, A.: Magnification of atmospheric mercury deposition to polar regions in springtime: The link to tropospheric ozone depletion chemistry, Geophysical Research Letters, 28, 3219-3222, 10.1029/2000gl012603, 2001.

Macdonald, R. W., and Loseto, L. L.: Are Arctic Ocean ecosystems exceptionally vulnerable to global emissions of mercury? A call for emphasised research on methylation and the consequences of climate change, Environ. Chem., 7, 133-138, 10.1071/en09127, 2010.

Muntean, M., Janssens-Maenhout, G., Song, S., Giang, A., Selin, N. E., Zhong, H., Zhao, Y., Olivier, J. G. J., Guizzardi, D., Crippa, M., Schaaf, E., and Dentener, F.: Evaluating EDGARv4.tox2 speciated mercury emissions ex-post scenarios and their impacts on modelled global and regional wet deposition patterns, Atmospheric Environment, 184, 56-68, https://doi.org/10.1016/j.atmosenv.2018.04.017, 2018.

Møller, A. K., Barkay, T., Al-Soud, W. A., Sørensen, S. J., Skov, H., and Kroer, N.: Diversity and characterization of mercury-resistant bacteria in snow, freshwater and sea-ice brine from the High Arctic, FEMS Microbiology Ecology, 75, 390-401, 10.1111/j.1574-6941.2010.01016.x, 2011.

Obrist, D., Tas, E., Peleg, M., Matveev, V., Faïn, X., Asaf, D., and Luria, M.: Bromine-induced oxidation of mercury in the mid-latitude atmosphere, Nature Geoscience, 4, 22-26, 10.1038/ngeo1018, 2010.

Skov, H., Christensen, J. H., Goodsite, M. E., Heidam, N. Z., Jensen, B., Wahlin, P., and Geernaert, G.: Fate of elemental mercury in the arctic during atmospheric mercury depletion episodes and the load of atmospheric mercury to the arctic, Environmental Science & Technology, 38, 2373-2382, 10.1021/es030080h, 2004.

Skov, H., Brooks, S., Goodsite, M., Lindberg, S., Meyers, T., Landis, M., Larsen, M., Jensen, B., McConville, G., and Christensen, J.: Fluxes of reactive gaseous mercury measured with a newly developed method using relaxed eddy accumulation, Atmospheric Environment, 40, 5452-5463, 10.1016/j.atmosenv.2006.04.061, 2006.

Steffen, A., Schroeder, W., Bottenheim, J., Narayan, J., and Fuentes, J. D.: Atmospheric mercury concentrations: measurements and profiles near snow and ice surfaces in the Canadian Arctic during Alert 2000, Atmospheric Environment, 36, 2653-2661, https://doi.org/10.1016/S1352-2310(02)00112-7, 2002.

Steffen, A., Bottenheim, J., Cole, A., Ebinghaus, R., Lawson, G., and Leaitch, W. R.: Atmospheric mercury speciation and mercury in snow over time at Alert, Canada, Atmos Chem Phys, 14, 2219-2231, 10.5194/acp-14-2219-2014, 2014.

Tarasick, D. W., and Bottenheim, J. W.: Surface ozone depletion episodes in the Arctic and Antarctic from historical ozonesonde records, Atmos. Chem. Phys., 2, 197-205, 10.5194/acp-2-197-2002, 2002.

UNEP: UNEP: Minamata Convention on Mercury: http://www.mercuryconvention.org/Convention/tabid/3426/Default.aspx access: 2020-11-12, 2013.

von Glasow, R.: Atmospheric chemistry in volcanic plumes, Proceedings of the National Academy of Sciences, 107, 6594-6599, 10.1073/pnas.0913164107, 2010.

Wang, S., McNamara, S. M., Moore, C. W., Obrist, D., Steffen, A., Shepson, P. B., Staebler, R. M., Raso, A. R. W., and Pratt, K. A.: Direct detection of atmospheric atomic bromine leading to mercury and ozone depletion, Proc Natl Acad Sci U S A, 116, 14479-14484, 10.1073/pnas.1900613116, 2019.

Ye, Z., Mao, H., Lin, C. J., and Kim, S. Y.: Investigation of processes controlling summertime gaseous elemental mercury oxidation at midlatitudinal marine, coastal, and inland sites, Atmos. Chem. Phys., 16, 8461-8478, 10.5194/acp-16-8461-2016, 2016.

Reply to Anonymous Referee # 3 Comment on 'Dynamics of gaseous oxidized mercury at Villum Research Station during the High Arctic summer'

The manuscript by Pernov et al. describes the measurement of mercury species and ancillary chemical and meteorological parameters at a site of great importance and interest in the high Arctic at 81°N in Greenland. Unlike many studies which concentrate on Spring when mercury depletion events are common, this study describes two measurement campaigns which were performed in the Summer, which is a relatively less well studied period of the year at these kinds of latitudes.

The manuscript is well written and mostly clear. There is one point however which I think could improve the clarity of the presentation and that is making it more clear when the authors are referring to the free troposphere, the planetary boundary layer or the troposphere in its entirety. As a large part of the discussion revolves around the height of origin and transport of the air masses arriving at the measurement site, it would be useful if the authors were explicit in their descriptions. For instance when they refer to the surface (see for example line 183), does this literally mean the soil or snow, or the surface layer, that is the boundary layer? Still on the same subject, it would be useful for the reader if in the Introduction, the authors could provide a brief description of the typical characteristics of the boundary layer. This would help the reader later on in the Discussion section.

I have a few more specific comments, which are listed below.

> We would like to thank Referee # 3 for the careful review of our manuscript. The comments and suggestions will improve the clarity, presentation, and discussion of the work. We have addressed the referee's concerns and corrected errors in the revised manuscript below with the author's responses in blue. Line numbers refer to the clean version of the revised manuscript. New references are highlighted in yellow.
>
> One of the referee's main points was to indicate where in the atmosphere the authors are referring to in the text. To address this, we have specified in the text which part of the atmosphere we are referring to, e.g., boundary layer, free troposphere, upper troposphere).
>
> The referee also states that a paragraph in the Introduction about boundary layer dynamics would help the reader later in the Discussion, specifically Sect. 3.6 in the previous version of the manuscript. We have made substantial changes to the text and ultimately decided to remove this section. After receiving pushback from all referees, we realize that our hypotheses were too speculative. We have opted not to include a paragraph about boundary layer dynamics in the Introduction, as this was mainly requested to aid the reader later in the Discussion on the section about possible halogen sources.

L19 does tropospheric in this sentence refer to the free troposphere?

Our original intention was to indicate free tropospheric air masses in this sentence. We have removed this sentence in the revised manuscript. We have also amended the text throughout the manuscript to be clear which part of the atmosphere we are referring to.

L24 I think it should be artisanal rather than artisan and in the list of 'natural' emissions, many would include re-emission of legacy mercury, perhaps the authors could make this clear.

We have replaced 'artisan' with 'artisanal'. We have included 'legacy mercury' in our description of previously deposited mercury.

Line 33-35: "The sources of mercury include anthropogenic emissions, e.g., fossil fuel/biomass combustion, and artisanal small-scale gold mines, in addition to natural emissions such as volcanoes, biomass burning, ocean/soil evasion, and reemission of previously deposited/legacy mercury (AMAP, 2011)."

L29 Hg(P) could include elemental mercury adsorbed (strongly) to soot particles as well maybe, which could be important in some instances.

There is ample literature demonstrating gaseous oxidized mercury is readily adsorbed onto particle surfaces. There is literature supporting the adsorption of GEM onto aerosols surfaces (Kim et al., 2012) and literature indicating this is negligible (Seigneur et al., 1998; Otani et al., 1986). Since the soot contained within Arctic aerosols are coated by sulfate and organic matter (Yu et al., 2019), the adsorption of GEM by soot containing aerosols appears negligible in the Arctic atmosphere, given this coating.

Kim, P.-R., Han, Y.-J., Holsen, T. M., and Yi, S.-M.: Atmospheric particulate mercury: Concentrations and size distributions, Atmospheric Environment, 61, 94-102, https://doi.org/10.1016/j.atmosenv.2012.07.014, 2012.

Seigneur, C., Abeck, H., Chia, G., Reinhard, M., Bloom, N. S., Prestbo, E., and Saxena, P.: Mercury adsorption to elemental carbon (soot) particles and atmospheric particulate matter, Atmospheric Environment, 32, 2649-2657, https://doi.org/10.1016/S1352-2310(97)00415-9, 1998.

Otani, Y., Kanaoka, C., Usui, C., Matsui, S., and Emi, H.: Adsorption of mercury vapor on particles, Environmental Science & Technology, 20, 735-738, 10.1021/es00149a014, 1986.

Yu, H., Li, W., Zhang, Y., Tunved, P., Dall'Osto, M., Shen, X., Sun, J., Zhang, X., Zhang, J., and Shi, Z.: Organic coating on sulfate and soot particles during late summer in the Svalbard Archipelago, Atmos. Chem. Phys., 19, 10433-10446, 10.5194/acp-19-10433-2019, 2019.

L34 references for the specific cases mentioned where rapid oxidation occurs would be better, the Angot et al. paper refers only to polar regions.

The authors agree with the referee's recommendation for additional references. We have added von Glasow (2010) which details atmospheric chemistry in volcanic plumes including halogen-induced mercury oxidation, Obrist et al. (2010) which investigated mercury oxidation over the Dead Sea, and Ye et al. (2016) which models mercury species at three sites in the midlatitudes. We have also replaced coastal regions with the marine boundary layer to be more specific and highlighted that these are reactive bromine species.

Line 35 "In locations with elevated reactive halogen concentrations (e.g., polar environments, the marine boundary layer, volcanic plumes, and salt lakes) and especially bromine radicals, GEM is quickly transformed into GOM (Obrist et al., 2010; von Glasow, 2010; Angot et al., 2016; Ye et al., 2016; Wang et al., 2019)."

von Glasow, R.: Atmospheric chemistry in volcanic plumes, Proceedings of the National Academy of Sciences, 107, 6594-6599, 10.1073/pnas.0913164107, 2010.

Obrist, D., Tas, E., Peleg, M., Matveev, V., Faïn, X., Asaf, D., and Luria, M.: Bromine-induced oxidation of mercury in the mid-latitude atmosphere, Nature Geoscience, 4, 22-26, 10.1038/ngeo1018, 2010.

Ye, Z., Mao, H., Lin, C. J., and Kim, S. Y.: Investigation of processes controlling summertime gaseous elemental mercury oxidation at midlatitudinal marine, coastal, and inland sites, Atmos. Chem. Phys., 16, 8461-8478, 10.5194/acp-16-8461-2016, 2016.

Wang, S., McNamara, S. M., Moore, C. W., Obrist, D., Steffen, A., Shepson, P. B., Staebler, R. M., Raso, A. R. W., and Pratt, K. A.: Direct detection of atmospheric atomic bromine leading to mercury and ozone depletion, Proc Natl Acad Sci U S A, 116, 14479-14484, 10.1073/pnas.1900613116, 2019.

L39 my curiosity here, to which type(s) of aerosol are the authors referring?

On Line 50, we refer to the conversion of GOM into PHg due to the cold temperatures which lowers the vapor pressure and because of the high aerosol surface area concentration. The Arctic spring experiences high surface area concentrations due to the Arctic Haze, which is anthropogenic pollution transported from the mid-latitudes caused by the expansion of the polar dome and inefficient removal processes and is characterized by higher concentrations of accumulation mode particles. This peak in surface area, volume, and mass concentration are observed across all Arctic stations in the spring. For clarity, we have specified it is aerosol surface area concentration we are referring to and added a reference to this observed peak in aerosol surface area concentration.

Lines 50-51: "(through condensational processes due to the cold temperatures and high aerosol surface area concentration from accumulation mode particles (Freud et al., 2017))"

Freud, E., Krejci, R., Tunved, P., Leaitch, R., Nguyen, Q. T., Massling, A., Skov, H., and Barrie, L.: Pan-Arctic aerosol number size distributions: seasonality and transport patterns, Atmos Chem Phys, 17, 8101-8128, 10.5194/acp-17-8101-2017, 2017.

L42-44 I was very surprised that none of the work by Dibble or Saiz-Lopez and their co-workers was included in the references here. Is there a reason for this? They would seem pertinent to me.

There is not a particular reason for the omissions of these authors' work. We acknowledge the references in this section could be more inclusive, so we have amended the text as seen in our reply to the comment below.

L50 Again, I think the references should be more inclusive here.

Lines 55-67: "GEM oxidation has been demonstrated to be initiated via photochemical reactions with the Br radical (R1-R2) through modeling studies (Holmes et al., 2006; Holmes et al., 2010; Horowitz et al., 2017), kinetic studies (Donohoue et al., 2006), theoretical studies (Goodsite et al., 2004; Dibble et al., 2012; Goodsite et al., 2012), and observations (Skov et al., 2004; Stephens et al., 2012; Wang et al., 2019).

$$Br + Hg^0 \leftrightarrow HgBr \qquad\qquad (R1)$$

$$HgBr + Y \rightarrow HgBrY \qquad\qquad (R2)$$

Where Y could be OH, O_3, NO_2, HO_2, Br, Cl, BrO, ClO, I, IO (Holmes et al., 2006; Hynes et al., 2009; Holmes et al., 2010; Dibble et al., 2012; Jiao and Dibble, 2017a, b). Of which Br, I, and OH have been postulated to be the main species for Y, both globally and in the Arctic (Goodsite et al., 2004, 2012), while NO_2, HO_2, ClO, or BrO have been demonstrated to be candidates for Y by Dibble et al. (2012). Recently, ozone was proposed to be a missing oxidation pathway of HgBr (Saiz-Lopez et al., 2020)."

Horowitz, H. M., Jacob, D. J., Zhang, Y., Dibble, T. S., Slemr, F., Amos, H. M., Schmidt, J. A., Corbitt, E. S., Marais, E. A., and Sunderland, E. M.: A new mechanism for atmospheric mercury redox chemistry: implications for the global mercury budget, Atmos. Chem. Phys., 17, 6353-6371, 10.5194/acp-17-6353-2017, 2017.

Dibble, T. S., Zelie, M. J., and Mao, H.: Thermodynamics of reactions of ClHg and BrHg radicals with atmospherically abundant free radicals, Atmos. Chem. Phys., 12, 10271-10279, 10.5194/acp-12-10271-2012, 2012.

Holmes, C. D., Jacob, D. J., and Yang, X.: Global lifetime of elemental mercury against oxidation by atomic bromine in the free troposphere, Geophysical Research Letters, 33, 10.1029/2006gl027176, 2006.

Hynes, A. J., Donohoue, D. L., Goodsite, M. E., and Hedgecock, I. M.: Our current understanding of major chemical and physical processes affecting mercury dynamics in the atmosphere and at the air-water/terrestrial interfaces, in: Mercury Fate and Transport in the Global Atmosphere: Emissions, Measurements and Models, edited by: Mason, R., and Pirrone, N., Springer US, Boston, MA, 427-457, 2009.

Holmes, C. D., Jacob, D. J., Corbitt, E. S., Mao, J., Yang, X., Talbot, R., and Slemr, F.: Global atmospheric model for mercury including oxidation by bromine atoms, Atmos. Chem. Phys., 10, 12037-12057, 10.5194/acp-10-12037-2010, 2010.

Jiao, Y., and Dibble, T. S.: First kinetic study of the atmospherically important reactions BrHg˙ + NO2 and BrHg˙ + HOO, Physical Chemistry Chemical Physics, 19, 1826-1838, 10.1039/C6CP06276H, 2017a.

Jiao, Y., and Dibble, T. S.: Structures, Vibrational Frequencies, and Bond Energies of the BrHgOX and BrHgXO Species Formed in Atmospheric Mercury Depletion Events, The Journal of Physical Chemistry A, 121, 7976-7985, 10.1021/acs.jpca.7b06829, 2017b.

L53 Some recent work by Gustin and her co-workers seem to be making progress on this front, see for example, Development of an Understanding of Reactive Mercury in Ambient Air: A Review MS Gustin, SM Dunham-Cheatham, J Huang, S Lindberg, SN Lyman, Atmosphere 12 (1), 73.

We thank the referee for sharing this reference. We have included a reference to this work to inform the reader that progress in this area is being made.

Line 69-71 "The exact chemical formulas for GOM and PHg are currently unknown so both species are operationally defined by their detection methods (Landis et al., 2002; Angot et al., 2016), although the development of improved analytical systems for their detection is currently underway (Gustin et al., 2021)."

Gustin, M. S., Dunham-Cheatham, S. M., Huang, J., Lindberg, S., and Lyman, S. N.: Development of an Understanding of Reactive Mercury in Ambient Air: A Review, Atmosphere, 12, 73, 2021.

L55 The sentence beginning Recently would be better at the end of the paragraph, where it is it interrupts the flow

The authors have agreed to the referee's suggestion and moved this sentence to the end of the paragraph.

L63 … thus posing a threat to … ?

The authors agree with the referee's suggested change and have amended the text accordingly.

L154 Here is a point where a little more description of local boundary layer dynamics would help the reader.

We have added a short statistical description of the modeled mixed layer depth from HYSPLIT during each campaign in the Methods and Materials sections to help the reader.

Lines 182-185: "For the 2019 campaign, the mixed layer varied from 25 to 554 m, with a median ± median absolute deviation (m.a.d.) of 74 ± 131 m, and a bimodal diurnal profile with minima at night and peaks at 5:00 and 15:00 of ~80 and ~85 m. For the 2020 campaign, the mixed layer varied from 25 to 204 m, with a median ± median absolute deviation (m.a.d.) of 34 ± 21 m, and a bimodal diurnal profile with minima at night and peaks at 13:00 and 18:00 of ~40 and ~50 m."

L163 to be honest I haven't checked all the references, but Greene 2020 is definitely missing.

The Greene, 2020 reference refers to

'Arctic Sea Ice: https://www.mathworks.com/matlabcentral/fileexchange/56923-arctic-sea-ice), access: 2020-01-26, 2020.'

Which was listed after Greene, 2017 in the bibliography. This is a webpage reference, so EndNote formatted it as such but without the author, year in the bibliography. This reference has been reformatted in Endnote to reflect the author and year, it is now properly referenced on Line 695.

Greene, C. A.: Arctic Sea ice: https://www.mathworks.com/matlabcentral/fileexchange/56923-arctic-sea-ice), access: 2020-01-26, 2020.

L168 In this section would it be possible to have a small summary table with the parameters listed simply as High or Low, when compared to the averages?

We have added two tables to the SI, Table S1 and S2 which lists the median and median absolute deviation of ground-level parameters and air mass history, respectively, for each event as well as event and non-event periods for each campaign.

L232 The reference list is rather scarce again.

We amended the text to include additional references.

Lines 432-436: "Interestingly, none of the events were linked to cold temperatures, which has been previously demonstrated to be associated with mercury oxidation through observations in the Arctic (Cole and Steffen, 2010; Ariya et al., 2015; Steffen et al., 2015), theoretical studies (Shepler et al., 2007), and modeling (Toyota et al., 2014). The stability of the Hg-Br intermediate is highly temperature-dependent (Goodsite et al., 2004; Donohoue et al., 2006; Dibble et al., 2012; Goodsite et al., 2012)."

Cole, A. S., and Steffen, A.: Trends in long-term gaseous mercury observations in the Arctic and effects of temperature and other atmospheric conditions, Atmos. Chem. Phys., 10, 4661-4672, 10.5194/acp-10-4661-2010, 2010.

Shepler, B. C., Balabanov, N. B., and Peterson, K. A.: Hg+Br→HgBr recombination and collision-induced dissociation dynamics, The Journal of Chemical Physics, 127, 164304, 10.1063/1.2777142, 2007.

Toyota, K., Dastoor, A. P., and Ryzhkov, A.: Air–snowpack exchange of bromine, ozone and mercury in the springtime Arctic simulated by the 1-D model PHANTAS – Part 2: Mercury and its speciation, Atmos. Chem. Phys., 14, 4135-4167, 10.5194/acp-14-4135-2014, 2014.

Donohoue, D. L., Bauer, D., Cossairt, B., and Hynes, A. J.: Temperature and Pressure Dependent Rate Coefficients for the Reaction of Hg with Br and the Reaction of Br with Br: A Pulsed Laser Photolysis-Pulsed Laser Induced Fluorescence Study, The Journal of Physical Chemistry A, 110, 6623-6632, 10.1021/jp054688j, 2006.

Dibble, T. S., Zelie, M. J., and Mao, H.: Thermodynamics of reactions of ClHg and BrHg radicals with atmospherically abundant free radicals, Atmos. Chem. Phys., 12, 10271-10279, 10.5194/acp-12-10271-2012, 2012.

L263-4 Are there not any more recent studies which support or further clarify the results from these studies?

We have updated the text to include more recent references about the link between cold temperatures and mercury oxidation.

Lines 432-442: "Interestingly, none of the events were linked to cold temperatures, which has been previously demonstrated to be associated with mercury oxidation through observations in the Arctic (Cole and Steffen, 2010; Ariya et al., 2015; Steffen et al., 2015), theoretical studies (Shepler et al., 2007), and modeling (Toyota et al., 2014). The stability of the Hg-Br intermediate is highly temperature-dependent (Goodsite et al., 2004; Donohoue et al., 2006; Dibble et al., 2012; Goodsite et al., 2012). Lower temperatures aid in the formation of GOM from HgBr, for example, Skov et al. (2004) and Christensen et al. (2004) modeled a surface temperature below -4 °C for mercury depletion to occur in the Arctic, while Brooks et al. (2011) observed a

temperature threshold of -15 °C for mercury oxidation to occur at Summit Station, atop the Greenlandic ice sheet. It should be noted that Brooks et al. (2011) detected oxidized mercury at temperatures above this threshold but not above 0 °C. Tarasick and Bottenheim (2002) analyzed ozonesonde records and observed surface temperatures below -20 °C were required for the occurrence of ozone depletion events. Furthermore, Halfacre et al. (2019) and Burd et al. (2017) demonstrated that a frozen heterogeneous surface is required for the propagation of halogen explosion events."

Cole, A. S., and Steffen, A.: Trends in long-term gaseous mercury observations in the Arctic and effects of temperature and other atmospheric conditions, Atmos. Chem. Phys., 10, 4661-4672, 10.5194/acp-10-4661-2010, 2010.

Shepler, B. C., Balabanov, N. B., and Peterson, K. A.: Hg+Br→HgBr recombination and collision-induced dissociation dynamics, The Journal of Chemical Physics, 127, 164304, 10.1063/1.2777142, 2007.

Toyota, K., Dastoor, A. P., and Ryzhkov, A.: Air–snowpack exchange of bromine, ozone and mercury in the springtime Arctic simulated by the 1-D model PHANTAS – Part 2: Mercury and its speciation, Atmos. Chem. Phys., 14, 4135-4167, 10.5194/acp-14-4135-2014, 2014.

Tarasick, D. W., and Bottenheim, J. W.: Surface ozone depletion episodes in the Arctic and Antarctic from historical ozonesonde records, Atmos. Chem. Phys., 2, 197-205, 10.5194/acp-2-197-2002, 2002.

Halfacre, J. W., Shepson, P. B., and Pratt, K. A.: pH-dependent production of molecular chlorine, bromine, and iodine from frozen saline surfaces, Atmos. Chem. Phys., 19, 4917-4931, 10.5194/acp-19-4917-2019, 2019.

Burd, J. A., Peterson, P. K., Nghiem, S. V., Perovich, D. K., and Simpson, W. R.: Snowmelt onset hinders bromine monoxide heterogeneous recycling in the Arctic, Journal of Geophysical Research: Atmospheres, 122, 8297-8309, 10.1002/2017jd026906, 2017.

L284 mixed layer height which is how high exactly and how does it vary over time, see introductory remarks

The mixed layer height is a modeled parameter that is included in the output of the HYSPLIT model along each step of the trajectory. The percentages above the mixed layer height were calculated by summing the number of hourly steps in which the modeled altitude of the trajectory was above the modeled mixed layer height and dividing by the total number of hourly steps during the event periods. We have included a statistical description of the boundary in the Methods section as described above.

L291 the characteristics of the trajectories for 2019 and 2020 seem very comparable, give or take a few hours, I would have emphasised this point, I think.

> We thank the referee for highlighting this point. One area of concern from other referees was the trajectory length was too short, we have recalculated the trajectory length from 120 to 240 hours to capture the lifetime of aerosols and to obtain a synoptic view of the air mass history. Calculating these statistics for 240 hours produced less clear results, and our analysis of individual events yielded unique features that were not revealed by grouping all event periods. Therefore, we have removed this paragraph from the discussion.

L312 Could the authors add a reference to Section 3.5 and or just include a short explanation of why fires might be important, otherwise the reader is at a bit of a loss as to why they are mentioned here.

> We have indicated in the text why we have included active fires in our analysis of air mass history.
>
> Lines 329-331: "Biomass burning (one of the possible causes of active fires) can emit aerosols covering a large size range and varying chemical composition (Reid et al., 2005), therefore active fires were included to analyze their effect on the air mass history during event periods."
>
> Reid, J. S., Koppmann, R., Eck, T. F., and Eleuterio, D. P.: A review of biomass burning emissions part II: intensive physical properties of biomass burning particles, Atmos. Chem. Phys., 5, 799-825, 10.5194/acp-5-799-2005, 2005.

L325 troposphere, all of it or just the free troposphere?

> We have amended the text on Lines 480-481 and throughout the manuscript to specify the region of the atmosphere we are referring to.
>
> Lines 480-481: "Previous studies have demonstrated the influence of the free troposphere on mercury concentrations within the boundary layer."

L330 This article might be useful in the discussion of free tropospheric Hg dynamics/reactions Weiss-Penzias, P., Amos, H. M., Selin, N. E., Gustin, M. S., Jaffe, D. A., Obrist, D., Sheu, G.-R., and Giang, A.: Use of a global model to understand speciated atmospheric mercury observations at five high-elevation sites, Atmos. Chem. Phys., 15, 1161–1173, https://doi.org/10.5194/acp-15-1161-2015, 2015.

> We greatly appreciate the referee's suggested article. This has provided valuable discussion for our results.

L355 and 358 both parentheses refer to median O3 from August 2010-2018 but the numbers are different, should one be July?

> This is a good catch. The month on Line 369 of the previous manuscript was incorrectly stated. It now correctly reads "July" on Line 376. We have also included another year of ozone observations into this average, which was not available at the time of submission.

L380 Good point, it is unlikely that small decreases in O3 would be noticed in the FT. But as we seem to be lacking oxidants

(Photochemistry of oxidized Hg(I) and Hg(II) species suggests missing mercury oxidation in the troposphere, Alfonso Saiz-Lopez, Oleg Travnikov, Jeroen E. Sonke, Colin P. Thackray, Daniel J. Jacob, Javier Carmona-García, Antonio Francés-Monerris, Daniel Roca-Sanjuán, A. Ulises Acuña, Juan Z. Dávalos, Carlos A. Cuevas, Martin Jiskra, Feiyue Wang, Johannes Bieser, John M. C. Plane, Joseph S. Francisco, Proceedings of the National Academy of Sciences Dec 2020, 117 (49) 30949-30956; DOI: 10.1073/pnas.1922486117)

Can we really ignore the possibility of O3/OH being an Hg oxidant, maybe through heterogeneous reactions? Just a thought.

> We thank the referee for bringing this to our attention and have incorporated this paper into the discussion.
>
> Lines 448-455: "While ozone mixing ratios were high during GOM enhancement events, they are an order of magnitude below levels reported in the upper troposphere/lower stratosphere (Talbot et al., 2007), and given the slow rate reaction coefficient (Pal and Ariya, 2004), ozone is an improbable first oxidant of mercury during these campaigns (Calvert and Lindberg, 2005), although ozone has recently been identified as a second oxidant of HgI (Saiz-Lopez et al., 2020). While ozone might be acting as a second oxidant of HgI, any depletions of ozone during GEM oxidation, either through reaction with the HgI intermediate or with halogen species, is likely masked by the elevated levels of ozone in the free troposphere. Therefore, the high ground-level temperatures, the increased ozone mixing ratios, and the positive correlations observed between ozone and GOM during all events cast doubt on the local in situ production of GOM in the boundary layer."
>
> Saiz-Lopez, A., Travnikov, O., Sonke, J. E., Thackray, C. P., Jacob, D. J., Carmona-García, J., Francés-Monerris, A., Roca-Sanjuán, D., Acuña, A. U., Dávalos, J. Z., Cuevas, C. A., Jiskra, M., Wang, F., Bieser, J., Plane, J. M. C., and Francisco, J. S.: Photochemistry of oxidized Hg(I) and Hg(II) species suggests missing mercury oxidation in the troposphere, Proceedings of the National Academy of Sciences, 117, 30949-30956, 10.1073/pnas.1922486117, 2020.

Calvert, J. G., and Lindberg, S. E.: Mechanisms of mercury removal by O3 and OH in the atmosphere, Atmospheric Environment, 39, 3355-3367, https://doi.org/10.1016/j.atmosenv.2005.01.055, 2005.

L390 common source as in emission source? Or do you mean source region or regions?

> We acknowledge that the wording could create confusion. The intended meaning was to illustrate a common formation source (both GOM and ozone being formed in the free troposphere) and a common source region (the free troposphere). While we cannot distinguish whether these species were formed in the free troposphere, they were both transported from the free troposphere. During our reorganization of the text, this sentence was however removed.

L405 surface level, is this literally ground level or within the boundary layer?

> Schulz et al. (2019) used aircraft campaigns to measure the vertical distribution of BC, they divided the vertical profiles into different levels based on potential temperature. The BC concentration was lowest in the lowermost level and compared well with measurements made over the Arctic Ocean. While these observations were not made at the surface, it is unclear if the lowermost level was within the boundary layer. Therefore, we have used their terminology of the surface level to represent their lowermost observations of BC.

L411 sources or source regions?

> Similar to the comment above, we acknowledge this wording can create confusion. We intended to show the different sources regions of aerosol particles and BC (the free troposphere) as well as a common source of GOM, aerosol particles, and BC (biomass burning). During our reorganization of the text, this sentence was however removed.

Section 3.6

In this discussion of possible halogen sources it would be useful to understand the dynamics of the mixing between the boundary layer and the free troposphere. The authors mention a number of surface sources and suggest that these are unlikely to play a role given that Hg oxidation seems to be occurring in the free troposphere L487.

However it is then postulated that biogenic halogen compound emissions and cycling on coarse mode aerosols are a potentially widespread source in the Arctic.

I would have thought that the coarse mode aerosol was less likely to reach the free troposphere than gaseous halogen containing compounds.

Some clarification of the reasoning behind the last two paragraphs of this section is required

We have opted to remove this section from the revised manuscript, although we have tried to explain our reasoning for this mechanism below:

While coarse mode aerosols are less likely to reach the free troposphere than gaseous compounds, the stability stratified atmosphere and reduced moisture in the Arctic inhibits its removal via gravitational setting and removal, respectively, compared to the mid-latitudes. The Arctic boundary layer is also different from mid-latitudes, where thermal convection drives the boundary layer structure. In the Arctic, heat fluxes from open leads, polynya, and wind shear cause convective mixing surface to free troposphere. Coarse mode sea salt can be emitted from these open leads and polynya as well as from sublimation of blowing snow at higher wind speeds. These aerosols are then transported via the free troposphere and subsided into the boundary layer through entrainment and frontal passages.

We realize this hypothesis, while based on literature, is highly speculative. We, therefore, removed this section to make the interpretation of the results more concise.

AMAP: AMAP Assessment 2011: Mercury in the Arctic, Arctic Monitoring and Assessment Programme (AMAP), Oslo, Norway, xiv + 193 pp., 2011.

Angot, H., Dastoor, A., De Simone, F., Gårdfeldt, K., Gencarelli, C. N., Hedgecock, I. M., Langer, S., Magand, O., Mastromonaco, M. N., Nordstrøm, C., Pfaffhuber, K. A., Pirrone, N., Ryjkov, A., Selin, N. E., Skov, H., Song, S., Sprovieri, F., Steffen, A., Toyota, K., Travnikov, O., Yang, X., and Dommergue, A.: Chemical cycling and deposition of atmospheric mercury in polar regions: review of recent measurements and comparison with models, Atmos Chem Phys, 16, 10735-10763, 10.5194/acp-16-10735-2016, 2016.

Ariya, P. A., Amyot, M., Dastoor, A., Deeds, D., Feinberg, A., Kos, G., Poulain, A., Ryjkov, A., Semeniuk, K., Subir, M., and Toyota, K.: Mercury physicochemical and biogeochemical transformation in the atmosphere and at atmospheric interfaces: a review and future directions, Chem Rev, 115, 3760-3802, 10.1021/cr500667e, 2015.

Brooks, S., Moore, C., Lew, D., Lefer, B., Huey, G., and Tanner, D.: Temperature and sunlight controls of mercury oxidation and deposition atop the Greenland ice sheet, Atmos Chem Phys, 11, 8295-8306, 10.5194/acp-11-8295-2011, 2011.

Burd, J. A., Peterson, P. K., Nghiem, S. V., Perovich, D. K., and Simpson, W. R.: Snowmelt onset hinders bromine monoxide heterogeneous recycling in the Arctic, Journal of Geophysical Research: Atmospheres, 122, 8297-8309, 10.1002/2017jd026906, 2017.

Christensen, J. H., Brandt, J., Frohn, L. M., and Skov, H.: Modelling of Mercury in the Arctic with the Danish Eulerian Hemispheric Model, Atmos. Chem. Phys., 4, 2251-2257, 10.5194/acp-4-2251-2004, 2004.

Cole, A. S., and Steffen, A.: Trends in long-term gaseous mercury observations in the Arctic and effects of temperature and other atmospheric conditions, Atmos. Chem. Phys., 10, 4661-4672, 10.5194/acp-10-4661-2010, 2010.

Dibble, T. S., Zelie, M. J., and Mao, H.: Thermodynamics of reactions of ClHg and BrHg radicals with atmospherically abundant free radicals, Atmos. Chem. Phys., 12, 10271-10279, 10.5194/acp-12-10271-2012, 2012.

Donohoue, D. L., Bauer, D., Cossairt, B., and Hynes, A. J.: Temperature and Pressure Dependent Rate Coefficients for the Reaction of Hg with Br and the Reaction of Br with Br: A Pulsed Laser Photolysis-Pulsed Laser Induced Fluorescence Study, The Journal of Physical Chemistry A, 110, 6623-6632, 10.1021/jp054688j, 2006.

Goodsite, M. E., Plane, J. M. C., and Skov, H.: A theoretical study of the oxidation of Hg-0 to HgBr2 in the troposphere, Environmental Science & Technology, 38, 1772-1776, 10.1021/es034680s, 2004.

Goodsite, M. E., Plane, J. M. C., and Skov, H.: Correction to A Theoretical Study of the Oxidation of Hg0 to HgBr2 in the Troposphere, Environmental Science & Technology, 46, 5262-5262, 10.1021/es301201c, 2012.

Halfacre, J. W., Shepson, P. B., and Pratt, K. A.: pH-dependent production of molecular chlorine, bromine, and iodine from frozen saline surfaces, Atmos. Chem. Phys., 19, 4917-4931, 10.5194/acp-19-4917-2019, 2019.

Holmes, C. D., Jacob, D. J., and Yang, X.: Global lifetime of elemental mercury against oxidation by atomic bromine in the free troposphere, Geophysical Research Letters, 33, 10.1029/2006gl027176, 2006.

Holmes, C. D., Jacob, D. J., Corbitt, E. S., Mao, J., Yang, X., Talbot, R., and Slemr, F.: Global atmospheric model for mercury including oxidation by bromine atoms, Atmos. Chem. Phys., 10, 12037-12057, 10.5194/acp-10-12037-2010, 2010.

Horowitz, H. M., Jacob, D. J., Zhang, Y., Dibble, T. S., Slemr, F., Amos, H. M., Schmidt, J. A., Corbitt, E. S., Marais, E. A., and Sunderland, E. M.: A new mechanism for atmospheric mercury redox chemistry: implications for the global mercury budget, Atmos. Chem. Phys., 17, 6353-6371, 10.5194/acp-17-6353-2017, 2017.

Hynes, A. J., Donohoue, D. L., Goodsite, M. E., and Hedgecock, I. M.: Our current understanding of major chemical and physical processes affecting mercury dynamics in the atmosphere and at the air-water/terrestrial interfaces, in: Mercury Fate and Transport in the Global Atmosphere: Emissions, Measurements and Models, edited by: Mason, R., and Pirrone, N., Springer US, Boston, MA, 427-457, 2009.

Jiao, Y., and Dibble, T. S.: First kinetic study of the atmospherically important reactions BrHg˙ + NO2 and BrHg˙ + HOO, Physical Chemistry Chemical Physics, 19, 1826-1838, 10.1039/C6CP06276H, 2017a.

Jiao, Y., and Dibble, T. S.: Structures, Vibrational Frequencies, and Bond Energies of the BrHgOX and BrHgXO Species Formed in Atmospheric Mercury Depletion Events, The Journal of Physical Chemistry A, 121, 7976-7985, 10.1021/acs.jpca.7b06829, 2017b.

Obrist, D., Tas, E., Peleg, M., Matveev, V., Faïn, X., Asaf, D., and Luria, M.: Bromine-induced oxidation of mercury in the mid-latitude atmosphere, Nature Geoscience, 4, 22-26, 10.1038/ngeo1018, 2010.

Reid, J. S., Koppmann, R., Eck, T. F., and Eleuterio, D. P.: A review of biomass burning emissions part II: intensive physical properties of biomass burning particles, Atmos. Chem. Phys., 5, 799-825, 10.5194/acp-5-799-2005, 2005.

Saiz-Lopez, A., Travnikov, O., Sonke, J. E., Thackray, C. P., Jacob, D. J., Carmona-García, J., Francés-Monerris, A., Roca-Sanjuán, D., Acuña, A. U., Dávalos, J. Z., Cuevas, C. A., Jiskra, M., Wang, F., Bieser, J., Plane, J. M. C., and Francisco, J. S.: Photochemistry of oxidized Hg(I) and Hg(II)

species suggests missing mercury oxidation in the troposphere, Proceedings of the National Academy of Sciences, 117, 30949-30956, 10.1073/pnas.1922486117, 2020.

Shepler, B. C., Balabanov, N. B., and Peterson, K. A.: Hg+Br→HgBr recombination and collision-induced dissociation dynamics, The Journal of Chemical Physics, 127, 164304, 10.1063/1.2777142, 2007.

Skov, H., Christensen, J. H., Goodsite, M. E., Heidam, N. Z., Jensen, B., Wahlin, P., and Geernaert, G.: Fate of elemental mercury in the arctic during atmospheric mercury depletion episodes and the load of atmospheric mercury to the arctic, Environmental Science & Technology, 38, 2373-2382, 10.1021/es030080h, 2004.

Steffen, A., Lehnherr, I., Cole, A., Ariya, P., Dastoor, A., Durnford, D., Kirk, J., and Pilote, M.: Atmospheric mercury in the Canadian Arctic. Part I: a review of recent field measurements, Sci Total Environ, 509-510, 3-15, 10.1016/j.scitotenv.2014.10.109, 2015.

Stephens, C. R., Shepson, P. B., Steffen, A., Bottenheim, J. W., Liao, J., Huey, L. G., Apel, E., Weinheimer, A., Hall, S. R., Cantrell, C., Sive, B. C., Knapp, D. J., Montzka, D. D., and Hornbrook, R. S.: The relative importance of chlorine and bromine radicals in the oxidation of atmospheric mercury at Barrow, Alaska, Journal of Geophysical Research: Atmospheres, 117, n/a-n/a, 10.1029/2011jd016649, 2012.

Tarasick, D. W., and Bottenheim, J. W.: Surface ozone depletion episodes in the Arctic and Antarctic from historical ozonesonde records, Atmos. Chem. Phys., 2, 197-205, 10.5194/acp-2-197-2002, 2002.

Toyota, K., Dastoor, A. P., and Ryzhkov, A.: Air–snowpack exchange of bromine, ozone and mercury in the springtime Arctic simulated by the 1-D model PHANTAS – Part 2: Mercury and its speciation, Atmos. Chem. Phys., 14, 4135-4167, 10.5194/acp-14-4135-2014, 2014.

von Glasow, R.: Atmospheric chemistry in volcanic plumes, Proceedings of the National Academy of Sciences, 107, 6594-6599, 10.1073/pnas.0913164107, 2010.

Wang, S., McNamara, S. M., Moore, C. W., Obrist, D., Steffen, A., Shepson, P. B., Staebler, R. M., Raso, A. R. W., and Pratt, K. A.: Direct detection of atmospheric atomic bromine leading to mercury and ozone depletion, Proc Natl Acad Sci U S A, 116, 14479-14484, 10.1073/pnas.1900613116, 2019.

Ye, Z., Mao, H., Lin, C. J., and Kim, S. Y.: Investigation of processes controlling summertime gaseous elemental mercury oxidation at midlatitudinal marine, coastal, and inland sites, Atmos. Chem. Phys., 16, 8461-8478, 10.5194/acp-16-8461-2016, 2016.

Dynamics of gaseous oxidized mercury at Villum Research Station during the High Arctic summer

Jakob Boyd Pernov, Bjarne Jensen, Andreas Massling, Daniel Charles Thomas, and Henrik Skov

Department of Environmental Science, iClimate, Arctic Research Center, Aarhus University, Frederiksborgvej 399, 4000 Roskilde, Denmark

Correspondence: Jakob Boyd Pernov (jbp@envs.au.dk)

Abstract. While much research has been devoted to the subject of gaseous elemental mercury (GEM) and gaseous oxidized mercury (GOM) in the Arctic spring, during atmospheric mercury depletion events, few studies have examined the behavior of GOM in the High Arctic summer. GOM, once ~~deposited and in~~troduced~~corporated~~ into the ecosystem, can pose a threat to human and wildlife health, though there remain large uncertainties regarding the transformation, deposition, and assimilation of mercury into the ~~ecosystem~~ food web. Therefore, to further our understanding of the dynamics of ~~gaseous oxidized mercury~~GOM in the High Arctic during the late summer, we performed measurements of GEM and GOM along with meteorological parameters, atmospheric constituents, and utilized modeled air mass history during two summer campaigns in 2019 and 2020 at Villum Research Station (Villum) in Northeastern Greenland. ~~Five~~ Seven events of enhanced GOM concentrations were identified and investigated in greater detail. In general, ~~The origin of these events was identified, through analysis of air mass back-trajectories, associated meteorological data, and other atmospheric constituents, to be the cold, dry free troposphere. These events were associated with low RH, limited precipitation, cold temperatures, and intense sunlight along the trajectory path.~~

~~The factors~~the common factors associated with ~~influencing~~ event periods at ground level ~~are~~were higher levels of radiation, lower H_2O mixing ratios, accumulated precipitation, and RH, although none were ~~linked~~connected ~~to~~with cold temperatures.

~~For the non-event periods in 2019, radiation and temperature were lower while H_2O mixing ratios, accumulated precipitation, and the RH were higher. For the 2020 campaign, n~~Non-event periods at ground level ~~were more diverse although~~ each displayed a ~~dissimilar~~different pattern, in one or more parameters, when compared to event periods. ~~-~~

~~In general,~~Generally, air masses during event periods for both campaigns were colder, drier, arrived from higher altitudes, spent more time above the mixed layer, and less time in a cloud ~~(Table S2)~~ compared to non-events, ~~a.~~ Although some events deviated from this general pattern. Non-event air masses displayed a different pattern in one or more parameters when compared to event periods although were generally warmer, wetter, arrived from lower altitudes with little radiation. Coarse mode aerosols were hypothesized to provide the heterogenous surface for halogen propagation during some of the events while

for others the source is unknown. While these general patterns were observed for event and non-event periods, analysis of individual events showed more specific origins.

Five of the seven events were associated with air masses that experienced similar conditions: transported from the cold, dry, sunlit free troposphere. However, two events experienced contrasting conditions, with air masses being warm and wet with surface layer contact under little radiation. , there are notable exceptions to this pattern

For example, during all non-event periods, air mass arrived from altitudes comparable to event periods although often experienced decreased radiation and high RH and H$_2$O mixing ratios,

The overall pattern of the air mass history for event periods appears to be cold, dry air masses arriving from above the mixed layer, higher altitudes, and having spent little time in a cloud.

Non-event periods were associated with….

Events were positively correlated with ozone, aerosol particle number, and black carbon mass concentration, which were interpreted as an indication of tropospheric air masses. Event 3 exhibited the highest levels of GOM observed during both campaigns, although at ground-level radiation, RH, and temperature displayed a contrasting pattern, relative to other events. While this event experienced air masses from aloft, they were warm and wet with little radiation, however, cold, dry, and sunlit conditions were present shortly before arrival followed by a quick descent into the surface layer. These conditions could favor GOM formation, and inhibit its removal. Event 4 experienced opposite conditions for RH, temperature, and radiation compared to Event 3 but similar conditions during transport although at later times during transport. Similar to Event 3, GOM formed during Event 4 appears to have formed in the cold, dry, sunlit free troposphere, although other processes cannot be ruled out, as such a specific origin of these events cannot be identified.

Event 5a….

Event 5b….

Event 5a displayed warm and wet air masses which arrived from low altitudes under little radiation, and the GOM observed during this event appears to be the result of emissions either from active fires or anthropogenic source in Northern Scandinavia. The origins of GOM during Event 5b appear to be the result of formation in the cold, dry, sunlit free troposphere over the Greenlandic ice sheet from an unknown source of halogens.

Two episodes of extremely high levels of N$_{Coarse}$ and BC, which appear to originate from flaring emissions in Russia, did not contribute to enhanced GOM levels.

This work aims to provide a better understanding of the dynamics of GOM during the High Arctic summer.

1 Introduction

65 Gaseous elemental mercury (Hg^0 or GEM) is a ubiquitous pollutant in the atmosphere due to its long relaxation time (6 to 12 months; relaxation time refers to the time delay between emission reductions and effect on ambient concentrations), thus being subject to long-range transport from source regions to remote environments through deposition and reemission cycling (Pirrone et al., 2010; Skov et al., 2020). The sources of mercury include anthropogenic emissions, e.g., fossil fuel /biomass combustion, and small artisanal small-scale gold mines, in addition to natural emissions such as volcanoes, biomass burning, ocean/ and

70 soil evasion, and reemission of previously deposited/legacy mercury (AMAP, 2011). In the atmosphere, GEM is oxidized to its divalent form (Hg^{II}), commonly known as gaseous oxidized mercury (GOM). GOM has a much shorter residence time than GEM in the atmosphere owing to its higher solubility, lower vapor pressure, and faster deposition velocity (Skov et al., 2006). Mercury can also be present in aerosol particles, referred to as particulate bound mercury (PHg), either through GOM condensation or through heterogeneous reactions of GEM on aerosol surfaces (Durnford and Dastoor, 2011). In the polar

75 regions, GEM typically dominates the atmospheric distribution throughout the year, with smaller contributions from GOM and PHg. However, during depletion events in the spring, GOM and PHg can constitute large fractions of total gaseous atmospheric mercury (Steffen et al., 2014). In contrast to the polar regions, in the mid-latitudes, and especially in locations close to anthropogenic emission point sources, GOM and PHg can be emitted directly to the atmosphere and represent larger significant fractions of the atmospheric mercury burden (Muntean et al., 2018).

80   In locations with elevated reactive halogen concentrations (e.g., polar environments, the coastal regionsmarine boundary layer, volcanic plumes, and salt lakes) and especially bromine radicals, GEM is quickly transformed into GOM (Obrist et al., 2010; von Glasow, 2010; Angot et al., 2016; Ye et al., 2016; Wang et al., 2019). In the Arctic, this process manifests as atmospheric mercury depletion events (AMDEs), which occur in spring following polar sunrise, and result in the rapid depletion (on the order of hours) of GEM and conversion to GOM (Schroeder et al., 1998; Lindberg et al., 2002; Berg et

85 al., 2003; Skov et al., 2004). In the early spring at Alert, Nunavut, Canada, it has been demonstrated that this GOM is converted to PHg (through condensational processes due to the cold temperatures and high aerosol surface area concentration (Freud et al., 2017)) while in the late spring oxidized mercury is mainly present as GOM (due to reduced surface area and increased temperatures) (Steffen et al., 2014). Late spring is also the peak of total Hg in surface snow at Alert, Nunavut, Canada and Utqiagvik, Alaska, USA (formerly Barrow), indicating that dry deposition of GOM is thea majorinajor deposition pathway of

90 mercury into the ecosystem (Lu et al., 2001; Lindberg et al., 2002; Steffen et al., 2002; Steffen et al., 2014). GEM oxidization has been demonstrated to be initiated via photochemical reactions with the Br radical (R1-R2) through modeling studies (Holmes et al., 2006; Holmes et al., 2010; Horowitz et al., 2017), kinetic studies (Donohoue et al., 2006), theoretical studies (Goodsite et al., 2004; Dibble et al., 2012; Goodsite et al., 2012), and observations (Skov et al., 2004; Stephens et al., 2012; Wang et al., 2019).

$$Br + Hg^0 \leftrightarrow HgBr \tag{R1}$$

$$HgBr + Y \rightarrow HgBrY \qquad (R2)$$

Where Y could be OH, O_3, NO_2, ~~NO,~~ HO_2, Br, Cl, BrO, ClO, I, IO (Holmes et al., 2006; Hynes et al., 2009; Holmes et al., 2010; Dibble et al., 2012; Jiao and Dibble, 2017a, b)~~,~~ ~~of~~ Of which Br, I, and OH have been postulated to be the main species for Y, both globally and in the Arctic (Goodsite et al., 2004, 2012), while NO_2, HO_2, ClO, or BrO have been demonstrated to be candidates for Y by Dibble et al. (2012). Recently, ozone was proposed to be a missing oxidation pathway of HgBr (Saiz-Lopez et al., 2020). Sources of these reactive halogen species include emissions from sea ice, snowpack, frost flowers, refreezing leads, sea-salt aerosol, and ~~liable~~ labile halogen reservoir species (i.e., halocarbons and inorganic bromine) (Brooks et al., 2006; Kaleschke et al., 2004; Peterson et al., 2018, 2019; Simpson et al., 2015). The exact chemical formulas for GOM and PHg are currently unknown so both species are operationally defined by their detection methods (Landis et al., 2002; Angot et al., 2016), although the development of improved analytical systems for their detection is currently underway (Gustin et al., 2021). Once formed, GOM can either bind to aerosol particles, becoming PHg, or deposit onto the snowpack through dry and wet deposition. ~~Recently, isotope analysis has revealed GEM uptake by vegetation and soils to be the main source of mercury input to the terrestrial environment in Alaska (Obrist et al., 2010; Douglas and Blum, 2019; Jiskra et al., 2019), although this process has yet to be confirmed in the High Arctic.~~ The majority of this deposited mercury is photo-reduced and emitted back into the atmosphere (Brooks et al., 2006; Dastoor et al., 2008; Kamp et al., 2018). The snowpack will retain a fraction of this mercury and release it with the ionic pulse during the melt season, introducing mercury into the ecosystem (Lu et al., 2001; Ariya et al., 2004; Durnford and Dastoor, 2011; Douglas et al., 2017). Recently, isotope analysis has revealed GEM uptake by vegetation and soils to be the main source of mercury input to the terrestrial environment in Alaska (Douglas and Blum, 2019; Jiskra et al., 2019), although this process has yet to be confirmed in the High Arctic.

After deposition ~~onto the Earth's surface~~, ~~GEM,~~ GOM~~, and PHg~~ can be methylated through biotic and abiotic processes to organic mercury (methyl- and dimethylmercury) (Macdonald and Loseto, 2010; Møller et al., 2011). Organic mercury is an extremely powerful neurotoxin that bio-accumulates in upper trophic levels thus posing ~~harmful effects~~a threat to ecosystems and human health (especially in indigenous peoples in high latitudes and societies that rely heavily on a seafood diet) (Park and Zheng, 2012). Therefore, as the Arctic becomes more populated and continues to change it is ~~pertinent~~ important to understand mercury oxidation in response to a changing climate, especially in high latitude regions (AMAP, 2011; Durnford and Dastoor, 2011; Stern et al., 2012).

While the majority of GOM formation and deposition occurs in the Arctic during spring, little attention has been given to the behavior of GOM outside of AMDEs. Steen et al. (2011) reported high amounts of GOM (max > 120 pg m^{-3}, mean 8 ± 13 pg m^{-3}) during the summers of 2007 and 2008 at Zeppelin Mountain (79.93° N 11.50° E, 474 m above sea level). This study revealed a pattern of GOM previously unknown to the Arctic, with elevated GOM concentrations during the summer, which postulates GOM deposition occurs ~~also~~ outside of AMDEs in the Arctic. They concluded the presence of GOM was of ~~local/~~regional origin, as long-range transport of direct emissions from anthropogenic sources ~~were~~ was unlikely. Other studies have found contrasting results regarding Arctic GOM concentrations during summer. During a research expedition in

the Arctic Ocean in June–August 2004, Aspmo et al. (2006) measured GEM, GOM, and PHg, and found increases in GEM over areas with > 70 % sea ice concentrations, which were attributed to an enhanced reduction potential and increased evasion of supersaturated dissolved mercury from the ocean through open leads. However, Tthey also found lower levels of GOM (< 20 pg m^{-3}) and PHg (< 10 pg m^{-3}) compared to Steen et al. (2011). Levels of Hg in snow and melt ponds were low (< 10 ng L^{-1}) suggesting little marginal accumulation of deposited mercury throughout the summer of deposited mercury from AMDEs in the spring. Concentrations of GEM, GOM, PHg, CO, and ozone were also reported on a research cruise throughout the Arctic basin from July–September 2005 (Sommar et al., 2010). They found low levels of GOM (3.2 ± 1.7 pg m^{-3}) and PHg (1.0 ± 0.7 pg m^{-3}), which were not correlated with GEM, sunlight, nor ozone. Steffen et al. (2014) analyzed GOM and PHg at Alert, Nunavut, CanadaCA from 2002–2011, they reported low median values during July–September of 5.3–7.36 pg m^{-3} and 1.01–14.78 pg m^{-3} for PHg and GOM, respectively. The source of GOM during this study was unclear. These studies show that mercury oxidation and deposition can occur outside of the springtime AMDEs, therefore warranting further study. While these latter studies found relatively low levels of GOM, the presence of GOM at all indicates that mercury oxidation and deposition are occurring outside of AMDEs in the Arctic.

With only limited measurements of GOM performed in the High Arctic summertime, there are many questions still unanswered. The dynamics of GOM in the Arctic are extremely complex; uncertainties in its spatiotemporal variability, annual cycle, and formation mechanisms emphasize the need for further examination. The variability of GOM reported during the Arctic summer (Aspmo et al., 2006; Sommar et al., 2010) as well as the previously unknown yearly cycle and lack of formation mechanism (Steen et al., 2011; Steffen et al., 2014) emphasize the need for further examination of the dynamics of GOM in the High Arctic summer. The Arctic region is undergoing rapid changes due to anthropogenic climate change and the dynamics of mercury oxidation are poorly resolved, especially in summer. Understanding these dynamics can offer insight into the general chemistry during Arctic summer and atmospheric mercury will respond to future changes in the Arctic climate.Resolving the sources and dynamics of mercury species in the High Arctic summer will help to infer the response of mercury in the context of a changing climate. It is also important to understand the changes in mercury concentrations in the Arctic to assess the effects of abatement strategies of the Minamata Convention It is also important to understand the dynamics of mercury to assess the effects of abatement strategies on atmospheric concentrations in the framework of the Minamata Convention (UNEP, 2013) .globally. This will aid in understanding what will be the effects of decreasing anthropogenic mercury emissions and global climate change on the recycling of mercury between different environmental matrixes and how it is ultimately sequestered.

Here we report measurements of GEM and GOM, outside of AMDEs, during the late summer of 2019 and GEM and GOM as well as PHg in the late summer of 2020 at Villum Research Station (Villum). We investigate the levels of GOM in connection with meteorological parameters, ozone, aerosol particle physical properties, and air mass history and examine existing interconnections and dependencies. In the following section, we describe the measurement site, analytical instrumentation, and analysis methods. We will then examine the behavior of GOMresults of the two campaigns in relation to meteorological parameters and atmospheric constituents as well as air mass history. We then discuss the factors influencing

165 event vs. non-event periods as well as individual events. ~~We compare our measurements to previous studies of GOM from the mid-latitudes and hypothesize on possible halogen sources.~~ We conclude with a summary and consider the implications for mercury oxidation in a future climate.

2 Methods and instrumentation

2.1 Measurement sites

170 Measurements were performed at Flyger's hut (N 81° 36′, W 16° 40′), which is part of Villum (81.6° N 16.67° W, 24 m above sea level) located on the Danish military base Station Nord in Northeastern Greenland. Villum and Flyger's hut are both located approx. 2 kilometers to the south of Station Nord, they are separated by approx. 200 meters' distance and they are both upwind > 95% of the time from local pollution sources at the military base. All times are reported as UTC.

2.2 Atmospheric mercury measurements

175 In 2019, atmospheric measurements of GEM and GOM at Flyger's hut started on August 16 and ended on September 1. In 2020, measurements of GEM, GOM, and PHg started on July 17 and ended on August 4. GEM was analyzed on a 5-minute time resolution by a Tekran 2537A vapor phase analyzer at a flow rate of 1 L min^{-1}. This technique is based on the pre-concentration of GEM on dual gold cartridges followed by thermal desorption in a stream of argon gas and detection by cold vapor atomic fluorescence spectroscopy (CVAFS) at a wavelength of 253.7 nm. Skov et al. (2004) determined a detection

180 limit of 0.1 ng m^{-3} and a reproducibility of 20 %, at a 95% confidence interval (CI) and above 0.5 ng m^{-3}. The instrument was manually calibrated with injections of a known amount of mercury before and after the campaigns and auto-calibrated in the field every 25th hour by an internal permeation source.

GOM and PHg were collected using a Tekran 1130 and 1135 speciation unit, respectively, upstream of the GEM analyzer, at a flow rate of 10 L min^{-1}. GOM was sampled onto potassium chloride (KCl) coated denuders. After sample

185 collection, the denuders were flushed in a stream of zero air supplied from the 1130 pump module, then heated to 500°C during which GOM was thermally decomposed to GEM and detected by the Tekran 2537A analyzer. Denuders were exchanged weekly. PHg was sampled onto quartz filters, thermally released in a stream of zero air at 800 °C, and pyrolyzed on quartz chips also at 800 °C (for details about denuder and quartz filter performance and coating procedure, see Landis et al. (2002)). The cutoff size for PHg was < 2.5 μm. For the 2019 campaign, the sampling time was 80 minutes, while for the 2020 campaign

190 the sampling time was 60 minutes. Due to technical issues during the 2019 campaign, measurements of PHg were not available. The limit of detection (LOD) for both GOM and PHg was calculated as three times the standard deviation (s.d.) of blanks values for the flush cycles, excluding the first measurement in a flush cycle as the heated sampling line still contains ambient air. The LODs for the 2019 and 2020 campaigns were 0.180 and 0.684 pg m^{-3}, respectively. With the KCl denuders being prone to unequal collection efficiencies for different GOM species and artifacts (Gustin et al., 2015) and the internal signal

integration routine biasing the concentrations low (Slemr et al., 2016; Ambrose, 2017), the GEM and GOM concentrations are likely a lower limit (Huang and Gustin, 2015; Huang et al., 2017; Marusczak et al., 2017).

2.3 Ancillary measurements

Meteorological parameters including wind speed, wind direction, air temperature, relative humidity, radiation, and snow depth were measured at Villum on a time resolution of 5 minutes. Ground-level H_2O mixing ratios were calculated using ambient temperature, RH, and pressure (Bolton, 1980; Weiss-Penzias et al., 2015). Ozone (O_3) was measured at Villum using a photometric O_3 analyzer (API M400) at 1 Hz, averaged to a 30-minute arithmetic means. The detection limit was 1 parts per billion by volume (ppbv), with an uncertainty of 3% for measured concentrations above 10 ppbv and 6% below, respectively, on a 95% CI (Nguyen et al., 2016). All measurements used in this study were averaged (median) to correspond temporally to GOM and PHg sampling intervals.

2.4 Particle number size distribution and black carbon

Particle number size distributions (PNSD) from 0.3 to 10 µm were measured using an optical particle sizer (OPS, TSI 3330) on a 10-minute time resolution. This size range is representative of coarse mode particles and a fraction of accumulation mode particles. The entire particle size spectrum was integrated to give the coarse mode particle number concentration (N_{Coarse}). The OPS was located at Villum and the data were vigorously quality controlled for abnormal instrument diagnostic parameters (RH, flow rate, and temperature) and the influence of local pollution (i.e., vehicles and activities from Station Nord).

Black carbon (BC) concentrations were measured using a MAGEE AE33 aethalometer (Drinovec et al., 2015) at a 1-minute time resolution. The instrument is an absorption photometer that continuously collects aerosol particles onto a filter and measures light absorption from the resulting filter spot containing the aerosol particles. The AE33 automatically corrects for filter-loading effects by measuring absorption on a reference filter and operates at seven wavelengths: λ = 370, 470, 520, 590, 660, 880, and 950 nm. By using a standard BC mass absorption cross-section (MAC) of 7.77 m^2 g^{-1} at 880 nm, these absorption coefficients are converted to equivalent black carbon (eBC) mass concentrations. It has been found that the aethalometer overestimates BC concentrations at Arctic sites compared to co-located absorption photometers (Backman et al., 2017). To account for this, an Arctic harmonization factor was used, adapted from Backman et al. (2017) to suit the newer aethalometer model. This has been widely used for Arctic datasets (Schmeisser et al., 2018; Zanatta et al., 2018; Schacht et al., 2019). Substantial uncertainties may arise from cross-sensitivity to scattering in the instrument, especially for Arctic aerosols, which are typically highly scattering. This uncertainty is estimated to be around 15% at Villum, using typical values of single scattering albedo (SSA) and previously determined uncertainty studies (Weingartner et al., 2003; Drinovec et al., 2015).

2.5 Air mass history analysis

Air mass history was interrogated by use of the HYSPLIT trajectory model (Draxler and Hess, 1998; Rolph et al., 2017). Air mass back-trajectories of ~~120~~240-hour length were calculated arriving at 50 m above ground level for every hour during the two campaigns. The trajectory starting height of 50 m was selected as a compromise between capturing air masses that are representative of our sampling site and avoiding trajectories intercepting the surface, which can produce unrepresentative trajectories (Stohl, 1998); trajectories were also initialized at 20 m, which produced similar trajectory paths but often intercepted the surface. For the 2019 campaign, the mixed layer varied from 25 to 554 m, with a median ± median absolute deviation (m.a.d.) of 74 ± 131 m, and a bimodal diurnal profile with minima at night and peaks at 5:00 and 15:00 of ~80 and ~85 m. For the 2020 campaign, the mixed layer varied from 25 to 204 m, with a median ± median absolute deviation (m.a.d.) of 34 ± 21 m, and a bimodal diurnal profile with minima at night and peaks at 13:00 and 18:00 of ~40 and ~50 m. The trajectory length of ~~120~~ 240 hours was selected to ~~produce accurate trajectories but also~~ capture the lifetime of GOM in the atmosphere and assess the geographical extent of air masses. Global Data Assimilation System (GDAS) meteorological data on a 1° spatial resolution, employing modeled vertical velocity, were used as input for the model. The HYSPLIT model output included meteorological variables along the trajectory path including relative humidity, precipitation, mixed layer height, and H_2O mixing ratio. Precipitation along each trajectory was integrated to calculate the amount of accumulated precipitation. These parameters along with ~~sea ice concentrations and~~ active fire data were utilized to inspect the geo-physical history of air masses arriving at Villum during the campaign periods (Greene et al., 2017; Greene, 2020). Active ~~Daily polar gridded sea ice concentrations for the measurement period were obtained through the Nimbus-7 SMMR and DMSP SSM/I-SSMIS Passive Microwave Data from the National Snow and Ice Data Center (NSIDC) (Cavalieri et al., 1996). F~~fire data were provided by NASA's Fire Information for Resource Management System (FIRMS), active fire data from NASA's Moderate Resolution Imaging Spectroradiometer (MODIS), and NASA's Visible Infrared Imaging Radiometer Suite (VIIRS) (Schroeder et al., 2014).

3 Results ~~& Discussion~~

3.1 Atmospheric mercury and ground-level meteorological parameters

From the two campaigns, ~~five~~ seven events of enhanced GOM concentrations were observed: ~~two~~ three during the 2019 campaign and ~~three~~ four during the 2020 campaign. These events were identified by enhancements of GOM over background levels as well as meteorological conditions and air mass classification. Results from the 2019 campaign, describing the time series of atmospheric mercury concentrations, ground-level meteorological parameters (radiation, H_2O mixing ratio, temperature, and RH), accumulated precipitation along the trajectory length, ozone ~~and atmospheric mercury concentrations~~, and aerosol properties (BC concentration and N_{Coarse}) are presented in Fig. 1. ~~Wind~~ Wind direction, wind speed, and snow depth are displayed in Fig. S1. ~~From Fig. 1,~~During the 2019 campaign, there ~~are~~ were ~~two~~ three distinct GOM enhancement events

~~during the 2019 campaign~~: Event 1a from August 20 at 17:45 to August ~~27~~ 26 at ~~0005:0~~10, Event 1b from August 26 at 9:00 to August 27 at 00:10, and Event 2 from August 29 at 20:10 to September 1 at 18:20.

During the first days of Event 1a (August 21 and 22), GEM increased slightly from ~1.6 to ~1.7 ng m^{-3}, then o. On the night of August 22, GEM suddenly dropped followed by a slow decrease until the afternoon of August 24 when it precipitously decreased, reaching a minimum of 1.1 ng m^{-3} on the morning of August 25. GEM then quickly increased back to consistent levels of ~1.5 ng m^{-3} for the remainder of the measurement campaign including Event 1b and 2. For Event 1, GOM gradually increased from zero on the afternoon of August 20 to the night of August 24, with the highest value (9.81 pg m^{-3}) on August 25. On the night of August 25 and into the morning of August 26, GOM quickly decreased from ~8 pg m^{-3} to zero, corresponding to a concurrent increase in RH and H$_2$O mixing ratio as well as a concurrent decrease in temperature. As RH then decreased for Event 1b throughout the day of August 26, GOM once again increased to levels ~~similar to~~comparable to those observed on the previous day. A back-trajectory analysis on August 26 revealed that, before arrival at Villum, air masses ~~arriving~~ traversed the Arctic Ocean, Greenland, then the North Atlantic while ~~on August 26 had significant surface~~experiencing low altitudes 50 hours before arrival~~contact~~ (Fig. S2). From August 27 to the evening of August 29, GOM is undetectable, before averaging (median ± m.a.d.) ~~2.8~~1.65 ± ~~01.6~~23 pg m^{-3} for Event 2~~, which started on August 29 and ended on September 1~~.

Concerning the meteorological parameters for Events 1a, 1b, and 2, the wind direction was mainly from the southwest (Fig. S1), with ~~low but~~ variable wind speed (~~34.9~~43 ± ~~2.02~~2.9 m s^{-1}, Table S1)). The relative humidity was low (< 90 % RH), averaging ~~63~~67.83 ± 8.53~~5~~ % RH for the ~~two~~ 2019 event periods, with Events 1a and 1b experiencing similar levels (~63 ± 5 %, Table S1) and Event 2 higher RHs (76.91 ± 7.82 %). During non-event periods, RH was considerably higher (95.70 ± 1.82 %). The temperature was routinely above freezing ~~(2.1 ± 0.8 °C)~~, with increased temperature during event periods vs non-event periods, 1.68 ± 1.23 vs -0.09 ± 0.43 °C, respectively. The skies were clear with peak solar radiation above 200 W m^{-2} during event periods.~~ ~~ Comparable to RH, H$_2$O mixing ratios and accumulated precipitation were noticeably higher during non-event periods than event periods with Event 2 experiencing higher values than Events 1a and 1b as well as the lowest levels of GOM (Table S1). On August 23, 24, 30, and 31, GOM experienced a reduction in concentration while accumulated precipitation simultaneously increased. A similar relationship between the H$_2$O mixing ratios and GOM levels is observed during the first part of Event 1a (August 21 and 22) and the aforementioned pattern during the transition of Event 1a to 1b. ~~Between the enhancement event periods and non-event periods of the 2019 campaign, temperature, relative humidity, wind direction, solar radiation, GEM, and GOM were significantly different (Wilcoxon Rank Sum Test, 95 % CI); however, there was no significant difference for wind speed.~~
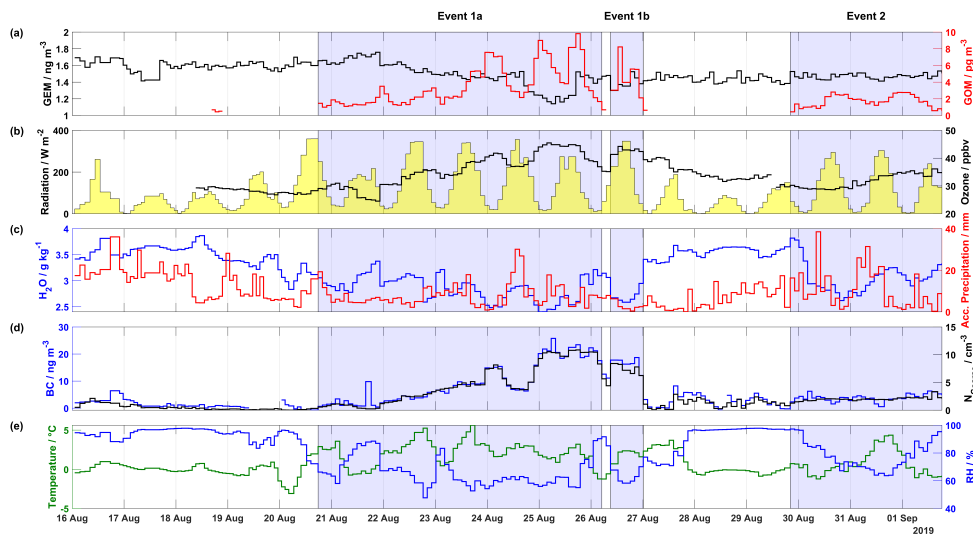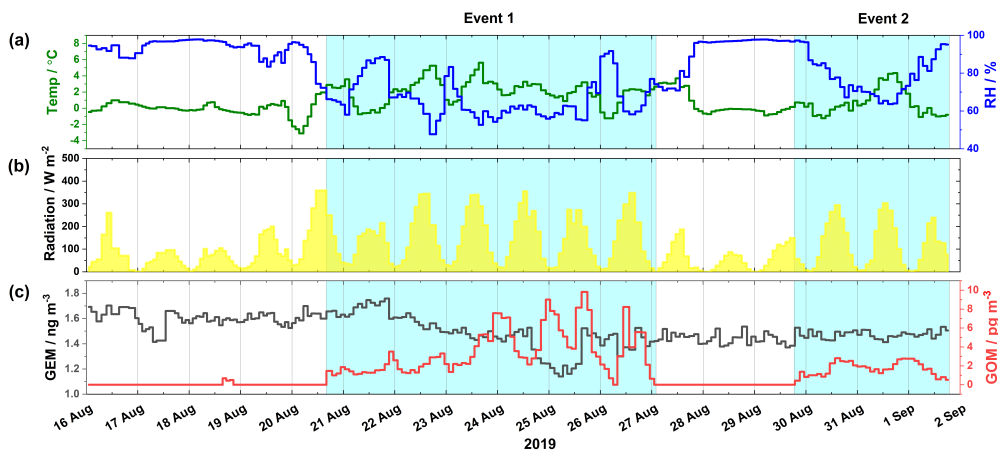
Figure. 1. Overview of mercury, ~~and~~ meteorological parameters, ozone, and aerosol properties (BC and N_{Coarse}) measured during the 2019 campaign including **(a)** GEM (ng m^{-3}) in black on the left axis and GOM (pg m^{-3}) in red on the right axis, ~~temperature (°C) in green on the left axis and relative humidity (%) in blue on the right axis,~~ **(b)** radiation (W m^{-2}) shaded in yellow on the left axis and ozone (ppbv) in black on the right axis, ~~and~~ **(c)** H$_2$O mixing ratio (g kg^{-1}) at ground level in blue

on the left axis and accumulated precipitation (mm) in red on the right axis, **(d)** BC (ng m^{-3}) in blue on the left axis and N$_{Coarse}$ (cm^{-3}) in black on the right axis, and **(d)** temperature (°C) in green on the left axis and relative humidity (%) in blue on the right axis ~~GEM (ng m^{-3}) in black on the left axis and GOM (pg m^{-3}) in red on the right axis~~. The areas shaded in blue indicate Events 1a, 1b, and 2, respectively.

295

     Results from the 2020 campaign, describing the time series of atmospheric mercury concentrations, ground-level meteorological parameters (radiation, H$_2$O mixing ratio, temperature, and RH), accumulated precipitation along the trajectory length, ozone, and aerosol properties (BC concentration and N$_{Coarse}$)~~describing the time series of atmospheric mercury species and meteorological parameters~~, are presented in Fig. 2. Wind direction, wind speed, and snow depth are displayed in Fig. S3.

300 ~~From Fig. 2~~During the 2020 campaign, ~~three~~ four distinct GOM enhancement events are observed: Event 3 from July 22 at 16:35 to July 23 at 13:15, Event 4 from July 24 at 11:55 to July 26 at 13:15, ~~and~~ Event 5a from July 30 at 17:00 to August 4~~1~~ at 13~~09~~:40, and Event 5a from August 13:40 to August 4 at 09:00. The 2020 campaign experienced higher GEM and GOM concentrations compared to the 2019 campaign. For example, GEM increased from ~1.7 ng m^{-3} on July 17 to ~2.8 ng m^{-3} on July 19, only to dip to ~1.7 ng m^{-3} on July 21 before increasing to ~2.4 ng m^{-3}. These elevated concentrations could be the result of oceanic evasion through open leads and fissures in the consolidated pack ice (Aspmo et al., 2006; DiMento et al., 2019), as air masses experienced extensive surface contact with sea ice on July 19–21 (Fig. S4a–c). Satellite images, which show fractured sea ice surrounding Villum are available at http://ocean.dmi.dk/arctic/nord.uk.php. ~~These elevated concentrations could be the result of oceanic evasion through open leads and fissures in the consolidated pack ice (Aspmo et al., 2006; DiMento et al., 2019), as air masses experienced extensive surface contact with sea ice on July 19–21 (Fig. S4a–c).~~

310 For Event 3, GEM and GOM averaged 1.7~~1~~ ± 0.1~~3~~ ng m^{-3} and 35.1~~3~~ ± 13.9~~8~~ pg m^{-3}, respectively (Table S1). At the beginning of Event 3, GEM dropped from ~2~~.1~~ to ~1.5 ng m^{-3}, while GOM increased from ~6~~.2~~ to ~62~~1~~.8 pg m^{-3}. For Event 4, GEM and GOM averaged 1.7~~9~~8 ± 0.0~~9~~1 ng m^{-3} and 8.7~~8~~ ± 2.3~~8~~4 pg m^{-3}, respectively (Table S1). During Event 4, GOM peaked at ~14 pg m^{-3} on July 24 at 13:55 and July 25 at 18:35, while GEM decreased from ~1.9 ng m^{-3} to ~1.4 ng m^{-3} before returning to levels of ~1.9 ng m^{-3} by the end of Event 4, this decrease in GEM during Event 4 is part of an overall decreasing pattern of GEM during the preceding and subsequent days (Fig. 2). For Event 5a, GEM was constant, ~~and GOM~~ averag~~ing~~ed 1.5~~4~~ ± 0.0~~2~~3 ng m^{-3}, with GOM increasing throughout the event while averaging ~~and~~ 9.1~~0~~8 ± 2.4~~3~~7 pg m^{-3}~~, respectively~~. ~~At the beginning of~~For Event 5b, GEM ~~was~~ displayed a slight decreasing pattern with an average of 1.51 ± 0.05 ng m^{-3}~~elevated at ~1.8 ng m^{-3} although quickly decreased to ~1.4 ng m^{-3} while GOM increased from near-zero values to enhanced concentrations of 20 pg m^{-3} for the remainder of Event 5~~, GOM decreased from ~14 pg m^{-3} on August 1 to ~5 pg m^{-3} on August 2 before

320 increasing until August 4 where GOM began to decrease. For Events 3, 4, and 5, PHg displayed no visible pattern and was constantly near or below LOD.

     Meteorological parameters during the 2020 campaign are displayed in Fig. 2 and S3 and summarized in Table S1. Event 3 experienced decreasing temperatures (from ~5 to ~1 °C) and increasing RH (~77 to ~92 %) while Event 4 displayed an opposite pattern of increasing temperatures (~5 to ~7, maximum 12 °C) and ~~decreasing~~ similar levels of RH at the beginning

Formatted: Font: Bold
Formatted: Superscript
Formatted: Subscript
Formatted: Superscript
Formatted: Font color: Auto

(~77 %) and end (~79 %) of the event (77 to 79, with a minimum ~52 %) in the middle. A similar relationship is observed for H_2O mixing ratios, with low values during Event 3 (3.83 ± 0.04 g kg^{-1}) and elevated values for Event 4 (4.61 ± 0.23 g kg^{-1}). Accumulated precipitation was slightly higher for Event 3 vs 4, 10.90 ± 4.10 and 8.90 ± 1.90 mm, respectively, although Event 4 experienced a higher maximum (~31 mm) on July 25. For Events 3 and 4, the wind direction was mainly from the east with low and stable wind speeds (Fig. S2S3 and Table S1). Radiation during the start of Event 3 was low (~125 W m^{-2}) but increased as the event progressed. For Event 5a, the temperature exhibited high values (10.81 ± 1.27 °C) and a diurnal pattern with maxima during the afternoon, (10.6 ± 1.2 °C) with llow (< 70 67 %) and decreasing RH (minimum ~30 42 %), and the wind direction was consistently from the southwest with high wind speeds (median 89.30 ± 1.058 m s^{-1}, max 12 11.5 m s^{-1}, Fig S3 and Table S1)). During the beginning of Event 5a, the H_2O mixing ratio was high (~5 g kg^{-1}) compared to the end of the event (~3.5 g kg^{-1}), and accumulated precipitation peaked at the beginning of the event (47.4 mm) and averaged 12.95 ± 3.4 mm. For Event 5b, the temperature continued to be elevated with a diurnal pattern while RH displayed a decreasing pattern till the end of the event, similar patterns were observed for the H_2O mixing ratios and accumulated precipitation (Fig. 2). During all three four events, snow cover was near zero (Fig. S2S3) and global radiation was high during all three events with peak values > 375 W m^{-2} (except during the beginning of Event 3 and end of Event 4, Fig 2). Between the enhancement event periods and non-event periods of the 2020 campaign, temperature, relative humidity, wind speed, wind direction, solar radiation, GEM, and GOM were significantly different (Wilcoxon Rank Sum Test, 95% CI).
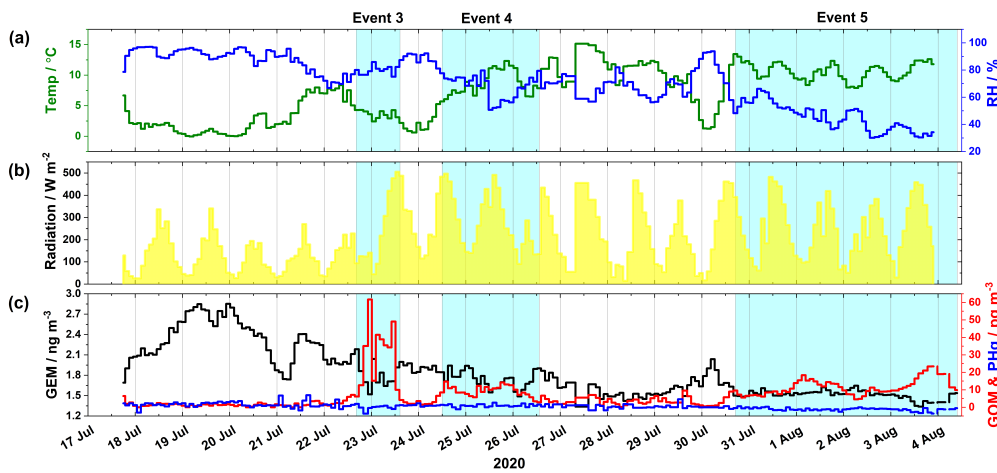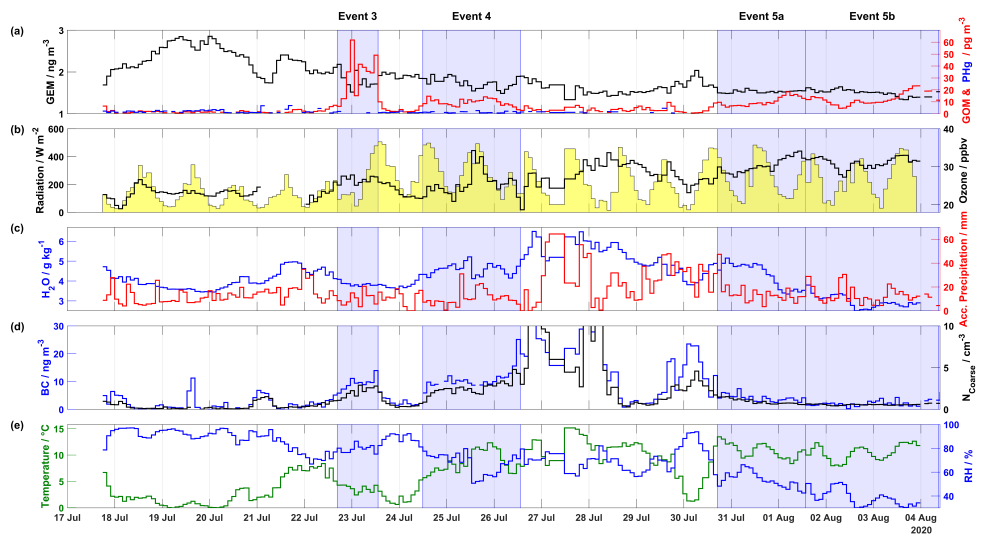
Figure. 2. Overview of mercury, meteorological parameters, ozone, and aerosol properties (BC and N_{Coarse}) measured during the 2020 campaign including **(a)** GEM (ng m^{-3}) in black on the left axis, GOM (pg m^{-3}) in red, and PHg (pg m^{-3}) in blue on the right axis, **(b)** radiation (W m^{-2}) shaded in yellow on the left axis and ozone (ppbv) in black on the right axis, **(c)** H_2O mixing ratio (g kg^{-1}) at ground level in blue on the left axis and accumulated precipitation (mm) in red on the right axis, **(d)** BC (ng

m^{-3}) in blue on the left axis and N$_{Coarse}$ (cm^{-3}) in black on the right axis, and **(d)** temperature (°C) in green on the left axis and relative humidity (%) in blue on the right axis. The areas shaded in blue indicate Events 3, 4, 5a, and 5b, respectively. The axis scale for **(d)** is truncated to show the fine structure of BC and N$_{Coarse}$ during event periods, for the full scale see Fig. 7. Overview of mercury and meteorological parameters during the 2020 campaign including **(a)** temperature (°C) in green on the left axis and relative humidity (%) in blue on the right axis, **(b)** radiation (W m^{-2}) shaded in yellow, and **(c)** GEM (ng m^{-3}) in black on the left axis, GOM (pg m^{-3}) in red on the right axis, and PHg (pg m^{-3}) in blue on the right axis. The area shaded in blue indicates Events 3, 4, and 5, respectively.

For Events 1, 2, 4, and 5, the ground level meteorological parameters mainly associated with GOM enhancement are high levels of radiation and low RH. Interestingly, these events were not linked to cold temperatures, which has been previously demonstrated to be associated with mercury oxidation (Shepler et al., 2007; Cole and Steffen, 2010; Toyota et al., 2014; Ariya et al., 2015; Steffen et al., 2015). The stability of the Hg-Br intermediate is highly temperature-dependent (Goodsite et al., 2004; Donohoue et al., 2006; Dibble et al., 2012; Goodsite et al., 2012). The temperature at Villum ranged from -3.1 to 5.6 °C and from 0.0 to 15.1 °C during the 2019 and 2020 campaign, respectively. Therefore, the ground-level temperatures are likely too high for local in situ production of GOM in the boundary layer to occur. This observation prompted the analysis of air mass back-trajectories with arriving at Villum, and their meteorological data, to investigate the dynamics of GOM during these enhancement events.

3.2 Air mass history

Analysis of air mass history including both the trajectories and the associated meteorology along the paths can provide useful information regarding the source regions and favorable conditions for GOM formation and removal. Contour plots for different meteorological parameters (temperature, relative humidity, solar radiation, H$_2$O mixing ratio, and precipitation) and altitude for each hourly trajectory along with GOM concentrations for the 2019 and 2020 campaigns are displayed in Fig. 3 and 4, respectively. Other meteorological parameters (H$_2$O mixing ratio and precipitationMixed layer height for each step of each hourly trajectory) for the 2019 and 2020 campaigns isare shown in Fig. S5a–b and Fig. S5c–d, respectively.
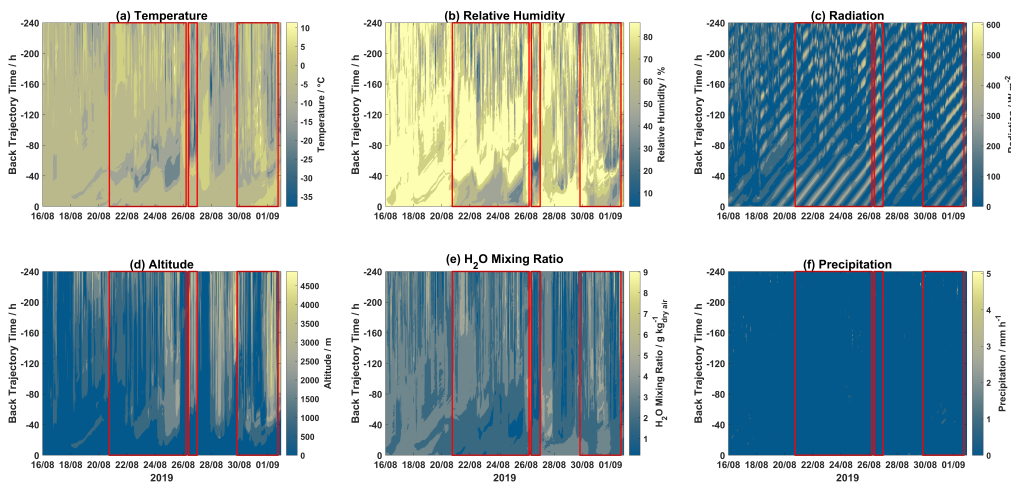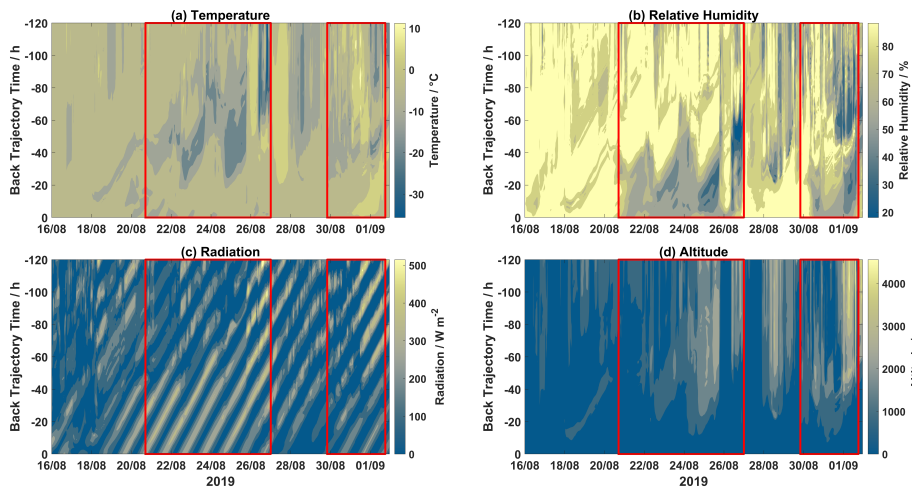
375   **Figure 3.** Contour plots of trajectory derived meteorological parameters **(a)** temperature, **(b)** relative humidity, **(c)** solar radiation, ~~and~~ **(d)** altitude, **(e)** H$_2$O mixing ratio, and **(f)** precipitation, along each trajectory for the 2019 campaign. Event

Formatted: Font: Bold

Formatted: Subscript

Formatted: Font: Bold

periods are outlined in red. The x-axis displays arrival time at Villum, the y-axis displays hours backward in time for each trajectory, and the color bar represents the meteorological parameter. ~~Trajectories were producing via the HYSPLIT model.~~

During Event 1a, after ~120 hours trajectory temperatures were warmer with lower RH values, while H_2O mixing ratios were increased after ~80 hours. Radiation was intense before 80 hours for the entirety of Event 1a, after this time air masses experienced variable radiation, especially on August 21, 22, 24, and 25. Air masses during Event 1a were consistently elevated with the highest altitudes on August 24-26. Precipitation was low except for several episodes which is reflected in the accumulated precipitation (Fig. 1). Event 1b experienced lower temperatures after 80 hours although lower RH before this time, radiation was intense and H_2O mixing ratios were low throughout the trajectory length for the entire event. For the first half of Event 2, air masses were slightly warmer and wetter with lower radiation and decreased altitudes when compared to the second half of this event. ~~In 2019, air masses arriving during Events 1 and 2 were, on average, colder (temperature: -2.8 ± 3.2 °C), dryer (RH: 80 ± 15 %, accumulated precipitation: 3.8 ± 2.5 mm, and H_2O mixing ratio: 2.6 ± 0.7 g / kg_{dry air}), and exposed to more intense solar radiation (110 ± 73 W m⁻²) when compared to non-event periods (temperature -1.1 ± 1.5 °C, RH: 90 ± 7 %, accumulated precipitation: 5.1 ± 3.0 mm, H_2O mixing ratio: 3.2 ± 0.4 g / kg_{dry air}, solar radiation: 100 ± 54 W m⁻²). Trajectory temperature, RH, precipitation, H_2O mixing ratio, solar radiation, and altitude were significantly different (Wilcoxon Rank Sum Test, 95% CI) between GOM enhancement event periods and non-event periods during the 2019 campaign.~~ During Event 3, temperatures were consistently warm except for a period of colder temperatures around ~60 hours backward. A similar observation is made for RH with high values after ~50 hours although the H_2O mixing ratios were elevated after ~70 hours. Radiation was intense before ~60 hours and low after that time. Event 4 experienced similar conditions to Event 3, although at later times throughout the air mass history. Interestingly, Event 5a and 5b experienced similar levels of GOM (Fig. 2), although Event 5a experienced higher temperatures as well as higher RH and H_2O mixing ratios with trajectories arriving from lower altitudes and being exposed to less radiation. ~~For the 2020 campaign, a similar pattern is observed for Events 3, 4, and 5 with air masses being, on average, colder (temperature: 0.4 ± 4.1 °C), drier (RH: 74 ± 17 %, accumulated precipitation: 1.9 ± 1.6 mm, and H_2O mixing ratio: 3.1 ± 0.7 g / kg_{dry air} and exposed to more intense solar radiation (214 ± 104 W m⁻²) when compared to non-event periods (temperature 1.3 ± 2 °C, RH: 91 ± 8 %, accumulated precipitation: 7.0 ± 3.6 mm, H_2O mixing ratio: 3.9 ± 0.6 g / kg_{dry air}, and solar radiation: 167 ± 85 W m⁻²). During the 2020 campaign, trajectory temperature, RH, H_2O mixing ratio, solar radiation, and altitude were significantly different (Wilcoxon Rank Sum Test, 95% CI) between GOM enhancement event periods and non-event periods.~~ Presuming that an RH greater than 95 % signifies air masses were within a cloud (Schmeissner et al., 2011; Freud et al., 2017), the time spent in-cloud could be calculated for each event. Air masses during Events 1a, 1b, and 2 spent 22.67, 11.67, and 14.28 % of the time in-cloud, respectively, and 19.15 % combined. For Events 3, 4, 5a, and 5b, air masses spent 52.58 %, 38.32 %, 20.37, and 14.68 % of the time in-cloud, and 27.37 % combined. For the 2019 campaign, event air masses spent less time in a cloud compared to non-event air masses (29.61 %), both when comparing individual events and combined event periods. For the 2020 campaign, the same

general pattern is observed when comparing combined event periods, although Events 3 and 4 spent more time in a cloud compared to non-event air masses (32.59 %, Table S2).

Higher levels of solar radiation enable the photolysis of reactive halogen species and lower relative humidity inhibits the partitioning of GOM into the liquid phase (Laurier, 2003; Soerensen et al., 2010; Brooks et al., 2011; Steen et al., 2011). Lower temperatures aid in the formation of GOM from HgBr; Skov et al. (2004) Jiao et al. 2015 and 2017 and Christensen et al. (2004) modeled a surface temperature below -4 °C for mercury depletion to occur in the Arctic, while Brooks et al. (2011) observed a temperature threshold of -15 °C for mercury oxidation to occur. Brooks et al. (2011)Therefore, it appears that while ground-level measurements showed no robust connection to cold temperatures, meteorological conditions along the trajectory path showed a relationship between GOM and subfreezing temperatures as well as dry, sunlit conditions.
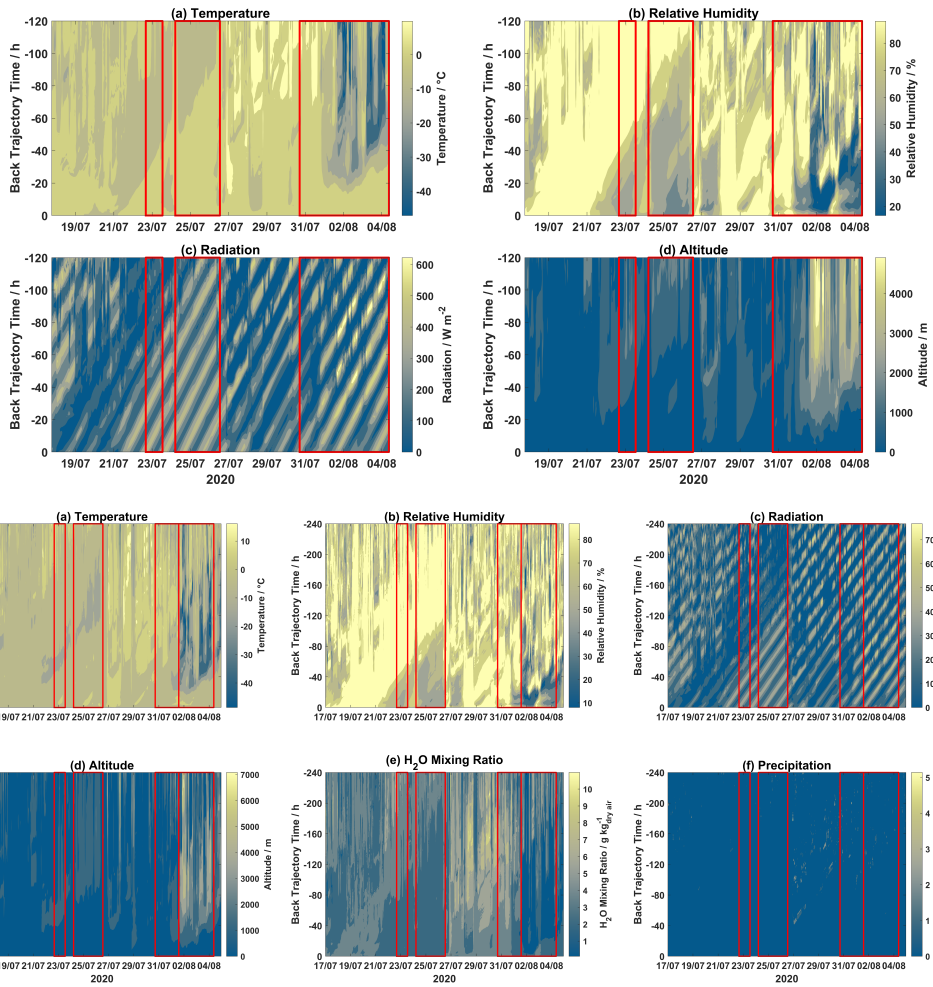
Figure 4. Contour plots of trajectory derived meteorological parameters **(a)** temperature, **(b)** relative humidity, **(c)** solar radiation, **(d)** altitude, **(e)** H$_2$O mixing ratio, and **(f)** precipitation~~and **(d)** altitude~~, along each trajectory for the 2020 campaign.

425   Event periods are outlined in red. The x-axis displays arrival time at Villum, the y-axis displays hours backward in time for

each trajectory, and the color bar represents the meteorological parameter. ~~Trajectories were producing via the HYSPLIT model.~~
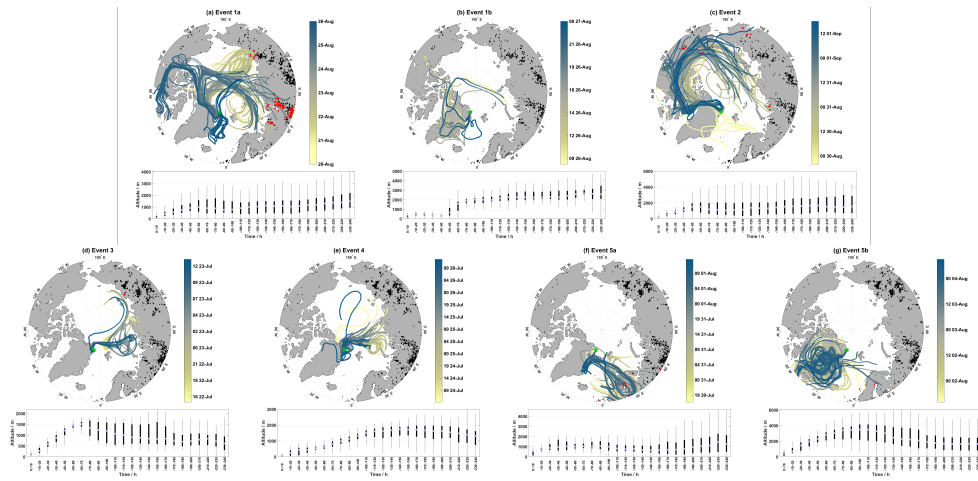
430 ~~The differences between ground-level and trajectory-derived meteorological parameters during enhancement events and non-events imply that these air masses are likely decoupled from the boundary layer. To examine the vertical origin of these air masses, an analysis of the altitude of trajectories arriving at Villum was performed. Figures 3d and 4d display a contour plot of the altitude for each hourly back-trajectory for the 2019 and 2020 campaign, respectively. From these figures, it is evident that during GOM enhancement events air masses spent considerable time aloft before arrival at Villum. For the 2019~~

435 ~~campaign, median back-trajectory altitudes during event periods were 754 ± 467 m, compared to 371 ± 351 m during non-event periods. For the 2020 campaign, median altitudes during event periods were 1075 ± 578 m, compared to 425 ± 352 m during non-event periods. Indeed, air masses that arrived during event periods were above the mixed layer height 90 and 99 % of the time in the 2019 and 2020 campaigns, respectively. Air masses that arrived during non-event periods were above the mixed layer height only 64 and 82 % of the time in the 2019 and 2020 campaigns, respectively. Together, the analysis of~~

440 ~~air mass history demonstrates that the origin of the GOM enhancement events is the free troposphere under favorable meteorological conditions (cold and dry with intense solar radiation along the trajectory path).~~
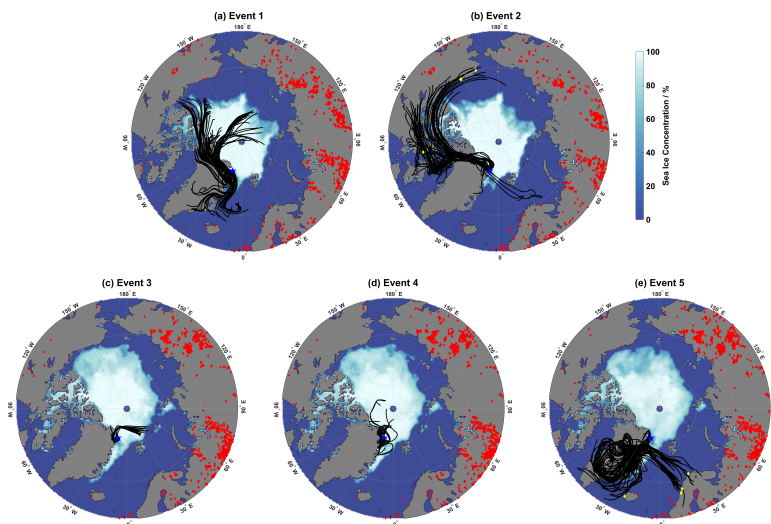
Figure. 5. Map of air mass back-trajectories during Events 1–5 in **(a)** through **(eg)**. The top panel shows ~~i~~individual hourly trajectories are ~~in black~~colored-coded by the arrival date at Villum as indicated by the color bar (the date format is HH dd-MMM), active fires during each event are in black~~red~~, active fires intersecting trajectories within 1° latitude/longitude and within 1 hour are in red~~yellow~~ (active fires from the previous 10~~5~~ days before the start of an event were included to reflect the trajectory length~~), and sea ice concentration is given by the color bar~~. The position of Villum is marked by the green~~blue~~ star. The bottom panel displays boxplots of the altitude for each event binned in increments of ten hours. ~~Trajectories were producing via the HYSPLIT model. Sea ice concentration was taken from NSIDC. Fire data were obtained from the FIRMS database.~~

Geospatially, the GOM enhancement events show different source regions. Figure 5a~~–e g~~ shows hourly air mass back-trajectories, combined with ~~sea ice concentrations and~~ active fire data, for each event. To capture the presence of fires in relation to the length of each trajectory, active fires from the previous 5~~10~~ days before the start of each event and up to the end of each event are marked in black ~~were included~~ and active fires intersecting trajectories within 2° latitude/longitude and within 2 hours are marked in red. The bottom panels in Figure 5a~~–g~~ displays the distribution of trajectory altitudes binned in ten-hour increments. Biomass burning (one of the possible causes of active fires) can emit aerosols covering a large size range and varying chemical composition (Reid et al., 2005), therefore active fires were included to analyze their effect on the air mass history during event periods. For Event 1, air masses circulated over the Barents Sea, Kara Sea, and the central Arctic

Ocean at the beginning of the event before transitioning to the East Siberian Sea. During the latter part of Event 1a, trajectories experienced continental influence from Eurasia before shifting to the Canadian archipelago, and finally arriving from the Greenland Sea. Trajectories in Event 1a were influenced by active fires during each circulation pattern except for the latter part when air masses passed over the Greenland Sea before arrival, corresponding to reduced GOM concentrations (Fig. 1). Trajectory altitudes during Event 1a were consistently above 1000 m after 120 hours, they experienced a minimum median altitude at 80–90 hours, and descended from ~1000 m approx. 50–60 hours before arrival. The distribution for trajectory altitudes during Event 1a were diverse, with each bin experiencing surface level contact as well as reaching the middle free troposphere (Fig. 5a). For Event 1b, air masses were mainly confined to the Arctic Ocean and central Greenland, with a few trajectories passing over the Canadian archipelago and the Greenland Sea. Median trajectories altitudes spent considerable time above 2000 m after 80 hours, followed by a quick descent to low altitudes for the last 50 hours before arrival at Villum. showed two main source regions: the first is the Arctic with air masses originating from either the central Arctic Ocean or the northern part of the Canadian archipelago and passing over Northern Greenland, and the other is the Northern Atlantic. Event 2 showed a major contribution of air masses from the central Arctic Ocean, North America, and the Canadian archipelago with smaller contributions from the Northern Atlantic just south of Svalbard. There is some influence of active fires from Eurasia, North America, and the Canadian archipelago during this event, although infrequent and at different stages of transport (Fig. 5c). Analogous to Event 1a, median trajectory altitudes during Event 2 were consistently elevated after 120 hours and resided in the surface layer and middle of the free troposphere. Event 2 experienced a minimum median altitude at 80–90 hours and started a descent from ~1500 m approx. 40–50 hours backward. Events 3 and 4 showed air masses originating from the Barents Sea and the AArctic Ocean with little spatial extentlittle influence of active fires. Trajectory altitudes for Event 3 experienced surface layer contact after 200 hours backward, thereafter, started an ascent in the free troposphere from 70–190 hours backward, which was followed by a steep descent from 1500 m at approx. 60–70 before arrival. Event 4 showed a similar spatial extent to Event 3 although with air masses located closer to Villum. Median trajectory altitudes for Event 4 resided at elevated altitudes with surface layer contact only after 200 hours, then started their descent from 1600 m approx. 120 before arrival. For Event 5a, air masses consistently arrived from Northern Scandinavia with extensive influence from active fires.showed the largest spatial extent, Trajectory altitudes were considerably lower (varying around 1000 m) and experienced surface layer contact after 100 hours, after which they started their descent closer to Villum (20–30 hours backward). For Event 5b, air masses shifted with air masses to arriving from circulating mainly over the Greenlandic Iice sSheet, although a few trajectoriescontributions were also found from the Northern Atlantic and parts of Northern Scandinavia also contributed. Trajectory altitudes showed the highest elevations compared to the other events (Table S2 and Fig. 5g), experienced altitudes around 1600 m after 200 hours, starting around 190 hours backward trajectories ascended from ~2000 m until approx. 90–100 backward where trajectories started to descend from ~3500 m. Other than Events 3 and 4, the geospatial origins of air masses during GOM enhancement events were quite diverse. Events 3 and 4 were only separated by a couple of hours and therefore similar air mass origin is expected for the two events, although interestingly Events 5a and 5b showed quite different air mass origins but were temporally consecutive. Each event displayed a gradual descent from elevated altitudes before reaching

Villum, except for Event 1b which experienced a steep descent around 50 hours backward followed by extensive surface layer contact. Figure 5a–e shows that the air mass origins during GOM enhancement events are heterogeneously distributed throughout the Arctic as well as the Canadian Archipelago and Scandinavia.

3.3 Comparison with mid-latitude studies

500 Previous studies have demonstrated the influence of the troposphere on mercury concentrations. In the mid-latitudes of the northern hemisphere, the free troposphere has been established as a source of GOM through modeling studies (Gratz et al., 2015; Shah and Jaeglé, 2017) and observations from both aircraft campaigns (Talbot et al., 2007; Gratz et al., 2015) and high altitude sites (Swartzendruber et al., 2006; Faïn et al., 2009; Fu et al., 2016). Depletions of GEM were observed onboard research flights in the upper troposphere (8–12 km) during the INTEX-B campaign in 2006 over the North Pacific (Talbot et 505 al., 2007). GEM was rarely detected when ozone was greater than 300 ppb; the authors ascribed this relationship as an indicator of time spent in the stratosphere. They hypothesized that the near-ppm levels of ozone in the stratosphere were the cause of the depleted GEM.

Add a sentence about altitude of flights vs b trajs

Faïn et al. (2009) reported similar observations of the free troposphere acting as a source of oxidized mercury at a high 510 elevation site (3220 m above sea level) in the Rocky Mountains, USA. They also observed that the presence of GOM was dependent on RH. They hypothesized that the build-up of GOM in the free troposphere was governed exclusively by the existence of low RH, possibly due to the lack of scavenging by particles at low RH levels. **Discuss article about comparison of high altitude sites, neg corr GOM Ozone**Weiss-Penzias et al. (2015)Modeling studies have also shown the troposphere to be a source of GOM. Using the GEOS-Chem global chemical transport model, Holmes et al. (2006) and Holmes et al. 515 (2010) identified Br to be the dominant oxidant of GEM globally, with most of the oxidation occurring in the middle and upper troposphere. Shah and Jaeglé (2017) arrived at a similar conclusion using GEOS-Chem that much of the mercury oxidation by Br occurs in the middle and upper troposphere. These studies show the free troposphere to be a source of GOM in the mid-latitudes, however, there are a limited number of field studies on GOM in the High Arctic summer and none, to the authors' knowledge, on the influence of the free troposphere on GOM levels. Similar chemistry is likely the cause of the observations 520 in this study; however, the Arctic atmosphere is largely separated from the mid-latitudes during summer on account of contraction of the polar dome, so there may be differences in the dynamics, albeit unlikely (Holmes et al., 2010). This study provides field validation of these previous modeling studies from the mid-latitudes by identifying the free troposphere as a source of GOM in the High Arctic summer.

3.4 Ozone

525 Ozone mixing ratios for the 2019 campaign are displayed in Fig. 1b. Due to technical difficulties, ozone measurements started on August 18 during the 2019 campaign. From August 18 to the beginning of Event 1a, ozone was slightly decreasing with values of ~30 ppbv. For Event 1a, ozone increased concurrently with GOM, both reaching max values of 45.50 ppbv and 9.81

ng m^{-3}, respectively, on August 25 (Fig. 1), while GEM exhibits a minimum on August 25 at 1.14 ng m^{-3}. The peak ozone level is abnormally high for the late summer (median ± m.a.d. ozone mixing ratio for August 2010–2019 is 24.64 ± 3.14 ppb).

530 Ozone decreased from this maximum to 35.30 ppbv at the end of Event 1a. For Event 1b, ozone returned to high levels observed at the peak of Event 1a (~40 ppbv). From the end of Event 1a to the beginning of Event 2, ozone steadily decreased. For Event 2, ozone steadily increased from ~29 to ~36 ppbv. For the 2020 campaign, a similar relationship between ozone and GOM is observed (Fig. 2b). Background levels during July (median ± m.a.d. ozone mixing ratio for July 2010–2019) is 23.92 ± 2.88 ppb. During Event 3, ozone is increasing simultaneously with GOM while GEM is decreasing; for this event, ozone averaged

535 26.69 ± 0.79 ppb. While this value is not considered elevated for the season, it is elevated over the preceding and subsequent days around Event 3. For Event 4, ozone averaged 25.30 ± 1.63 ppb and is at background levels for much of the event. On July 25, ozone peaked at ~34 ppb before returning to background levels. For Event 5a and 5b, ozone experienced similar levels (Table S1) and followed a similar pattern as GOM, increasing during Event 5a followed by a dip on August 2, then increasing for the remainder of Event 5b.

540 GEM and GOM concentrations along with ozone mixing ratios for the 2019 and 2020 campaigns are displayed in Fig. 6a and Fig. 6d, respectively. During non-event periods in the 2019 campaign, ozone is either low or decreasing. During Event 1, ozone increases concurrently with GOM, when they both peak on August 25 at 45.5 ppb and 9.8 pg m^{-3} for ozone and GOM, respectively, while GEM exhibits a minimum on August 25 at 1.1 ng m^{-3} (Fig. 6a). For Event 1, ozone averaged 36.9 ± 4.7 ppb. The peak ozone level is abnormally high for the late summer (median ± m.a.d. ozone mixing ratio for August 2010–

545 2018 is 24.6 ± 3.1 ppb). Ozone then decreases during the second non-event period and only increases again during Event 2 to an average of 31.9 ± 2.6 ppb.

Given the source of the enhanced GOM concentrations was identified to be the cold, dry free troposphere, our analysis now turns to other atmospheric constituents, particularly ozone. An analysis of ground-level ozone measurements can help to provide insight into the dynamics of GOM as mercury depletion events and ozone depletion events often occur concurrently

550 through reactions with halogen species.

GEM and GOM concentrations along with ozone mixing ratios for the 2019 and 2020 campaigns are displayed in Fig. 6a and Fig. 6d, respectively. During non-event periods in the 2019 campaign, ozone is either low or decreasing. During Event 1, ozone increases concurrently with GOM, when they both peak on August 25 at 45.5 ppb and 9.8 pg m^{-3} for ozone and GOM, respectively, while GEM exhibits a minimum on August 25 at 1.1 ng m^{-3} (Fig. 6a). For Event 1, ozone averaged 36.9

555 ± 4.7 ppb. The peak ozone level is abnormally high for the late summer (median ± m.a.d. ozone mixing ratio for August 2010–2018 is 24.6 ± 3.1 ppb). Ozone then decreases during the second non-event period and only increases again during Event 2 to an average of 31.9 ± 2.6 ppb.

For the 2020 campaign, a similar relationship between ozone and GOM is observed (Fig. 6d). During Event 3, ozone is increasing simultaneously with GOM while GEM is decreasing; for this event, ozone averaged 26.7 ± 0.8 ppb. For Event 4,

560 ozone averaged 25.3 ± 1.6 ppb and is at background levels for much of the event. On July 25, ozone peaked at 34 ppb before returning to background levels. For the non-event period from July 26 to 30, ozone is significantly elevated over background

Formatted: Superscript
Formatted: Superscript
Formatted: Font color: Auto
Formatted: Font color: Auto
Formatted: Font color: Auto
Formatted: Font color: Auto
Formatted: Font color: Auto
Formatted: Font color: Auto
Formatted: Font color: Auto
Formatted: Font color: Auto
Formatted: Font color: Auto
Formatted: Font color: Auto
Formatted: Font color: Auto
Formatted: Font color: Auto
Formatted: Font color: Light Green
Formatted: Font color: Auto
Formatted: Font color: Auto
Formatted: Font color: Auto
Formatted: Font color: Auto
Formatted: Font color: Auto
Formatted: Font color: Auto

Commented [JBP1]: Add a sentence about neg corr ozone G for FT influence. Boundary layer sink for ozone while FT source

Formatted: Font color: Red

levels, although there is an absence of enhanced GOM concentrations. This discrepancy can again be accounted for by the meteorological conditions along the trajectory path (Fig. 4 and S3); elevated temperature, RH, precipitation, and H_2O mixing ratios lead to the removal of GOM, while ozone is only slightly water-soluble leading to less efficient wet removal (Sander, 2015). For Event 5, ozone follows a similar pattern as GOM, increasing at the beginning of the event and remaining elevated for the duration. Event 5 experienced the highest average trajectory altitudes (1530 ± 813 m) as well as highest average ozone mixing ratios (30.7 ± 1.7 ppb), which were elevated over normal levels during July (median $\pm$ m.a.d. ozone mixing ratio for August 2010–2018 is 23.6 ± 2.8 ppb).

For the GOM enhancement events in 2019, there is a moderate negative correlation between GEM and ozone (Spearman's rank coefficient -0.62, Fig. 6b), as well as a moderate positive correlation between GOM and ozone (Spearman's rank coefficient 0.71, Fig. 6c). For the 2020 campaign, this moderate negative relationship between GEM and ozone is retained (Spearman's rank coefficient -0.72, Fig. 6e), although for GOM and ozone the correlation is moderate to weak (Spearman's rank coefficient 0.45, Fig. 6e). This is likely due to the high concentrations observed during Event 3, when removing this event from the correlation analysis for the 2020 campaign, the Spearman's rank coefficient increases to 0.62. These relationships cast doubt on the boundary layer production of GOM, analogous to the mechanisms of AMDEs. During AMDEs, ozone and GEM are positively correlated due to mutual reaction with halogen species and are both extremely depleted due to strong halogen explosion events (Schroeder et al., 1998; Lindberg et al., 2002; Berg et al., 2003; Skov et al., 2004; Brooks et al., 2006; Simpson et al., 2015). While ozone mixing ratios were high during GOM enhancement events, they are an order of magnitude below levels reported in the upper troposphere/lower stratosphere (Talbot et al., 2007), and given the slow rate reaction coefficient (Pal and Ariya, 2004), ozone is an improbable oxidant of mercury during these campaigns(Saiz-Lopez et al., 2020). Any depletions of ozone during GEM oxidation is likely masked by the elevated levels of ozone in the free troposphere.
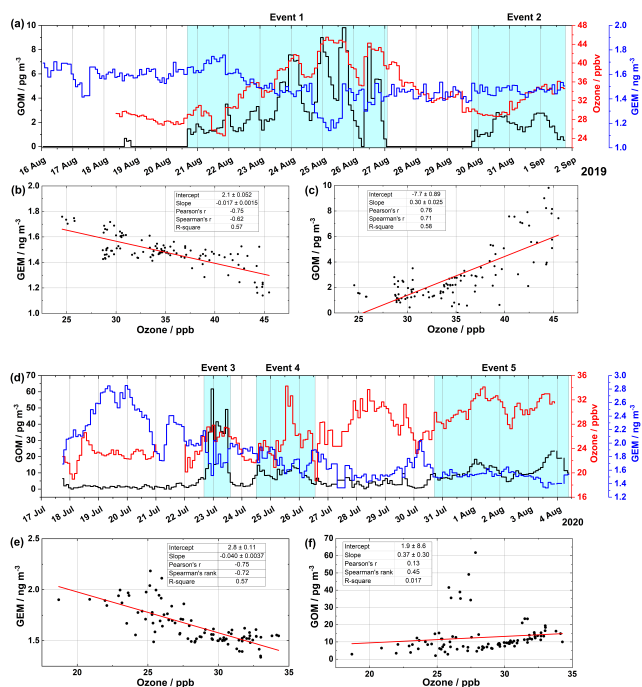
585 **Figure. 6.** Time series of GOM concentrations (pg m⁻²) in black on the left axis, ozone mixing ratios (ppbv) in red on the first right axis, and GEM concentrations (ng m⁻³) in blue on the second right axis for **(a)** the 2019 and **(d)** the 2020 campaign. Correlation between GEM and ozone for **(b)** the 2019 and **(e)** the 2020 campaign. Correlation between GOM and ozone for **(c)** the 2019 campaign and **(f)** the 2020 campaign. The areas shaded in blue indicate events periods. Correlations were calculated using the event periods. The slopes for **(b)**, **(c)**, **(e)**, and **(f)** are significantly different from zero at the 95 % CI.

590

The relationship between GOM and ozone suggests a common source or source regions for these two species. Sources of ozone in the High Arctic include transport from mid-latitudes, local production from NOₓ present in the snowpack, peroxyacetyl nitrate (PAN) photolysis, and intrusion from the free troposphere/stratosphere (Dibb et al., 2002; Walker et al., 2012; Law et al., 2014). During the winter and spring, transport from the mid-latitudes (Hirdman et al., 2009) and the free
595 troposphere/stratosphere (Semane et al., 2007; Arnold et al., 2015) are dominant ozone sources. During the summer and autumn, contraction of the polar dome decreases transport of ozone and its precursors (e.g., CO, PAN, NOₓ) from the mid-latitudes, making intrusion from the free troposphere/stratosphere a more dominant source of ozone. Elevated ozone mixing

ratios have been observed with increasing altitude in the Arctic during the ARCTAS aircraft campaigns (Jacob et al., 2010; Monks et al., 2015). Conversely, increased photochemical activity and deposition are important sinks for ozone at the ground level during the summer (Helmig et al., 2007; Arnold et al., 2015). Enhancements of GOM, which exhibited a positive correlation with ozone, have also been observed during subsidence events on Antarctica (Brooks et al., 2008; Pfaffhuber et al., 2012). Therefore, the elevated ozone levels during GOM enhancement events and positive correlation between these two species are an indicator of influence from air masses in the free troposphere, strengthening our hypothesis of the free troposphere as the source of GOM during summer (Sect. 2.2).

3.5 Particle number and black carbon

Our attention now turns to other atmospheric constituents, namely aerosol particles and black carbon content. The free troposphere has been shown to be a source of aerosol particles to the boundary layer in the Arctic (Igel et al., 2017) and contains elevated concentrations of BC over the surface level (Schulz et al., 2019). The presence of coarse mode aerosol particles has also been shown to be a necessary condition for observing BrO (a tracer for halogen activation) in the Arctic (Bognar et al., 2020). A common source of aerosol particles, black carbon, and mercury species is biomass burning (Friedli et al., 2009; Soerensen et al., 2010; Winiger et al., 2019). Therefore, we analyzed these constituents to examine their interaction with GOM with respect to the different sources.

During the non-event periods of the 2019 campaign, the coarse mode particle number concentration (N_{Coarse}) and black carbon (BC) are both low, 0.5 46 ± 0.34 cm^{-3} and 1.22 ± 1.061 ng m^{-3}, respectively. For Event 1a, N_{Coarse} and BC are both elevated (4.23.92 ± 3.12.82 cm^{-3} and 8.67.30 ± 6.04.94 ng m^{-3}, respectively) and increase concurrently with GOM, reaching a maximum concentration of ~11 cm^{-3} and ~26 ng m^{-3}, respectively, on August 25 (Fig. 7a1d). In-between Event 1a and 1b, N_{Coarse} and BC showed a reduction in concentration, consistent with other parameters during this time (Fig. 1). For Event 1b, N_{Coarse} and BC were elevated and relatively constant, 7.19 ± 0.95 cm^{-3} and 16.44 ± 1.32 ng m^{-3}, Forrespectively. For Event 2, N_{Coarse} and BC returned to low values, although at a higher level compared to non-event periods, 1.992 ± 0.13 cm^{-3} and 3.80 ± 0.596 ng m^{-3}, respectively. This pattern is comparable to the behavior of ozone (Sect. 2.33.4, Fig. 6a1b). For the enhancement events during the 2019 campaign, there is a positive correlation for event periods between GOM and N_{Coarse} (Spearman's rank coefficient 0.71), as well as between GOM and BC (Spearman's rank coefficient 0.62). For the 2020 campaign, a different scenario is observed between N_{Coarse}, BC, and GOM (Fig. 7b2a and d). For Events 3 and 4, there is a slight enhancement of N_{Coarse} and BC levels when compared to the preceding non-event periods (Fig. 7b2d). For Event 5a and 5b, both N_{Coarse} and BC are decreasing and low (Fig. 2d and Table S1). , 0.6 ± 0.1 cm^{-3} and 2.8 ± 1.1 ng m^{-3}, respectively. For enhancement events during the 2020 campaign, GOM is not correlated with N_{Coarse} and BC (Spearman's rank coefficient -0.02 and -0.07, respectively). Given the high concentrations during Event 3, these measurements may be skewing the results of the correlation analysis, however, if they are removed, the Spearman's rank coefficient between GOM and both N_{Coarse} and BC becomes moderately negative (Spearman's rank -0.25 and -0.33, respectively). This moderate negative correlation is due to decreasing concentrations during Event 5. Air masses during this event arrived from high altitudes from over the Greenlandic ice sheet

(Sect. 2.2), therefore the low concentrations of N_{Coarse} and BC are likely a representation of upper tropospheric air masses above the polar dome, which are extremely pristine (Schulz et al., 2019).

635
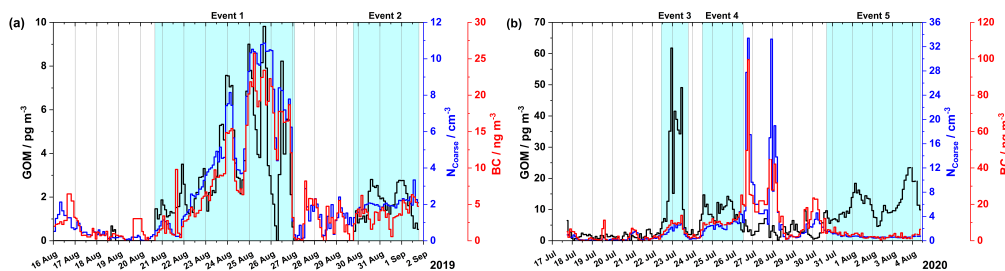
Figure. 7. Gaseous oxidized mercury (pg m^{-3}) in black on the left axis, coarse mode particle number concentration (cm^{-3}) in blue on the first right axis, and black carbon (ng m^{-3}) in red on the second right axis for **(a)** the 2019 and **(b)** the 2020 campaign. The areas shaded in blue indicate event periods.

640   Given the correlation between GOM, BC, and N_{Coarse} during enhancement events, biomass burning could be a potential source. To investigate the influence of biomass burning emission on GOM concentrations and the two episodes of high N_{Coarse} and BC concentrations during the 2020 campaign, active fire data from the FIRMS database were utilized in connection with air mass back-trajectory analysis for each event (active fires from the previous 5 days before the start of an event were included to reflect the trajectory length). As seen in Fig. 5a–e in Sect. 3.2, the geospatial origins of air masses during GOM enhancement

645   events are heterogeneously distributed. During the enhancement events, there are few intersections between air mass back-trajectories and active fires during Events 2 and 5 and none for Events 1, 3, and 4. GOM levels during Events 2 and 5 were low compared to other events (Fig. 1 and 2) and there is minimal intersection of back-trajectories and fires. Therefore, it appears that biomass burning and/or combustion related emissions have little to no influence on GOM levels observed at Villum.

650   During the 2020 campaign, there are two episodes, the first from July 26 at 17:15 to July 27 at 03:35 and the second from July 27 at 19:05 to July 28 at 09:05, where N_{Coarse} and BC are significantly elevated, reaching up to ~33 cm^{-3} and ~100 ng m^{-3}, respectively, compared to the rest of the campaign (Fig. 7b). These two episodes are observed during non-event periods (Fig. 7b). GOM during these episodes is low, 2.95 ± 1.78 pg m^{-3} for the first episode and 2.20 ± 1.9 pg m^{-3} for the second episode. These episodes are likely long-range transported, as they are too gradual and long to be identified as local

655   pollution from activities at Station Nord. Another indicator that these episodes were of non-local origin is that ozone remained at constant levels throughout both episodes. If these episodes were of local pollution, then we would expect ozone to decrease as it is titrated by local NO$_x$ emissions. Figures 6a-c show the time series of GOM, N_{Coarse}, and BC on a full-scale axis and

~~b show~~, and air mass back-trajectories for the first and second episodes, ~~respectively,~~ combined with active fire data from the previous ~~5,~~10 days to the end of the episode. ~~These episodes, which originate mainly from Fennoscandia with smaller contributions from the Arctic Ocean and the Barents Sea, are influenced by biomass burning emissions from active fires around the Bay of Bothnia (Fig. 8). GOM during these episodes is low, 2.6 ± 1.1 pg m⁻² for the first episode and 1.8 ± 0.9 pg m⁻² for the second episode.~~

~~Zheng et al. (2021)This shows that while biomass burning emissions can influence the Arctic atmospheric composition, they do not impact GOM concentrations.~~

(a) 26 July 2020 15:00 - 27 July 2020 12:00   (b) 27 July 2020 19:00 - 28 July 2020 09:00
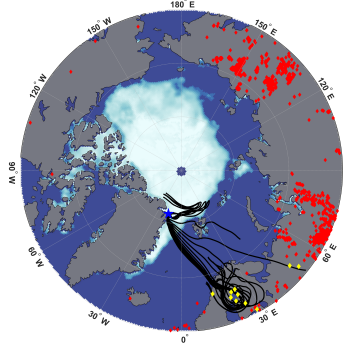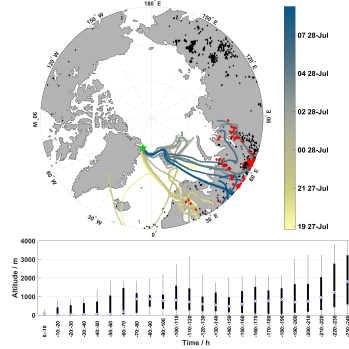
Figure. ~~8~~6. Time series ~~displaying~~demonstrating the full scale of N$_{Coarse}$ and BC, along with GOM concentrations shown in (a). The event periods are shaded in blue while the two episodes are shaded in red. Map of air mass back-trajectories during (~~a~~b) the first episode and (~~b~~c) the second episode of elevated N$_{Coarse}$ and BC concentrations. The top panels in (b) and (c) show individual hourly trajectories are colored-coded by the arrival date at Villum as indicated by the color bar (the date format is HH dd-MMM), active fires during each event are in black, active fires intersecting trajectories within 2° latitude/longitude and within 2 hours are in red (active fires from the previous 10 days before the start of an event were included to reflect the trajectory length). The position of Villum is marked by the green star. The bottom panel displays boxplots of the altitude for each event binned in increments of ten hours. ~~Individual hourly trajectories are in black, active fires during each event are in red, active fires intersecting trajectories within 1° latitude/longitude and within 1 hour are in yellow (active fires from the previous 5 days before the start of an episode were included to reflect the trajectory length), and sea ice concentration is given by the color bar. The position of Villum is marked by the blue star. Trajectories were producing via the HYSPLIT model. Sea ice concentration was taken from NSIDC. Fire data were obtained from the FIRMS database.~~

~~While these positive correlations between GOM and both N$_{Coarse}$ and BC appear not to be indicative of a common source, they do suggest a common sink. A dominant sink for aerosol particles is scavenging by cloud droplets and removal via wet deposition (Browse et al., 2012). Tunved et al. (2013) observed a decrease in particle mass and diameter with increased accumulated precipitation at Ny Ålesund for the period 2000–2010, while Croft et al. (2016) used the GEOS-Chem-TOMAS model to simulate the Arctic aerosol annual cycle and found coagulation scavenging of interstitial aerosols to be a strong control on accumulation mode particles. Presuming that an RH greater than 95 % signifies air masses were within a cloud (Schmeissner et al., 2011; Freud et al., 2017), the time spent in-cloud could be calculated for each event. Air masses during Events 1 and 2 spent 23 and 12 % of the time in-cloud, respectively, and 20 % combined. For Events 3, 4, and 5, air masses spent 50 %, 8 %, and 16 % of the time in-cloud, and 15 % combined. Interestingly, Event 3 exhibited both the highest GOM concentrations and the most time in-cloud, an observation for which we do not have an explanation thus far. While Event 3 followed the general pattern displayed by the other events (cold, dry air from the free troposphere under sunlit conditions), there appears other factors influencing the high concentrations of GOM during this event that we are unable to detect at this time. Overall, we hypothesize that the lack of sinks in the free troposphere for accumulation mode particles and BC due to the absence of wet removal processes and diminished water content is likely the reason for the observed increase in N$_{Coarse}$ and BC during the enhancement events. Furthermore, we did not find evidence of biomass burning emissions influencing GOM levels at Villum.~~

4 Discussion

700 **4.1 Factors influencing event vs. non-event periods**

~~Event 1a was the only event during 2019 to experience a simultaneous decrease in GEM and an increase in GOM. Event 3 was the only event during the 2020 to experience a simultaneous decrease in GEM and increase in GOM.~~

705 For Events 1a, 1b, 2, 4, and 5, the ~~ground~~ ground-level meteorological parameters mainly associated with GOM enhancement are higher levels of radiation, lower RH, H_2O mixing ratios, and accumulated precipitation when compared to non-event periods (Table S1). For Event 3, radiation was low at the beginning of the event, and temperature and RH displayed an opposite pattern relative to the rest of the events, although H_2O mixing ratios and accumulated precipitation were both low. For the non-event periods in 2019, radiation and temperature were lower while H_2O mixing ratios, accumulated precipitation, and the RH

710 were higher. For the 2020 campaign, non-event periods were more diverse although each displayed a dissimilar pattern in one or more parameters when compared to event periods. For example, at the beginning of the 2020 campaign and during the non-event period between Event 3 and 4, both H_2O mixing ratios and accumulated precipitation were low, however, radiation was also low, while the RH was high (Fig. 2). For the non-event period between Event 4 and 5a, radiation was sufficiently high but H_2O mixing ratios and accumulated precipitation were exceptionally high, while the temperature and RH fluctuated

715 throughout this period (Fig. 2). ~~Between the event periods and non-event periods of the 2019 campaign, temperature, RH, H_2O mixing ratio, accumulated precipitation, wind direction, solar radiation, GEM, and GOM were significantly different (Wilcoxon Rank Sum Test, 95 % CI); however, there was no significant difference for wind speed. Between the event periods and non-event periods of the 2020 campaign, temperature, RH, wind speed, wind direction, H_2O mixing ratio, accumulated precipitation, solar radiation, GEM, and GOM were significantly different (Wilcoxon Rank Sum Test, 95% CI).~~

720 The factors influencing event periods at ground level are high levels of radiation, low H_2O mixing ratios, accumulated precipitation, and RH. Higher levels of solar radiation enable the photolysis of reactive halogen species and lower RH and H_2O mixing ratios inhibit the partitioning of GOM into the liquid phase (Laurier, 2003; Soerensen et al., 2010; Brooks et al., 2011; Steen et al., 2011). Interestingly, none of the events were ~~not~~ linked to cold temperatures, which has been previously demonstrated to be associated with mercury oxidation through observations in the Arctic (Cole and Steffen, 2010; Ariya et al.,

725 2015; Steffen et al., 2015), theoretical studies (Shepler et al., 2007), and modeling (Toyota et al., 2014). The stability of the Hg-Br intermediate is highly temperature-dependent (Goodsite et al., 2004; Donohoue et al., 2006; Dibble et al., 2012; Goodsite et al., 2012). Lower temperatures aid in the formation of GOM from HgBr, for example, Skov et al. (2004) and Christensen et al. (2004) modeled a surface temperature below -4 °C for mercury depletion to occur in the Arctic, while Brooks et al. (2011) observed a temperature threshold of -15 °C for mercury oxidation to occur at Summit Station, atop the Greenlandic

730 ice sheet. It should be noted that Brooks et al. (2011) detected oxidized mercury at temperatures above this threshold but not above 0 °C. Tarasick and Bottenheim (2002) analyzed ozonesonde records and observed surface temperatures below -20 °C

were required for the occurrence of ozone depletion events. Furthermore, Halfacre et al. (2019) and Burd et al. (2017) demonstrated that a frozen heterogeneous surface is required for the propagation of halogen explosion events. Tarasick and Bottenheim (2002)The temperature at Villum ranged from -1.2 to 5.6 °C and from 2.4 to 13.5 °C during the 2019 and 2020 event periods, respectively. During AMDEs, ozone and GEM are positively correlated due to mutual reaction with halogen species and are both extremely depleted due to strong halogen explosion events in the boundary layer (Schroeder et al., 1998; Lindberg et al., 2002; Berg et al., 2003; Skov et al., 2004; Brooks et al., 2006; Simpson et al., 2015). However, during event periods ozone was consistently elevated over not only non-event periods but also background levels and displayed positive correlations with GOM during all events (Sect. 3.4, Table S1, and Fig. 7). While ozone mixing ratios were high during GOM enhancement events, they are an order of magnitude below levels reported in the upper troposphere/lower stratosphere (Talbot et al., 2007), and given the slow rate reaction coefficient (Pal and Ariya, 2004), ozone is an improbable first oxidant of mercury during these campaigns (Calvert and Lindberg, 2005), although ozone has recently been identified as a second oxidant of Hg^I (Saiz-Lopez et al., 2020). While ozone might be acting as a second oxidant of Hg^I, any depletions of ozone during GEM oxidation, either through reaction with the Hg^I intermediate or with halogen species, is likely masked by the elevated levels of ozone in the free troposphere. Therefore, the high ground-level temperatures, the increased ozone mixing ratios, and the positive correlations observed between ozone and GOM during all events cast doubt on the local in situ production of GOM in the boundary layer, given the thermal instability of the Hg^I intermediate.

To evaluate the differences between the air mass history for event periods and non-event periods, we used meteorological data at each step over the length of each back trajectory arriving during an event vs. non-event period, calculated an average (median ± m.a.d.), and utilized the Wilcoxon Rank Sum Test to compare the two datasets. For example, only meteorological data included in the red outline of Figs. 2 and 3 were used for calculating event period averages and testing for statistically significant differences against data not included in the red outline for non-event periods.

For Events 1a, 1b, 2, 3, and 5, air masses were, on average, colder, dryer, and experienced higher altitudes when compared to non-event periods, although there is considerable variability which is logical given the average is calculated over the entire trajectory length (see Table S2 for a statistical comparison). During the 2019 campaign, trajectory temperature, RH, precipitation, H_2O mixing ratio, radiation, and altitude were significantly different (Wilcoxon Rank Sum Test, 95% CI) between GOM enhancement event periods and non-event periods.

For the 2020 campaign, Events 3, 4, 5a, and 5b were , on average, colder, drier, experienced higher altitudes, and exposed to more intense solar radiation when compared to non-event periods, there is again considerable variability with m.a.d. values often overlapping between medians. During the 2020 campaign, trajectory temperature, RH, precipitation, H_2O mixing ratio, and altitude were significantly different (Wilcoxon Rank Sum Test, 95% CI) between GOM enhancement event periods and non-event periods. Radiation was not significantly different; this likely arises from the high levels of radiation experienced during non-event periods further backwards along the trajectories (Fig. 4).

The differences in air mass history between the event and non-event periods ~~might~~ may offer insight into the origin of GOM, given the doubt associated with in situ oxidation at the surface. In general, air masses during event periods were colder, drier, arrived from higher altitudes, spent more time above the mixed layer, and less time in a cloud (Table S2). Although, there are notable exceptions to this pattern: Event 3 experienced high RH values and spent over half of the 240 hours in a cloud, and Event 5a experienced high temperatures and elevated H_2O mixing ratios. Analogous to the ground-level meteorological parameters, the air mass history during non-event periods was missing one or more of these conditions compared to event periods. For example, during all non-event periods, air mass arrived from altitudes comparable to event periods although often experienced decreased radiation and high RH and H_2O mixing ratios, especially closer to Villum. The overall pattern of the air mass history for event periods appears to be cold, dry air masses arriving from above the mixed layer, higher altitudes, and having spent little time in a cloud. These temperature and altitude parameters are ~~also~~ interconnected, since with increasing altitude the temperature ~~and RH~~ will ~~naturally~~ decrease as the air becomes less dense.

This suggests the cold, dry, high altitudes of the free troposphere are facilitating the formation of GOM. ~~source of GOM during event periods~~

~~These parameters are also interconnected, since with increasing altitude temperature and RH will naturally decrease.~~

~~Given the favorable (Jiao and Dibble, 2015, 2017a)~~Colder temperatures in the free troposphere are likely facilitating the formation of GOM, by increasing the stability of the Hg^I intermediate, while low RHs, H_2O mixing ratios, and less time spent within a cloud are limiting uptake of GOM into the aqueous phase. Additionally, given the low surface resistance of GOM over snowpack (Skov et al. (2006) estimated a surface resistance of GOM close to zero), the occurrence of dry (and possibly wet) deposition will increase when air masses come in close contact with the surface layer (i.e., below the mixed layer), resulting in decreased concentrations. ~~(Lampert et al., 2012; Brooks et al., 2017), coupled with the trajectory altitude analysis of Sect. 3.2 showing event air masses following a gradual descent before reaching Villum, this could explain the warmer temperatures observed at ground level compared to the trajectory temperature, as air masses would bring warmer air from this temperature inversion to ground level.~~

N_{Coarse} was enhanced during event periods vs non-event periods and for every individual event except for 5b (Table S2). Coarse mode particles and aerosol optical depth have been shown to be connected to the recycling of bromine during spring in the free troposphere leading to a prolonged lifetime of BrO (Peterson et al., 2017; Bognar et al., 2020), through the recycling of halogens on aerosol surfaces. This suggests coarse mode particles could be providing a surface for the propagation of halogen plumes aloft as demonstrated by Peterson et al. (2017) and Simpson et al. (2017). ~~Thus, t~~hese observations ~~strongly~~ suggest coarse mode particles may be providing a heterogenous surface for the propagation of halogen species required for the formation of GOM and this process is facilitated in the cold, dry, and sunlit environment of the free troposphere ~~and the survival is governed by aqueous phase parameters (RH and H_2O mixing ratio) closer to the surface layer, as well as the~~

800 ~~accumulated precipitation along the trajectory path.~~ . These findings highlight the complex relationship between GOM formation, removal, and meteorological parameters during transport.

Previous studies have demonstrated the influence of the free troposphere on mercury concentrations within the boundary layer. In the northern hemisphere, the free troposphere has been established as a source of GOM through modeling studies (Gratz et al., 2015; Shah and Jaeglé, 2017) and observations from both aircraft campaigns (Talbot et al., 2007; Gratz

805 et al., 2015) and high altitude sites (Swartzendruber et al., 2006; Faïn et al., 2009; Weiss-Penzias et al., 2015; Fu et al., 2016). Faïn et al. (2009) reported similar observations of the free troposphere acting as a source of oxidized mercury at a high elevation site (3220 m above sea level) in the Rocky Mountains, USA. They also observed that the presence of GOM was dependent on RH. They hypothesized that the build-up of GOM in the free troposphere was governed exclusively by the existence of low RH, possibly due to the lack of scavenging by particles at low RH levels. Modeling studies have also shown the free

810 troposphere to be a source of GOM. Using the GEOS-Chem global chemical transport model, Holmes et al. (2006) and Holmes et al. (2010) identified ~~Br~~ bromine to be the dominant oxidant of GEM globally, with most of the oxidation occurring in the middle and upper troposphere. Shah and Jaeglé (2017) arrived at a similar conclusion using GEOS-Chem that much of the mercury oxidation by ~~Br~~ bromine occur~~s~~ in the middle and upper troposphere. Weiss-Penzias et al. (2015) compared the GEOS-Chem model output from two different mercury oxidation schemes (a standard run using ~~Br~~ bromine and an alternative

815 run using $OH–O_3$) with observations of mercury speciation (GEM and reactive mercury, which is a combination of GOM and PHg) from five high elevation sites. In both the model output and observations, they observed RM was negatively correlated with GEM and H_2O mixing ratios and positively correlated with ozone. They hypothesized RM was formed in the free tropospheric air from the photo-oxidation of GEM. These studies show the free troposphere to be a source of GOM globally, however, there are a limited number of field studies on GOM in the High Arctic summer and none, to the authors' knowledge,

820 on the influence of the free troposphere on GOM levels. These observations from other locations around the globe add credence to our hypothesis, as they all observed similar conditions during high levels of GOM as we did during event periods. Similar chemi~~cal processes~~tsy ~~ar~~eis likely the cause of the observations in this study; however, the Arctic atmosphere is largely separated from the mid-latitudes during summer on account of contraction of the polar dome, so there may be some differences in the dynamics, albeit unlikely (Holmes et al., 2010).

825 **4.2 Factors influencing individual events**

The general pattern associated with event vs non-event periods showed the cold, dry, sunlit free troposphere the likely origin of the GOM enhancement, although individual events did not always fit this description. Individual events displayed unique features which can offer insight into the specific origins of GOM in the Arctic summer.

Event 1a ~~and 1b both~~ followed the general pattern for ~~ground~~ ground-level meteorological parameters and air mass

830 history of dry, warm, and sunlit conditions at ground level (Fig. 1) and cold, dry, sunlit air masses arriving from elevated altitudes (Fig. 3 and 5), along with elevated N_{Coarse} and ozone. GOM during Event 1a was moderately negatively correlated with the H_2O mixing ratio and significant on the 95 % confidence level (CL) using the Spearman Rank correlation (Fig. 7a),

although no correlation was found for accumulated precipitation ~~possibly due to the high frequency of low values during times of elevated GOM concentrations~~ (Fig. 7b). GOM during Event 1a was also strongly positively correlated with ozone, N_{Coarse}, and BC on the 95 % CL (Fig. 7e, g, and i), indicating. ~~Given the correlation between GOM, BC, and N_{Coarse} during enhancement events,~~ biomass burning could be a potential factor influencing this event. While active fires might not be directly producing GOM (Friedli et al., 2003), they can explain elevated levels of N_{Coarse}, BC, and ozone (Andreae, 2019). Indeed, trajectories during Event 1a experienced extensive ~~influence from~~ intersection with active fires, especially during the first half of the event, ~~on times scales of 240 hours and~~ under a range of altitudes during transport (Fig. 5a). This range of altitudes could allow for injected active fire emissions to be entrained into the event air mass. ~~. This range of altitudes could allow for injected active fire emissions to be entrained in the event air mass (Fig 5a).~~ Coarse mode particles emitted from active fires could provide a heterogenous surface for halogen recycling. Although there were no intersections with trajectories and active fires during the second half of this event, coarse mode particles could arise from other sources (e.g., sea salt aerosol) or result from interactions occurring beyond the length of the trajectories. ~~It is important to note that on timescales of 120 hours, there were no intersections of trajectories and active fires.~~ Thus, while Event 1a exhibited the general pattern for GOM formation in the cold, dry, and sunlit free troposphere, emissions of coarse mode aerosols from active fires likely ~~had an influence during~~ influenced this event.~~.~~

On the morning of August 26, GOM concentrations dropped to zero which marked the end of Event 1a and the beginning of Event 1b. Event 1b experienced similar conditions at ground level, although the air masses were colder, drier, and from higher altitudes with increased radiation (Table S2 and Fig. 3). During Event 1b, GOM displayed a moderately negative correlation with H_2O mixing ratios, although was only significant on the 90 % CL, and was not correlated with accumulated precipitation (Fig. 7a and c). ~~This is possibly due to a small range of values for accumulated precipitation and the low number of data points used in this correlation.~~ GOM during Event 1b was strongly positively correlated with ozone on the 95 % CL and displayed moderate correlations with N_{Coarse} and BC however they were not statistically significant (Fig. 7e, g, and i). Air masses during this event were confined to the Arctic, exhibited no intersection with active fires, and experienced extensive surface layer contact 50 hours before arrival, yet this event showed similar levels of GOM when compared to Event 1a. Even though air masses experienced surface layer contact 50 hours backward, they were extremely dry and previously resided aloft under cold temperatures (Fig. 3). These conditions are conducive for the formation of GOM and inhibit its removal. The source of coarse mode particles could be emissions from active fires on timescales greater than 240 hours, given the strong correlation with ozone and the moderate yet insignificant correlations with N_{Coarse} and BC (Fig. 7g and i), or possibly other sources such as sea salt. GOM during Event 1b appears to be formed in the cold, dry, sunlit free troposphere, with an unknown source of coarse mode aerosols.

~~Given the strong correlation with ozone, the moderate yet insignificant correlations with N_{Coarse} and BC, and the spatial as well as vertical extent, it appears Event 1b was likely the result of residual emissions from active fires and any direct influence of active fires probably occurred on timescales greater than 240 hours.~~

Event 2 displayed the overall pattern of warm, dry, sunlit conditions at ground level accompanied by cold, dry, sunlit conditions in the free troposphere, ~~like~~ similar to Event 1a and 1b, although Event 2 exhibited increased accumulated precipitation and H_2O mixing ratios relative to the other events in 2019 (Fig. 1c). GOM during Event 2 showed a weak correlation with H_2O mixing ratios and accumulated precipitation, with only the former being significant on the 95 % CL (Fig. 7a and c). N_{Coarse} and BC showed no enhancement and were constant, while ozone started low and increased throughout the event. GOM during Event 2 was weakly positively correlated with ozone, N_{Coarse}, and BC and none showed a significant correlation at the 95 % CL (Fig. 7e, g, and i). Air masses at the beginning of Event 2 originated from the Greenland Sea then transitioned ~~followed~~to a circulation pattern starting near Eurasia before traversing over North America (Fig. 5), and the intersection with active fires was present albeit infrequent. If active fires were influencing GOM concentrations during this event, their signature is likely masked by the increased levels of accumulated precipitation and H_2O mixing ratios, which is also likely responsible for the decreased levels of GOM, N_{Coarse}, and BC during Event 2 relative to ~~Events~~ 1a and 1b (Table S2), as well as weak correlations. Therefore, the observed levels during Event 2 ~~is~~are likely the result of GOM formation in the cold, dry, sunlit free troposphere and the source of coarse mode particles was possibly active fires, ~~wh~~with the decreased levels of GOM, N_{Coarse}, and BC ~~ich~~ ~~was affected by~~due to wet removal ~~before arrival at Villum~~.

Event 3 ~~exhibited~~showed the largest observed levels of GOM but showed no obvious features indicating the cause. Radiation, RH, and temperature displayed the opposite pattern for GOM formation, with low levels of radiation, high and increasing values of RH, and decreasing temperatures during the beginning of the event. H_2O mixing ratio and accumulated precipitation both showed low values compared to non-event periods (Fig. 2b), with GOM showing ~~and~~ a moderate correlation with H_2O mixing ratios and no correlation with accumulated precipitation (Fig. 7b and c). Ozone showed an enhancement during this event but was low compared to other events, and did not show a correlation with GOM (Fig. 7f). N_{Coarse} and BC both displayed enhancements during this event and were both strongly correlated with GOM (Fig. 7h and j). Air masses originated from the Arctic Ocean and the Barents Sea, with only one active fire intersecting trajectories in western Russia (Fig. 5d). The air mass history of this event exhibited the highest temperatures and RHs, the lowest altitudes, as well as the most time spent above the mixed layer and the most time within a cloud (Table S2). However, this event did experience cold, dry, and sunlit conditions several hours before arrival (Fig. 4), and a steep descent before arrival (Fig 5d). The free troposphere has been shown to be a source of aerosol particles to the boundary layer in the Arctic through entrainment and cloud-mediated transport (Igel et al., 2017). It is possible that the extended time this event spent within a cloud resulted in the cloud mediated transport of free troposphere constituents to the surface layer (Igel et al., 2017), although possible aqueous phase oxidation of Hg^0 cannot be ruled out (Lin and Pehkonen, 1998; Lyman et al., 2020). Activated and interstitial aerosol particles and GOM could also have undergone evaporation in the warm surface layer temperatures (Fig. 2). This event experienced favorable conditions for GOM formation (cold, dry, and sunlit air masses from aloft) shortly before arrival followed by a quick descent

into the surface layer, and these conditions could create a situation where GOM formation is favored and the removal is inhibited, resulting in the high levels. This is however a hypothesis that requires further research.

Event 4 occurred approx. one day after Event 3, experienced a similar geographical origin, similar levels of ozone, accumulated precipitation, N_{Coarse}, and BC, however, the ground level meteorological parameters showed differences in the amount of radiation, H_2O mixing ratios, temperatures, and RHs (Fig. 2 and 5, Table S1). The temperature and RH during Event 4 displayed the general pattern observed for GOM formation although contrasted with the pattern of temperature and RH during Event 3. While the H_2O mixing ratios at ground level were higher during Event 4 compared to Event 3, they showed no correlation with GOM (Fig. 7b). GOM and ozone during Event 4 showed a weak and insignificant correlation (95 % CL) and showed a moderate significant negative correlation with BC and none with N_{Coarse} (Fig. 7f, h, and j). The air mass history showed Event 4 experienced lower temperatures, RHs, H_2O mixing ratios, and time spent within a cloud as well as higher radiation and altitudes but a similar amount of time above the mixed layer compared to Event 3 (Table S2). Event 4 did not show as steep of a descent as Event 3 (Fig. 5d and e). The amount of time spent within a cloud could indicate cloud-mediated transport to the surface layer and the slower rate of descent, coupled with the increased H_2O mixing ratios at ground level, could lead to increased removal of GOM before being observed at Villum. Event 3 and 4 showed similarities that could indicate cloud-mediated transport from the free troposphere to the surface layer, however, there exist dissimilarities that suggest that Event 4 could be the result of entrainment of GOM formed in the cold, dry, sunlit free troposphere. It appears that the increased H_2O mixing ratios at ground level during Event 4 is the reason for the decreased levels of GOM compared to Event 3. A definitive conclusion for the origin of this event is currently unavailable.

Event 5a exhibited high radiation, H_2O mixing ratios, ozone, and temperature along with low accumulated precipitation, RH, N_{Coarse}, and BC at ground level (Fig. 2.). GOM during this event was strongly negatively and significantly correlated with H_2O mixing ratios but displayed no correlation with accumulated precipitation on the 95% CL (Fig. 7b and d). This event showed a strongly positive correlation between GOM and ozone and moderately negative, albeit significant, correlations with N_{Coarse} and BC (Fig. 7f, h, and j). This event showed air massesAir masses for this event arriveding consistently from Northern Scandinavia after low low-level transport with high temperatures, RHs, and H_2O mixing ratios and being exposed to less radiation (Fig. 4 and 5f). Air masses circulated in the vicinity of active fires in Northern Scandinavia before being transported to Villum with several intersections between trajectories and active fires (Fig. 5f). These conditions

are opposite to the pattern identified for GOM formation, the cause of the observed GOM levels could therefore be the extensive interactions between trajectories and active fires, although the influence of anthropogenic pollution cannot be ruled out. ~~Air masses circulated in the vicinity of active fires in Northern Scandinavia before being transported to Villum.~~ Air masses were, however, warm, wet, and traveled at low altitudes under little radiation, and therefore it is reasonable to expect this air mass to be depleted in N_{Coarse} and BC as well as GOM, given the high values of hydrological-related parameters, ~~Additional emissions of GOM from the European continent could have added to the GOM reservoir, thus sustaining the GOM levels as N_{Coarse} and BC were removed via the aqueous phase.~~ Ozone was elevated and strongly correlated with GOM during Event 5a (Fig. 2 and 7). ~~o~~ Ozone could originate from both anthropogenic and natural sources and ozone is only slightly water-soluble leading to less efficient wet removal (Sander, 2015). ~~It is perplexing how active fire emissions under such adverse conditions to GOM formation could lead to the observed levels of GOM and low concentrations of N_{Coarse} and BC without the influence of unrevealed factors such as additional emissions either occurring after 240 hours or during transport to Villum. A plausible explanation is that the biomass burning was at a high temperature lead to emission of small aerosols and low levels of BC. In the absence of extra material in the atmosphere they will remain in the nucleation and Aitken mode that has a short atmospheric lifetime towards deposition leaving GOM as the only constituent. The low altitudes and surface layer contact air masses experienced during transport could lead to the removal of aerosol particles, and any BC contained within them, through deposition (Fig. 5f). Particles smaller than 300 nm will not be detected by the OPS, although it is conceivable that they were still aiding in the recycling of halogen species.~~ GOM observed during Event 5a appears to be the result of emissions either from active fires or anthropogenic sources in Northern Scandinavia~~Further measurements and modeling of GOM in the High Arctic during summertime are required to investigate these processes in greater detail~~.

Air masses shifted from circulating Northern Scandinavia to the Greenlandic continent on August 1, which coincided with the start of Event 5b. This event is a good example ~~for~~ of the observed pattern of GOM formation: warm, dry, sunlit conditions at ground level and cold, dry, sunlit air masses from the free troposphere (Fig 2 and 4)~~(Brooks et al., 2011)~~. GOM during this event exhibited no correlation with H_2O mixing ratio, accumulated precipitation, or BC while being strongly correlated with ozone and moderately positively correlated with N_{Coarse} (Fig. 7). Enhancements of GOM, which exhibited a positive correlation with ozone, have also been observed during subsidence events in Antarctica as well (Brooks et al., 2008; Pfaffhuber et al., 2012). However, concentrations of N_{Coarse} and BC were extremely low, which is expected of upper tropospheric air masses above the polar dome, which is extremely pristine (Schulz et al., 2019). With the low concentration of N_{Coarse}, there appears not to be a heterogenous surface for halogen propagation, although this could be due to particles smaller than 0.3 µm facilitating halogen propagation. Another source of reactive halogen species is the photolysis of halocarbons (Yang et al., 2005; Simpson et al., 2015), although Gratz et al. (2015) found this source to be too slow to explain mercury oxidation in the upper troposphere. (Yang et al., 2005); Brooks et al. (2011); (Thomas et al., 2012; Simpson et al., 2015)The origins of GOM during Event 5b appear to be the result of formation in the cold, dry, sunlit free troposphere over the Greenlandic ice sheet from an unknown source of halogens.

It is interesting to note the vast differences in air mass history for Events 5a and 5b even though both events observed similar levels of GEM, GOM, ozone, and N_{Coarse} (Fig 2). The main differences between these events lie in the H_2O mixing ratios and RH (both at ground level and during transport), the temperature during transport, and the altitude (Table S1 and S2). The median BC concentration for Event 5a was over double that of 5b, although was low compared to other events influenced by active fires i.e., Events 1a and 1b. (Table S1). During Event 5a, air masses were warmer, wetter, and traveled at lower altitudes compared to Event 5b; these conditions could lead to the removal of GOM, N_{Coarse}, and BC through deposition and uptake into the aqueous phase. It is an intriguing observation that air masses that originated from the European continent and were subject to increased hydrological-related parameters during transport (Event 5a) have a similar composition of GOM, ozone, N_{Coarse}, and BC to air masses that originated over Greenland (Event 5b). Currently, an explanation for these observations is unknown and further research is required to fully resolve the interactions of anthropogenic and natural emissions, transport-related processes, and removal mechanisms that are responsible for these observations.

There were two episodes of enhanced N_{Coarse} and BC, as presented in Sect. 3.5 and shown in Fig. 6, which appear to be the result of active fire emissions. These two events were interrupted by large amounts of accumulated precipitation on August 27 (Fig. 2). The air mass history during these two episodes shows warm and wet low altitude trajectories with little radiation (Fig. 3); these conditions are inconducive towards GOM formation as indicated by the low levels of GOM, however, they show greatly enhanced concentrations of N_{Coarse} and BC. Figures 6b and c show the geographical extent and intersection of air masses with active fires during the two episodes, respectively. The first few hours of the first episode show trajectories arriving from the central Arctic Ocean, which could arise from emissions in western Russia on longer timescales than 240 hours, however, the reason is unknown at this time. it might be explained by the The trajectories for both episodes intersect active fires in Northern Scandinavia and Russia, this region of Russia has been shown to emit large amounts of BC through flaring (Huang et al., 2015; Böttcher et al., 2021). It should be noted that the term active fires represent a thermal anomaly detected by MODIS and VIIRS and cannot be distinguished between vegetation fires and fires due to flaring (Schroeder et al., 2014). The low-level transport, under wet conditions, will likely result in the removal of a fraction of the emissions from these active fires. However, fresh BC emissions are very hydrophobic (Dusek et al., 2006), and might not be removed as efficiently during transport. Event 5a experienced air mass arriving from Northern Scandinavia having circulated over several active fires, although no large increase in BC was observed (Fig. 2 and 5). The large increase in N_{Coarse} and BC during these two episodes is therefore likely due to the flaring activities in Russia while the observed GOM in Event 5a could possibly be due to vegetation fires, although this cannot be confirmed in this study and anthropogenic sources remain a possibility.

1000 Stohl (2006); Zheng et al. (2021)Event 1a was the only event during 2019 to experience a simultaneous decrease in GEM and an increase in GOM.
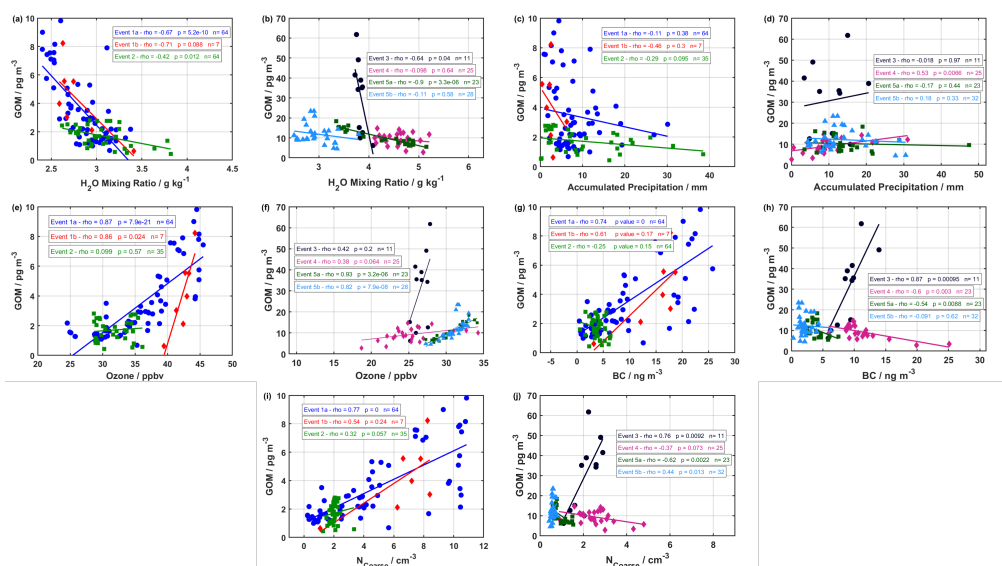
Figure. 7. Correlation analysis of GOM with **(a)** and **(b)** H_2O mixing ratio, **(c)** and **(d)** accumulated precipitation, **(e)** and **(f)** ozone, **(g)** and **(h)** BC, **(i)**, and **(j)** N_{Coarse}, for the 2019 and 2020 campaigns, respectively. The Spearman Rank correlation
1005 coefficient (rho), the p-value, and the number of observations are listed for each event in each panel.

3.6 Possible halogen sources

With the source region of the observed GOM identified as the cold, dry free troposphere, what are the possible sources of
halogen species? Sources in the Arctic boundary layer of these reactive halogen species include snowpack, sea ice, frost
1010 flowers, refreezing leads, sea-salt aerosol, and liable halogen reservoir species (i.e., halocarbons and inorganic bromine)
(Kaleschke et al., 2004; Brooks et al., 2006; Simpson et al., 2015; Peterson et al., 2018). As demonstrated by Halfacre et al.
(2019) and Burd et al. (2017), a frozen heterogeneous surface is required for the propagation of halogen explosions. However,
with the altitude and meteorological conditions of back-trajectories indicating free tropospheric air masses (Sect. 3.2), as well
as ground-level temperatures regularly above 0 °C and little snow cover during both campaigns, emissions from snowpack,
1015 sea ice, and frost flowers appear to be unlikely sources in this study.

Studies in the subtropics have revealed that the degradation of organobromides in the free troposphere is insufficient to explain the Br needed for Hg oxidation (Gratz et al., 2015)and they speculated that Br_y originated from strong convection in intertropical convection zone. Thus, focus needs to be on Br_y input from surface sources also in the Arctic as organo bromides are expected to be distributed ubiquitously in the troposphere due to their atmospheric lifetime.

Coarse mode particles and aerosol optical depth have been shown to be connected to reactivation of brominewith BrO enhancement events during spring in the free troposphere leading to a prolonged lifetime of Br_y (Peterson et al., 2017; Bognar et al., 2020), through the recycling of halogens on sea salt aerosol surfaces in the troposphere. Indeed, previous studies have found that enhancement of sea salt aerosols (SSA) and heterogeneous reactions on SSA are the main key processes for atmospheric BrOx cycle activation depletions of bromine in coarse mode particles in the polar regions (Giordano et al., 2018; Hara et al., 2018; Frey et al., 2020). In the present study during Arctic summer and 10 degrees further north compared to the study area in the previous cited studies, tThe positive correlation between GOM and N_{Coarse} observed during our study (Fig. 7), could consequently likewise be due to halogens being activated and recycled on coarse mode aerosol particle surfaces. As stated in Sect. 3.5, we hypothesize isupportingnstead that the positive correlation between GOM and N_{Coarse} is due to reactivation of BrOx decreased sinks in the free troposphere enhancing Br induced oxidation of GEM, although the contribution from halogen activation and recycling cannot be ruled out without high time resolution measurements of aerosol chemical composition. While N_{Coarse} is low throughout both campaigns, coarse mode particles are likely one of the few heterogeneous surfaces in the free troposphere, therefore, they could have a large impact on halogen recycling.

One biogenic source of halogen species is the emission of halocarbons from marine emissions by micro-organisms, e.g., macroalgae, ice algae, and phytoplankton (Sturges et al., 1992; Quack and Wallace, 2003). Thin, porous sea ice has been shown to readily emit halocarbons during the Arctic summer (Atkinson et al., 2014), and our studies were conducted in July–September when sea ice is at a minimum (Comiso, 2012). Once emitted from the ocean, these halocarbons are photolyzed in the troposphere to produce reactive halogen species (Yang et al., 2005). In our study, the vertical extent of air mass back-trajectories during enhancement events was consistently from aloft, under cold, dry, and sunlit conditions. The spatial extent showed no consistent source regions, indicating that GEM oxidation is ubiquitous in the free troposphere of the High Arctic. Given the vertical profile and spatial extent of air masses during enhancement events, biogenic emissions of halocarbons and emissions of coarse mode aerosol particles from open waters and marginal ice zones would therefore represent a widespread source throughout the Arctic but transport from previously enriched air masses from more southern latitudes might be important as well.

Therefore, we hypothesize that the oxidants responsible for the mercury oxidation result from the photolysis of short-lived halocarbons emitted from marine biological activity and were possibly sustained via recycling on aerosol surfaces. However, this is a working hypothesis and further research is needed to confirm this theory, specifically column and in situ measurements of reactive halogen species, their precursors, aerosol chemical composition, and mercury species.

4 5 Summary and cConclusion

While the behavior of GEM and GOM during the spring in the High Arctic has received much attention, the dynamics of GOM in the late summer/autumn have seldom been investigated. Therefore, we conducted measurements of GEM, GOM, PHg (only in 2020), meteorological parameters, ozone, and aerosol particle physical properties at Villum Research Station in Northeastern Greenland during the High Arctic summer in 2019 and 2020. The general pattern observed for events of GOM enhancement appears to be cold, dry, sunlit air masses from the free troposphere, as opposed to the low levels of GOM connected with warm and wet air masses with little radiation observed during non-event periods. Coarse mode aerosols provided a heterogenous surface for halogen propagation during certain events while the source of halogens during other events remains unknown. Analysis of individual events displayed unique origins. GOM observed during Events 1a, 1b, and 2 were likely formed in the cold, dry, sunlit free troposphere with contributions of coarse mode particles from active fires and possibly other sources. Decreased concentrations of GOM during Event 2 were likely due to wet removal. GOM observed during Events 3 and 4 appears to have formed in the cold, dry, sunlit free troposphere from an unknown source of halogens, other processes are likely contributing, and therefore specific origins of these events cannot be ascertained. The observed GOM during Event 5a was likely the result of emissions from either active fires or anthropogenic activities in Northern Scandinavia. The origins of GOM during Event 5b appear to be the result of formation in the cold, dry, sunlit free troposphere over the Greenlandic ice sheet from an unknown source of halogens. Two episodes of flaring emissions from Russia were observed which did not contribute to enhanced GOM levels.

By probing the air mass history during five GOM enhancement events, we show that enhancements of GOM are largely controlled by temperature, RH, and solar radiation. Analysis of air mass history provides direct evidence of influence from the free troposphere, while measurements of ozone, BC, and coarse mode particle number concentration support this conclusion. Biomass burning was not found to contribute to GOM enhancement events, although it affects N_{Coarse} and BC concentrations through long-range transport. These measurements and analyses provide insight into the behavior of GOM during summer in at athe High Arctic station and highlight the complex relationships between GOM formation, removal mechanisms, atmospheric constituents, and meteorological parameters during transportprovide validation for previous studies from the mid-latitudes, where the free troposphere has been identified to be a source of GOM. . The behavior of mercury in a changing Arctic climate is still an area with many knowledge gaps, and this work seeks to bridge those gaps, although further research (especially long-term, mercury speciation measurements) is needed.

With changing conditions in the Arctic (i.e., rising temperatures, melting sea ice, longer melt seasons), there is large uncertainty regarding the oxidation and deposition of mercury in response to these changes (Stern et al., 2012). For example, with the Arctic becoming warmer (Jiang et al., 2020) and therefore wetter, the feedback mechanisms on mercury oxidation remain an important scientific question. Warming temperatures will decrease the stability of the Hg^I intermediate and possibly increase biogenic production of halocarbons as well as increasing atmospheric water vapor, which will favor increased uptake of oxidized mercury into the particulate aqueous phase and its removal by wet deposition. Forest fires are

expected to increase in the future (Flannigan et al., 2009; Kelly et al., 2013), which could lead to an increase in coarse mode particles. The magnitude of these contrasting effects and their consequences for GOM levels in the High Arctic is still an open question. Given the positive correlation between GOM and aerosol coarse mode particles, and their role in halogen activation, changes in the size distribution and chemical composition of aerosol particles could have implications for mercury oxidation. Recent trends in declining sea ice (Stroeve et al., 2012) could increase the sea salt and total aerosol burden, thus potentially increasing mercury oxidation and deposition via increased halogen recycling and particulate mercury deposition. Declining sea ice could also increase GEM evasion from the Arctic Ocean, shifting the Arctic Ocean from a sink to a source (Ariya et al., 2004; Dastoor and Durnford, 2014). Future studies addressing the contribution of the free troposphere to boundary layer GOM concentrations along with flux measurements of dry and wet deposition of GOM in the summer will help answer these questions. The presented work aims to bridge some of the knowledge gaps in mercury processing although further research is needed to better advance our understanding of how how the behavior of atmospheric mercury will respond in a changing climate. Specifically, we recommend long-term measurements of mercury speciation at more High Arctic stations to obtain more information on seasonality, trends, and the geospatial distribution of atmospheric mercury species.

Financial Support. This study was funded by the Danish Environmental Protection Agency (DANCEA funds for Environmental Support to the Arctic Region project; grant no. 2019-7975) and by the European ERA-PLANET projects of iGOSP and iCUPE (consortium agreement no. 689443 for both projects). Villum Foundation is gratefully acknowledged for financing Villum Research Station.

Acknowledgments. Thanks to the Royal Danish Air Force, Arctic Command, and the staff at Station Nord for providing logistic support to the project. Christel Christoffersen and Keld Mortensen are gratefully acknowledged for their technical support. We thank NOAA for use of the HYSPLIT model. We thank the NSIDC for use of sea ice data. We acknowledge the use of data from the NASA FIRMS application (https://firms.modaps.eosdis.nasa.gov/).

Data availability. All data used in this publication are available to the community and can be accessed by request to the corresponding author Jakob Boyd Pernov (jbp@envs.au.dk).

Author contributions. JBP, BJ, HSK designed the study. JBP and BJ performed the mercury and aerosol sizing measurements. DCT and AM performed the black carbon measurements. JBP performed all data analysis and air mass history analysis. HSK was the project leader led the project. JBP wrote the manuscript with comments from all co-authors.

Competing interests. The authors declare that they have no conflict of interest.

1115

References

AMAP: AMAP Assessment 2011: Mercury in the Arctic, Arctic Monitoring and Assessment Programme (AMAP), Oslo, Norway, xiv + 193 pp., 2011.

Ambrose, J. L.: Improved methods for signal processing in measurements of mercury by Tekran® 2537A and 2537B instruments, Atmos. Meas. Tech., 10, 5063-5073, 10.5194/amt-10-5063-2017, 2017.

Andreae, M. O.: Emission of trace gases and aerosols from biomass burning - an updated assessment, Atmos Chem Phys, 19, 8523-8546, 10.5194/acp-19-8523-2019, 2019.

Angot, H., Dastoor, A., De Simone, F., Gårdfeldt, K., Gencarelli, C. N., Hedgecock, I. M., Langer, S., Magand, O., Mastromonaco, M. N., Nordstrøm, C., Pfaffhuber, K. A., Pirrone, N., Ryjkov, A., Selin, N. E., Skov, H., Song, S., Sprovieri, F., Steffen, A., Toyota, K., Travnikov, O., Yang, X., and Dommergue, A.: Chemical cycling and deposition of atmospheric mercury in polar regions: review of recent measurements and comparison with models, Atmos Chem Phys, 16, 10735-10763, 10.5194/acp-16-10735-2016, 2016.

Ariya, P. A., Dastroor, A. P., Amyot, M., Schroeder, W. H., Barrie, L., Anlauf, K., Raofie, F., Ryzhkov, A., Davignon, D., Lalonde, J., and Steffen, A.: The Arctic: a sink for mercury, Tellus B: Chemical and Physical Meteorology, 56, 397-403, 10.3402/tellusb.v56i5.16458, 2004.

Ariya, P. A., Amyot, M., Dastoor, A., Deeds, D., Feinberg, A., Kos, G., Poulain, A., Ryjkov, A., Semeniuk, K., Subir, M., and Toyota, K.: Mercury physicochemical and biogeochemical transformation in the atmosphere and at atmospheric interfaces: a review and future directions, Chem Rev, 115, 3760-3802, 10.1021/cr500667e, 2015.

Arnold, S. R., Emmons, L. K., Monks, S. A., Law, K. S., Ridley, D. A., Turquety, S., Tilmes, S., Thomas, J. L., Bouarar, I., Flemming, J., Huijnen, V., Mao, J., Duncan, B. N., Steenrod, S., Yoshida, Y., Langner, J., and Long, Y.: Biomass burning influence on high-latitude tropospheric ozone and reactive nitrogen in summer 2008: a multi-model analysis based on POLMIP simulations, Atmos. Chem. Phys., 15, 6047-6068, 10.5194/acp-15-6047-2015, 2015.

Aspmo, K., Temme, C., Berg, T., Ferrari, C., Gauchard, P. A., Fain, X., and Wibetoe, G.: Mercury in the atmosphere, snow and melt water ponds in the North Atlantic Ocean during Arctic summer, Environmental Science & Technology, 40, 4083-4089, 10.1021/es052117z, 2006.

Atkinson, H. M., Hughes, C., Shaw, M. J., Roscoe, H. K., Carpenter, L. J., and Liss, P. S.: Halocarbons associated with Arctic sea ice, Deep Sea Research Part I: Oceanographic Research Papers, 92, 162-175, https://doi.org/10.1016/j.dsr.2014.05.012, 2014.

Backman, J., Schmeisser, L., Virkkula, A., Ogren, J. A., Asmi, E., Starkweather, S., Sharma, S., Eleftheriadis, K., Uttal, T., Jefferson, A., Bergin, M., Makshtas, A., Tunved, P., and Fiebig, M.: On Aethalometer measurement uncertainties and an instrument correction factor for the Arctic, Atmos. Meas. Tech., 10, 5039-5062, 10.5194/amt-10-5039-2017, 2017.

Berg, T., Sekkesæter, S., Steinnes, E., Valdal, A.-K., and Wibetoe, G.: Springtime depletion of mercury in the European Arctic as observed at Svalbard, Science of The Total Environment, 304, 43-51, https://doi.org/10.1016/S0048-9697(02)00555-7, 2003.

Bognar, K., Zhao, X., Strong, K., Chang, R. Y.-W., Frieß, U., Hayes, P. L., McClure-Begley, A., Morris, S., Tremblay, S., and Vicente-Luis, A.: Measurements of Tropospheric Bromine Monoxide Over Four Halogen Activation Seasons in the Canadian High Arctic, Journal of Geophysical Research: Atmospheres, 125, e2020JD033015, 10.1029/2020jd033015, 2020.

Bolton, D.: The Computation of Equivalent Potential Temperature, Monthly Weather Review, 108, 1046-1053, 10.1175/1520-0493(1980)108<1046:Tcoept>2.0.Co;2, 1980.

Brooks, I. M., Tjernström, M., Persson, P. O. G., Shupe, M. D., Atkinson, R. A., Canut, G., Birch, C. E., Mauritsen, T., Sedlar, J., and Brooks, B. J.: The Turbulent Structure of the Arctic Summer Boundary Layer During The Arctic Summer Cloud-Ocean Study, Journal of Geophysical Research: Atmospheres, 122, 9685-9704, https://doi.org/10.1002/2017JD027234, 2017.

Brooks, S., Arimoto, R., Lindberg, S., and Southworth, G.: Antarctic polar plateau snow surface conversion of deposited oxidized mercury to gaseous elemental mercury with fractional long-term burial, Atmospheric Environment, 42, 2877-2884, https://doi.org/10.1016/j.atmosenv.2007.05.029, 2008.

Brooks, S., Moore, C., Lew, D., Lefer, B., Huey, G., and Tanner, D.: Temperature and sunlight controls of mercury oxidation and deposition atop the Greenland ice sheet, Atmos Chem Phys, 11, 8295-8306, 10.5194/acp-11-8295-2011, 2011.

Brooks, S. B., Saiz-Lopez, A., Skov, H., Lindberg, S. E., Plane, J. M. C., and Goodsite, M. E.: The mass balance of mercury in the springtime arctic environment, Geophysical Research Letters, 33, 10.1029/2005gl025525, 2006.

Browse, J., Carslaw, K. S., Arnold, S. R., Pringle, K., and Boucher, O.: The scavenging processes controlling the seasonal cycle in Arctic sulphate and black carbon aerosol, Atmos. Chem. Phys., 12, 6775-6798, 10.5194/acp-12-6775-2012, 2012.

Burd, J. A., Peterson, P. K., Nghiem, S. V., Perovich, D. K., and Simpson, W. R.: Snowmelt onset hinders bromine monoxide heterogeneous recycling in the Arctic, Journal of Geophysical Research: Atmospheres, 122, 8297-8309, 10.1002/2017jd026906, 2017.

Böttcher, K., Paunu, V.-V., Kupiainen, K., Zhizhin, M., Matveev, A., Savolahti, M., Klimont, Z., Väätäinen, S., Lamberg, H., and Karvosenoja, N.: Black carbon emissions from flaring in Russia in the period 2012–2017, Atmospheric Environment, 254, 118390, https://doi.org/10.1016/j.atmosenv.2021.118390, 2021.

Calvert, J. G., and Lindberg, S. E.: Mechanisms of mercury removal by O3 and OH in the atmosphere, Atmospheric Environment, 39, 3355-3367, https://doi.org/10.1016/j.atmosenv.2005.01.055, 2005.

Cavalieri, D. J., Parkinson, C. L., Gloersen, P., and Zwally, H. J.: Sea Ice Concentrations from Nimbus-7 SMMR and DMSP SSM/I-SSMIS Passive Microwave Data, Version 1., https://doi.org/10.5067/8GQ8LZQVL0VL. , 1996.

Christensen, J. H., Brandt, J., Frohn, L. M., and Skov, H.: Modelling of Mercury in the Arctic with the Danish Eulerian Hemispheric Model, Atmos. Chem. Phys., 4, 2251-2257, 10.5194/acp-4-2251-2004, 2004.

Cole, A. S., and Steffen, A.: Trends in long-term gaseous mercury observations in the Arctic and effects of temperature and other atmospheric conditions, Atmos. Chem. Phys., 10, 4661-4672, 10.5194/acp-10-4661-2010, 2010.

Comiso, J. C.: Large Decadal Decline of the Arctic Multiyear Ice Cover, Journal of Climate, 25, 1176-1193, 10.1175/jcli-d-11-00113.1, 2012.

Croft, B., Martin, R. V., Leaitch, W. R., Tunved, P., Breider, T. J., amp, apos, Andrea, S. D., and Pierce, J. R.: Processes controlling the annual cycle of Arctic aerosol number and size distributions, Atmos Chem Phys, 16, 3665-3682, 10.5194/acp-16-3665-2016, 2016.

Dastoor, A. P., Davignon, D., Theys, N., Van Roozendael, M., Steffen, A., and Ariya, P. A.: Modeling Dynamic Exchange of Gaseous Elemental Mercury at Polar Sunrise, Environmental Science & Technology, 42, 5183-5188, 10.1021/es800291w, 2008.

Dastoor, A. P., and Durnford, D. A.: Arctic Ocean: Is It a Sink or a Source of Atmospheric Mercury?, Environmental Science & Technology, 48, 1707-1717, 10.1021/es404473e, 2014.

Dibb, J. E., Arsenault, M., Peterson, M. C., and Honrath, R. E.: Fast nitrogen oxide photochemistry in Summit, Greenland snow, Atmospheric Environment, 36, 2501-2511, 10.1016/s1352-2310(02)00130-9, 2002.

Dibble, T. S., Zelie, M. J., and Mao, H.: Thermodynamics of reactions of ClHg and BrHg radicals with atmospherically abundant free radicals, Atmos. Chem. Phys., 12, 10271-10279, 10.5194/acp-12-10271-2012, 2012.

DiMento, B. P., Mason, R. P., Brooks, S., and Moore, C.: The impact of sea ice on the air-sea exchange of mercury in the Arctic Ocean, Deep Sea Research Part I: Oceanographic Research Papers, 144, 28-38, https://doi.org/10.1016/j.dsr.2018.12.001, 2019.

Donohoue, D. L., Bauer, D., Cossairt, B., and Hynes, A. J.: Temperature and Pressure Dependent Rate Coefficients for the Reaction of Hg with Br and the Reaction of Br with Br: A Pulsed Laser Photolysis-Pulsed Laser Induced Fluorescence Study, The Journal of Physical Chemistry A, 110, 6623-6632, 10.1021/jp054688j, 2006.

1225

Douglas, T. A., Sturm, M., Blum, J. D., Polashenski, C., Stuefer, S., Hiemstra, C., Steffen, A., Filhol, S., and Prevost, R.: A Pulse of Mercury and Major Ions in Snowmelt Runoff from a Small Arctic Alaska Watershed, Environmental Science & Technology, 51, 11145-11155, 10.1021/acs.est.7b03683, 2017.

1230

Douglas, T. A., and Blum, J. D.: Mercury Isotopes Reveal Atmospheric Gaseous Mercury Deposition Directly to the Arctic Coastal Snowpack, Environmental Science & Technology Letters, 6, 235-242, 10.1021/acs.estlett.9b00131, 2019.

Draxler, R. R., and Hess, G. D.: An overview of the HYSPLIT_4 modelling system for trajectories, dispersion and deposition, Australian Meteorological Magazine, 47, 295-308, 1998.

1235

Drinovec, L., Močnik, G., Zotter, P., Prévôt, A. S. H., Ruckstuhl, C., Coz, E., Rupakheti, M., Sciare, J., Müller, T., Wiedensohler, A., and Hansen, A. D. A.: The "dual-spot" Aethalometer: an improved measurement of aerosol black carbon with real-time loading compensation, Atmos. Meas. Tech., 8, 1965-1979, 10.5194/amt-8-1965-2015, 2015.

1240

Durnford, D., and Dastoor, A.: The behavior of mercury in the cryosphere: A review of what we know from observations, Journal of Geophysical Research, 116, 10.1029/2010jd014809, 2011.

Dusek, U., Reischl, G. P., and Hitzenberger, R.: CCN Activation of Pure and Coated Carbon Black Particles, Environmental Science & Technology, 40, 1223-1230, 10.1021/es0503478, 2006.

1245

Faïn, X., Obrist, D., Hallar, A. G., McCubbin, I., and Rahn, T.: High levels of reactive gaseous mercury observed at a high elevation research laboratory in the Rocky Mountains, Atmos. Chem. Phys., 9, 8049-8060, 10.5194/acp-9-8049-2009, 2009.

Flannigan, M., Stocks, B., Turetsky, M., and Wotton, M.: Impacts of climate change on fire activity and fire management in the circumboreal forest, Global Change Biology, 15, 549-560, https://doi.org/10.1111/j.1365-2486.2008.01660.x, 2009.

1250

Freud, E., Krejci, R., Tunved, P., Leaitch, R., Nguyen, Q. T., Massling, A., Skov, H., and Barrie, L.: Pan-Arctic aerosol number size distributions: seasonality and transport patterns, Atmos Chem Phys, 17, 8101-8128, 10.5194/acp-17-8101-2017, 2017.

1255

Frey, M. M., Norris, S. J., Brooks, I. M., Anderson, P. S., Nishimura, K., Yang, X., Jones, A. E., Nerentorp Mastromonaco, M. G., Jones, D. H., and Wolff, E. W.: First direct observation of sea salt aerosol production from blowing snow above sea ice, Atmos. Chem. Phys., 20, 2549-2578, 10.5194/acp-20-2549-2020, 2020.

Friedli, H. R., Radke, L. F., Lu, J. Y., Banic, C. M., Leaitch, W. R., and MacPherson, J. I.: Mercury emissions from burning of biomass from temperate North American forests: laboratory and airborne measurements, Atmospheric Environment, 37, 253-267, https://doi.org/10.1016/S1352-2310(02)00819-1, 2003.

1260

Friedli, H. R., Arellano, A. F., Cinnirella, S., and Pirrone, N.: Initial Estimates of Mercury Emissions to the Atmosphere from Global Biomass Burning, Environmental Science & Technology, 43, 3507-3513, 10.1021/es802703g, 2009.

1265

Fu, X., Marusczak, N., Heimbürger, L. E., Sauvage, B., Gheusi, F., Prestbo, E. M., and Sonke, J. E.: Atmospheric mercury speciation dynamics at the high-altitude Pic du Midi Observatory, southern France, Atmos. Chem. Phys., 16, 5623-5639, 10.5194/acp-16-5623-2016, 2016.

1270

Giordano, M. R., Kalnajs, L. E., Goetz, J. D., Avery, A. M., Katz, E., May, N. W., Leemon, A., Mattson, C., Pratt, K. A., and DeCarlo, P. F.: The importance of blowing snow to halogen-containing aerosol in coastal Antarctica: influence of source region versus wind speed, Atmos. Chem. Phys., 18, 16689-16711, 10.5194/acp-18-16689-2018, 2018.

Goodsite, M. E., Plane, J. M. C., and Skov, H.: A theoretical study of the oxidation of Hg-0 to HgBr2 in the troposphere, Environmental Science & Technology, 38, 1772-1776, 10.1021/es034680s, 2004.

1275

Goodsite, M. E., Plane, J. M. C., and Skov, H.: Correction to A Theoretical Study of the Oxidation of Hg0 to HgBr2 in the Troposphere, Environmental Science & Technology, 46, 5262-5262, 10.1021/es301201c, 2012.

1280   Gratz, L. E., Ambrose, J. L., Jaffe, D. A., Shah, V., Jaegle, L., Stutz, J., Festa, J., Spolaor, M., Tsai, C., Selin, N. E., Song, S., Zhou, X., Weinheimer, A. J., Knapp, D. J., Montzka, D. D., Flocke, F. M., Campos, T. L., Apel, E., Hornbrook, R., Blake, N. J., Hall, S., Tyndall, G. S., Reeves, M., Stechman, D., and Stell, M.: Oxidation of mercury by bromine in the subtropical Pacific free troposphere, Geophysical Research Letters, 42, 10494-10502, 10.1002/2015gl066645, 2015.

1285   Greene, C. A., Gwyther, D. E., and Blankenship, D. D.: Antarctic Mapping Tools for MATLAB, Computers & Geosciences, 104, 151-157, 10.1016/j.cageo.2016.08.003, 2017.

Greene, C. A.: Arctic Sea ice: https://www.mathworks.com/matlabcentral/fileexchange/56923-arctic-sea-ice), access: 2020-01-26, 2020.

1290   Gustin, M. S., Amos, H. M., Huang, J., Miller, M. B., and Heidecorn, K.: Measuring and modeling mercury in the atmosphere: a critical review, Atmos. Chem. Phys., 15, 5697-5713, 10.5194/acp-15-5697-2015, 2015.

Gustin, M. S., Dunham-Cheatham, S. M., Huang, J., Lindberg, S., and Lyman, S. N.: Development of an Understanding of Reactive Mercury in Ambient Air: A Review, Atmosphere, 12, 73, 2021.

1295

Halfacre, J. W., Shepson, P. B., and Pratt, K. A.: pH-dependent production of molecular chlorine, bromine, and iodine from frozen saline surfaces, Atmos. Chem. Phys., 19, 4917-4931, 10.5194/acp-19-4917-2019, 2019.

Hara, K., Osada, K., Yabuki, M., Takashima, H., Theys, N., and Yamanouchi, T.: Important contributions of sea-salt aerosols to atmospheric bromine cycle in the Antarctic coasts, Scientific Reports, 8, 13852, 10.1038/s41598-018-32287-4, 2018.
1300

Helmig, D., Oltmans, S. J., Carlson, D., Lamarque, J.-F., Jones, A., Labuschagne, C., Anlauf, K., and Hayden, K.: A review of surface ozone in the polar regions, Atmospheric Environment, 41, 5138-5161, https://doi.org/10.1016/j.atmosenv.2006.09.053, 2007.

1305   Hirdman, D., Aspmo, K., Burkhart, J. F., Eckhardt, S., Sodemann, H., and Stohl, A.: Transport of mercury in the Arctic atmosphere: Evidence for a spring-time net sink and summer-time source, Geophysical Research Letters, 36, 10.1029/2009gl038345, 2009.

Holmes, C. D., Jacob, D. J., and Yang, X.: Global lifetime of elemental mercury against oxidation by atomic bromine in the free troposphere, Geophysical Research Letters, 33, 10.1029/2006gl027176, 2006.
1310

Holmes, C. D., Jacob, D. J., Corbitt, E. S., Mao, J., Yang, X., Talbot, R., and Slemr, F.: Global atmospheric model for mercury including oxidation by bromine atoms, Atmos. Chem. Phys., 10, 12037-12057, 10.5194/acp-10-12037-2010, 2010.

Horowitz, H. M., Jacob, D. J., Zhang, Y., Dibble, T. S., Slemr, F., Amos, H. M., Schmidt, J. A., Corbitt, E. S., Marais, E. A., and Sunderland,
1315   E. M.: A new mechanism for atmospheric mercury redox chemistry: implications for the global mercury budget, Atmos. Chem. Phys., 17, 6353-6371, 10.5194/acp-17-6353-2017, 2017.

Huang, J., and Gustin, M. S.: Uncertainties of Gaseous Oxidized Mercury Measurements Using KCl-Coated Denuders, Cation-Exchange Membranes, and Nylon Membranes: Humidity Influences, Environmental Science & Technology, 49, 6102-6108,
1320   10.1021/acs.est.5b00098, 2015.

Huang, J., Miller, M. B., Edgerton, E., and Sexauer Gustin, M.: Deciphering potential chemical compounds of gaseous oxidized mercury in Florida, USA, Atmos. Chem. Phys., 17, 1689-1698, 10.5194/acp-17-1689-2017, 2017.

1325   Huang, K., Fu, J. S., Prikhodko, V. Y., Storey, J. M., Romanov, A., Hodson, E. L., Cresko, J., Morozova, I., Ignatieva, Y., and Cabaniss, J.: Russian anthropogenic black carbon: Emission reconstruction and Arctic black carbon simulation, Journal of Geophysical Research: Atmospheres, 120, 11,306-311,333, https://doi.org/10.1002/2015JD023358, 2015.

Hynes, A. J., Donohoue, D. L., Goodsite, M. E., and Hedgecock, I. M.: Our current understanding of major chemical and physical processes
1330   affecting mercury dynamics in the atmosphere and at the air-water/terrestrial interfaces, in: Mercury Fate and Transport in the Global Atmosphere: Emissions, Measurements and Models, edited by: Mason, R., and Pirrone, N., Springer US, Boston, MA, 427-457, 2009.

Igel, A. L., Ekman, A. M. L., Leck, C., Tjernström, M., Savre, J., and Sedlar, J.: The free troposphere as a potential source of arctic boundary
1335   layer aerosol particles, Geophysical Research Letters, 44, 7053-7060, 10.1002/2017gl073808, 2017.

Jacob, D. J., Crawford, J. H., Maring, H., Clarke, A. D., Dibb, J. E., Emmons, L. K., Ferrare, R. A., Hostetler, C. A., Russell, P. B., Singh, H. B., Thompson, A. M., Shaw, G. E., McCauley, E., Pederson, J. R., and Fisher, J. A.: The Arctic Research of the Composition of the Troposphere from Aircraft and Satellites (ARCTAS) mission: design, execution, and first results, Atmos. Chem. Phys., 10, 5191-5212, 10.5194/acp-10-5191-2010, 2010.

Jiang, S., Ye, A., and Xiao, C.: The temperature increase in Greenland has accelerated in the past five years, Global and Planetary Change, 194, 103297, https://doi.org/10.1016/j.gloplacha.2020.103297, 2020.

Jiao, Y., and Dibble, T. S.: Quality Structures, Vibrational Frequencies, and Thermochemistry of the Products of Reaction of BrHg• with NO2, HO2, ClO, BrO, and IO, The Journal of Physical Chemistry A, 119, 10502-10510, 10.1021/acs.jpca.5b04889, 2015.

Jiao, Y., and Dibble, T. S.: First kinetic study of the atmospherically important reactions BrHg˙ + NO2 and BrHg˙ + HOO, Physical Chemistry Chemical Physics, 19, 1826-1838, 10.1039/C6CP06276H, 2017a.

Jiao, Y., and Dibble, T. S.: Structures, Vibrational Frequencies, and Bond Energies of the BrHgOX and BrHgXO Species Formed in Atmospheric Mercury Depletion Events, The Journal of Physical Chemistry A, 121, 7976-7985, 10.1021/acs.jpca.7b06829, 2017b.

Jiskra, M., Sonke, J. E., Agnan, Y., Helmig, D., and Obrist, D.: Insights from mercury stable isotopes on terrestrial–atmosphere exchange of Hg(0) in the Arctic tundra, Biogeosciences, 16, 4051-4064, 10.5194/bg-16-4051-2019, 2019.

Kaleschke, L., Richter, A., Burrows, J., Afe, O., Heygster, G., Notholt, J., Rankin, A. M., Roscoe, H. K., Hollwedel, J., Wagner, T., and Jacobi, H. W.: Frost flowers on sea ice as a source of sea salt and their influence on tropospheric halogen chemistry, Geophysical Research Letters, 31, 10.1029/2004gl020655, 2004.

Kamp, J., Skov, H., Jensen, B., and Sorensen, L. L.: Fluxes of gaseous elemental mercury (GEM) in the High Arctic during atmospheric mercury depletion events (AMDEs), Atmos Chem Phys, 18, 6923-6938, 10.5194/acp-18-6923-2018, 2018.

Kelly, R., Chipman, M. L., Higuera, P. E., Stefanova, I., Brubaker, L. B., and Hu, F. S.: Recent burning of boreal forests exceeds fire regime limits of the past 10,000 years, Proceedings of the National Academy of Sciences, 110, 13055-13060, 10.1073/pnas.1305069110, 2013.

Lampert, A., Maturilli, M., Ritter, C., Hoffmann, A., Stock, M., Herber, A., Birnbaum, G., Neuber, R., Dethloff, K., Orgis, T., Stone, R., Brauner, R., Kässbohrer, J., Haas, C., Makshtas, A., Sokolov, V., and Liu, P.: The Spring-Time Boundary Layer in the Central Arctic Observed during PAMARCMiP 2009, Atmosphere, 3, 320-351, 2012.

Landis, M. S., Stevens, R. K., Schaedlich, F., and Prestbo, E. M.: Development and characterization of an annular denuder methodology for the measurement of divalent inorganic reactive gaseous mercury in ambient air, Environmental Science & Technology, 36, 3000-3009, 10.1021/es015887t, 2002.

Laurier, F. J. G.: Reactive gaseous mercury formation in the North Pacific Ocean's marine boundary layer: A potential role of halogen chemistry, Journal of Geophysical Research, 108, 10.1029/2003jd003625, 2003.

Law, K. S., Stohl, A., Quinn, P. K., Brock, C. A., Burkhart, J. F., Paris, J.-D., Ancellet, G., Singh, H. B., Roiger, A., Schlager, H., Dibb, J., Jacob, D. J., Arnold, S. R., Pelon, J., and Thomas, J. L.: Arctic Air Pollution: New Insights from POLARCAT-IPY, Bulletin of the American Meteorological Society, 95, 1873-1895, 10.1175/bams-d-13-00017.1, 2014.

Lin, C.-J., and Pehkonen, S. O.: Oxidation of elemental mercury by aqueous chlorine (HOCl/OCl−): Implications for tropospheric mercury chemistry, Journal of Geophysical Research: Atmospheres, 103, 28093-28102, https://doi.org/10.1029/98JD02304, 1998.

Lindberg, S. E., Brooks, S., Lin, C. J., Scott, K. J., Landis, M. S., Stevens, R. K., Goodsite, M., and Richter, A.: Dynamic oxidation of gaseous mercury in the Arctic troposphere at polar sunrise, Environmental Science & Technology, 36, 1245-1256, 10.1021/es0111941, 2002.

1390 Lu, J. Y., Schroeder, W. H., Barrie, L. A., Steffen, A., Welch, H. E., Martin, K., Lockhart, L., Hunt, R. V., Boila, G., and Richter, A.: Magnification of atmospheric mercury deposition to polar regions in springtime: The link to tropospheric ozone depletion chemistry, Geophysical Research Letters, 28, 3219-3222, 10.1029/2000gl012603, 2001.

Lyman, S. N., Cheng, I., Gratz, L. E., Weiss-Penzias, P., and Zhang, L.: An updated review of atmospheric mercury, Science of The Total
1395 Environment, 707, 135575, https://doi.org/10.1016/j.scitotenv.2019.135575, 2020.

Macdonald, R. W., and Loseto, L. L.: Are Arctic Ocean ecosystems exceptionally vulnerable to global emissions of mercury? A call for emphasised research on methylation and the consequences of climate change, Environ. Chem., 7, 133-138, 10.1071/en09127,
1400 2010.

Maruszczak, N., Sonke, J. E., Fu, X., and Jiskra, M.: Tropospheric GOM at the Pic du Midi Observatory—Correcting Bias in Denuder Based Observations, Environmental Science & Technology, 51, 863-869, 10.1021/acs.est.6b04999, 2017.

Monks, S. A., Arnold, S. R., Emmons, L. K., Law, K. S., Turquety, S., Duncan, B. N., Flemming, J., Huijnen, V., Tilmes, S., Langner, J.,
1405 Mao, J., Long, Y., Thomas, J. L., Steenrod, S. D., Raut, J. C., Wilson, C., Chipperfield, M. P., Diskin, G. S., Weinheimer, A., Schlager, H., and Ancellet, G.: Multi-model study of chemical and physical controls on transport of anthropogenic and biomass burning pollution to the Arctic, Atmos. Chem. Phys., 15, 3575-3603, 10.5194/acp-15-3575-2015, 2015.

Muntean, M., Janssens-Maenhout, G., Song, S., Giang, A., Selin, N. E., Zhong, H., Zhao, Y., Olivier, J. G. J., Guizzardi, D., Crippa, M.,
1410 Schaaf, E., and Dentener, F.: Evaluating EDGARv4.tox2 speciated mercury emissions ex-post scenarios and their impacts on modelled global and regional wet deposition patterns, Atmospheric Environment, 184, 56-68, https://doi.org/10.1016/j.atmosenv.2018.04.017, 2018.

Møller, A. K., Barkay, T., Al-Soud, W. A., Sørensen, S. J., Skov, H., and Kroer, N.: Diversity and characterization of mercury-resistant
1415 bacteria in snow, freshwater and sea-ice brine from the High Arctic, FEMS Microbiology Ecology, 75, 390-401, 10.1111/j.1574-6941.2010.01016.x, 2011.

Nguyen, Q. T., Glasius, M., Sorensen, L. L., Jensen, B., Skov, H., Birmili, W., Wiedensohler, A., Kristensson, A., Nojgaard, J. K., and Massling, A.: Seasonal variation of atmospheric particle number concentrations, new particle formation and atmospheric oxidation
1420 capacity at the high Arctic site Villum Research Station, Station Nord, Atmos Chem Phys, 16, 11319-11336, 10.5194/acp-16-11319-2016, 2016.

Obrist, D., Tas, E., Peleg, M., Matveev, V., Faïn, X., Asaf, D., and Luria, M.: Bromine-induced oxidation of mercury in the mid-latitude atmosphere, Nature Geoscience, 4, 22-26, 10.1038/ngeo1018, 2010.
1425

Pal, B., and Ariya, P. A.: Studies of ozone initiated reactions of gaseous mercury: kinetics, product studies, and atmospheric implications, Physical Chemistry Chemical Physics, 6, 572-579, 10.1039/B311150D, 2004.

Park, J.-D., and Zheng, W.: Human Exposure and Health Effects of Inorganic and Elemental Mercury, J Prev Med Public Health, 45, 344-
1430 352, 10.3961/jpmph.2012.45.6.344, 2012.

Peterson, P. K., Pöhler, D., Sihler, H., Zielcke, J., General, S., Frieß, U., Platt, U., Simpson, W. R., Nghiem, S. V., Shepson, P. B., Stirm, B. H., Dhaniyala, S., Wagner, T., Caulton, D. R., Fuentes, J. D., and Pratt, K. A.: Observations of bromine monoxide transport in the Arctic sustained on aerosol particles, Atmos. Chem. Phys., 17, 7567-7579, 10.5194/acp-17-7567-2017, 2017.
1435

Peterson, P. K., Pöhler, D., Zielcke, J., General, S., Frieß, U., Platt, U., Simpson, W. R., Nghiem, S. V., Shepson, P. B., Stirm, B. H., and Pratt, K. A.: Springtime Bromine Activation over Coastal and Inland Arctic Snowpacks, ACS Earth and Space Chemistry, 2, 1075-1086, 10.1021/acsearthspacechem.8b00083, 2018.

1440 Pfaffhuber, K. A., Berg, T., Hirdman, D., and Stohl, A.: Atmospheric mercury observations from Antarctica: seasonal variation and source and sink region calculations, Atmos Chem Phys, 12, 3241-3251, 10.5194/acp-12-3241-2012, 2012.

Pirrone, N., Cinnirella, S., Feng, X., Finkelman, R. B., Friedli, H. R., Leaner, J., Mason, R., Mukherjee, A. B., Stracher, G. B., Streets, D. G., and Telmer, K.: Global mercury emissions to the atmosphere from anthropogenic and natural sources, Atmos Chem Phys, 10,
1445 5951-5964, 10.5194/acp-10-5951-2010, 2010.

Quack, B., and Wallace, D. W. R.: Air-sea flux of bromoform: Controls, rates, and implications, Global Biogeochemical Cycles, 17, 10.1029/2002gb001890, 2003.

Reid, J. S., Koppmann, R., Eck, T. F., and Eleuterio, D. P.: A review of biomass burning emissions part II: intensive physical properties of biomass burning particles, Atmos. Chem. Phys., 5, 799-825, 10.5194/acp-5-799-2005, 2005.

Rolph, G., Stein, A., and Stunder, B.: Real-time Environmental Applications and Display sYstem: READY, Environmental Modelling & Software, 95, 210-228, 10.1016/j.envsoft.2017.06.025, 2017.

Saiz-Lopez, A., Travnikov, O., Sonke, J. E., Thackray, C. P., Jacob, D. J., Carmona-García, J., Francés-Monerris, A., Roca-Sanjuán, D., Acuña, A. U., Dávalos, J. Z., Cuevas, C. A., Jiskra, M., Wang, F., Bieser, J., Plane, J. M. C., and Francisco, J. S.: Photochemistry of oxidized Hg(I) and Hg(II) species suggests missing mercury oxidation in the troposphere, Proceedings of the National Academy of Sciences, 117, 30949-30956, 10.1073/pnas.1922486117, 2020.

Sander, R.: Compilation of Henry's law constants (version 4.0) for water as solvent, Atmos. Chem. Phys., 15, 4399-4981, 10.5194/acp-15-4399-2015, 2015.

Schacht, J., Heinold, B., Quaas, J., Backman, J., Cherian, R., Ehrlich, A., Herber, A., Huang, W. T. K., Kondo, Y., Massling, A., Sinha, P. R., Weinzierl, B., Zanatta, M., and Tegen, I.: The importance of the representation of air pollution emissions for the modeled distribution and radiative effects of black carbon in the Arctic, Atmos. Chem. Phys., 19, 11159-11183, 10.5194/acp-19-11159-2019, 2019.

Schmeisser, L., Backman, J., Ogren, J. A., Andrews, E., Asmi, E., Starkweather, S., Uttal, T., Fiebig, M., Sharma, S., Eleftheriadis, K., Vratolis, S., Bergin, M., Tunved, P., and Jefferson, A.: Seasonality of aerosol optical properties in the Arctic, Atmos. Chem. Phys., 18, 11599-11622, 10.5194/acp-18-11599-2018, 2018.

Schmeissner, T., Krejci, R., Ström, J., Birmili, W., Wiedensohler, A., Hochschild, G., Gross, J., Hoffmann, P., and Calderon, S.: Analysis of number size distributions of tropical free tropospheric aerosol particles observed at Pico Espejo (4765 m a.s.l.), Venezuela, Atmos. Chem. Phys., 11, 3319-3332, 10.5194/acp-11-3319-2011, 2011.

Schroeder, W., Oliva, P., Giglio, L., and Csiszar, I. A.: The New VIIRS 375 m active fire detection data product: Algorithm description and initial assessment, Remote Sensing of Environment, 143, 85-96, 10.1016/j.rse.2013.12.008, 2014.

Schroeder, W. H., Anlauf, K. G., Barrie, L. A., Lu, J. Y., Steffen, A., Schneeberger, D. R., and Berg, T.: Arctic springtime depletion of mercury, Nature, 394, 331-332, 10.1038/28530, 1998.

Schulz, H., Zanatta, M., Bozem, H., Leaitch, W. R., Herber, A. B., Burkart, J., Willis, M. D., Kunkel, D., Hoor, P. M., Abbatt, J. P. D., and Gerdes, R.: High Arctic aircraft measurements characterising black carbon vertical variability in spring and summer, Atmos. Chem. Phys., 19, 2361-2384, 10.5194/acp-19-2361-2019, 2019.

Semane, N., Peuch, V. H., El Amraoui, L., Bencherif, H., Massart, S., Cariolle, D., Attie, J. L., and Abida, R.: An observed and analysed stratospheric ozone intrusion over the high Canadian Arctic UTLS region during the summer of 2003, Quarterly Journal of the Royal Meteorological Society, 133, 171-178, 10.1002/qj.141, 2007.

Shah, V., and Jaeglé, L.: Subtropical subsidence and surface deposition of oxidized mercury produced in the free troposphere, Atmos. Chem. Phys., 17, 8999-9017, 10.5194/acp-17-8999-2017, 2017.

Shepler, B. C., Balabanov, N. B., and Peterson, K. A.: Hg+Br→HgBr recombination and collision-induced dissociation dynamics, The Journal of Chemical Physics, 127, 164304, 10.1063/1.2777142, 2007.

Simpson, W. R., Brown, S. S., Saiz-Lopez, A., Thornton, J. A., and Glasow, R.: Tropospheric halogen chemistry: sources, cycling, and impacts, Chem Rev, 115, 4035-4062, 10.1021/cr5006638, 2015.

Simpson, W. R., Peterson, P. K., Frieß, U., Sihler, H., Lampel, J., Platt, U., Moore, C., Pratt, K., Shepson, P., Halfacre, J., and Nghiem, S. V.: Horizontal and vertical structure of reactive bromine events probed by bromine monoxide MAX-DOAS, Atmos. Chem. Phys., 17, 9291-9309, 10.5194/acp-17-9291-2017, 2017.

Skov, H., Christensen, J. H., Goodsite, M. E., Heidam, N. Z., Jensen, B., Wahlin, P., and Geernaert, G.: Fate of elemental mercury in the arctic during atmospheric mercury depletion episodes and the load of atmospheric mercury to the arctic, Environmental Science & Technology, 38, 2373-2382, 10.1021/es030080h, 2004.

Skov, H., Brooks, S., Goodsite, M., Lindberg, S., Meyers, T., Landis, M., Larsen, M., Jensen, B., McConville, G., and Christensen, J.: Fluxes of reactive gaseous mercury measured with a newly developed method using relaxed eddy accumulation, Atmospheric Environment, 40, 5452-5463, 10.1016/j.atmosenv.2006.04.061, 2006.

Skov, H., Hjorth, J., Nordstrøm, C., Jensen, B., Christoffersen, C., Bech Poulsen, M., Baldtzer Liisberg, J., Beddows, D., Dall'Osto, M., and Christensen, J.: The variability in Gaseous Elemental Mercury at Villum Research Station, Station Nord in North Greenland from 1999 to 2017, Atmos. Chem. Phys. Discuss., 2020, 1-22, 10.5194/acp-2019-912, 2020.

Slemr, F., Weigelt, A., Ebinghaus, R., Kock, H. H., Bödewadt, J., Brenninkmeijer, C. A. M., Rauthe-Schöch, A., Weber, S., Hermann, M., Becker, J., Zahn, A., and Martinsson, B.: Atmospheric mercury measurements onboard the CARIBIC passenger aircraft, Atmos. Meas. Tech., 9, 2291-2302, 10.5194/amt-9-2291-2016, 2016.

Soerensen, A. L., Skov, H., Jacob, D. J., Soerensen, B. T., and Johnson, M. S.: Global Concentrations of Gaseous Elemental Mercury and Reactive Gaseous Mercury in the Marine Boundary Layer, Environmental Science & Technology, 44, 7425-7430, 10.1021/es903839n, 2010.

Sommar, J., Andersson, M. E., and Jacobi, H. W.: Circumpolar measurements of speciated mercury, ozone and carbon monoxide in the boundary layer of the Arctic Ocean, Atmos Chem Phys, 10, 5031-5045, 10.5194/acp-10-5031-2010, 2010.

Steen, A. O., Berg, T., Dastoor, A. P., Durnford, D. A., Engelsen, O., Hole, L. R., and Pfaffhuber, K. A.: Natural and anthropogenic atmospheric mercury in the European Arctic: a fractionation study, Atmos Chem Phys, 11, 6273-6284, 10.5194/acp-11-6273-2011, 2011.

Steffen, A., Schroeder, W., Bottenheim, J., Narayan, J., and Fuentes, J. D.: Atmospheric mercury concentrations: measurements and profiles near snow and ice surfaces in the Canadian Arctic during Alert 2000, Atmospheric Environment, 36, 2653-2661, https://doi.org/10.1016/S1352-2310(02)00112-7, 2002.

Steffen, A., Bottenheim, J., Cole, A., Ebinghaus, R., Lawson, G., and Leaitch, W. R.: Atmospheric mercury speciation and mercury in snow over time at Alert, Canada, Atmos Chem Phys, 14, 2219-2231, 10.5194/acp-14-2219-2014, 2014.

Steffen, A., Lehnherr, I., Cole, A., Ariya, P., Dastoor, A., Durnford, D., Kirk, J., and Pilote, M.: Atmospheric mercury in the Canadian Arctic. Part I: a review of recent field measurements, Sci Total Environ, 509-510, 3-15, 10.1016/j.scitotenv.2014.10.109, 2015.

Stephens, C. R., Shepson, P. B., Steffen, A., Bottenheim, J. W., Liao, J., Huey, L. G., Apel, E., Weinheimer, A., Hall, S. R., Cantrell, C., Sive, B. C., Knapp, D. J., Montzka, D. D., and Hornbrook, R. S.: The relative importance of chlorine and bromine radicals in the oxidation of atmospheric mercury at Barrow, Alaska, Journal of Geophysical Research: Atmospheres, 117, n/a-n/a, 10.1029/2011jd016649, 2012.

Stern, G. A., Macdonald, R. W., Outridge, P. M., Wilson, S., Chetelat, J., Cole, A., Hintelmann, H., Loseto, L. L., Steffen, A., Wang, F., and Zdanowicz, C.: How does climate change influence Arctic mercury?, Sci Total Environ, 414, 22-42, 10.1016/j.scitotenv.2011.10.039, 2012.

Stohl, A.: Computation, accuracy and applications of trajectories - A review and bibliography, Atmospheric Environment, 32, 947-966, 10.1016/s1352-2310(97)00457-3, 1998.

Stohl, A.: Characteristics of atmospheric transport into the Arctic troposphere, Journal of Geophysical Research, 111, 10.1029/2005jd006888, 2006.

Stroeve, J. C., Serreze, M. C., Holland, M. M., Kay, J. E., Malanik, J., and Barrett, A. P.: The Arctic's rapidly shrinking sea ice cover: a research synthesis, Climatic Change, 110, 1005-1027, 10.1007/s10584-011-0101-1, 2012.

Sturges, W. T., Cota, G. F., and Buckley, P. T.: Bromoform emission from Arctic ice algae, Nature, 358, 660-662, 10.1038/358660a0, 1992.

Swartzendruber, P. C., Jaffe, D. A., Prestbo, E. M., Weiss-Penzias, P., Selin, N. E., Park, R., Jacob, D. J., Strode, S., and Jaeglé, L.: Observations of reactive gaseous mercury in the free troposphere at the Mount Bachelor Observatory, Journal of Geophysical Research, 111, 10.1029/2006jd007415, 2006.

Talbot, R., Mao, H., Scheuer, E., Dibb, J., and Avery, M.: Total depletion of Hg degrees in the upper troposphere-lower stratosphere, Geophysical Research Letters, 34, 5, 10.1029/2007gl031366, 2007.

Tarasick, D. W., and Bottenheim, J. W.: Surface ozone depletion episodes in the Arctic and Antarctic from historical ozonesonde records, Atmos. Chem. Phys., 2, 197-205, 10.5194/acp-2-197-2002, 2002.

Thomas, J. L., Dibb, J. E., Huey, L. G., Liao, J., Tanner, D., Lefer, B., von Glasow, R., and Stutz, J.: Modeling chemistry in and above snow at Summit, Greenland – Part 2: Impact of snowpack chemistry on the oxidation capacity of the boundary layer, Atmos. Chem. Phys., 12, 6537-6554, 10.5194/acp-12-6537-2012, 2012.

Toyota, K., Dastoor, A. P., and Ryzhkov, A.: Air–snowpack exchange of bromine, ozone and mercury in the springtime Arctic simulated by the 1-D model PHANTAS – Part 2: Mercury and its speciation, Atmos. Chem. Phys., 14, 4135-4167, 10.5194/acp-14-4135-2014, 2014.

Tunved, P., Ström, J., and Krejci, R.: Arctic aerosol life cycle: linking aerosol size distributions observed between 2000 and 2010 with air mass transport and precipitation at Zeppelin station, Ny-Ålesund, Svalbard, Atmos Chem Phys, 13, 3643-3660, 10.5194/acp-13-3643-2013, 2013.

UNEP: UNEP: Minamata Convention on Mercury: http://www.mercuryconvention.org/Convention/tabid/3426/Default.aspx access: 2020-11-12, 2013.

von Glasow, R.: Atmospheric chemistry in volcanic plumes, Proceedings of the National Academy of Sciences, 107, 6594-6599, 10.1073/pnas.0913164107, 2010.

Walker, T. W., Jones, D. B. A., Parrington, M., Henze, D. K., Murray, L. T., Bottenheim, J. W., Anlauf, K., Worden, J. R., Bowman, K. W., Shim, C., Singh, K., Kopacz, M., Tarasick, D. W., Davies, J., von der Gathen, P., Thompson, A. M., and Carouge, C. C.: Impacts of midlatitude precursor emissions and local photochemistry on ozone abundances in the Arctic, Journal of Geophysical Research-Atmospheres, 117, 10.1029/2011jd016370, 2012.

Wang, S., McNamara, S. M., Moore, C. W., Obrist, D., Steffen, A., Shepson, P. B., Staebler, R. M., Raso, A. R. W., and Pratt, K. A.: Direct detection of atmospheric atomic bromine leading to mercury and ozone depletion, Proc Natl Acad Sci U S A, 116, 14479-14484, 10.1073/pnas.1900613116, 2019.

Weingartner, E., Saathoff, H., Schnaiter, M., Streit, N., Bitnar, B., and Baltensperger, U.: Absorption of light by soot particles: determination of the absorption coefficient by means of aethalometers, Journal of Aerosol Science, 34, 1445-1463, https://doi.org/10.1016/S0021-8502(03)00359-8, 2003.

Weiss-Penzias, P., Amos, H. M., Selin, N. E., Gustin, M. S., Jaffe, D. A., Obrist, D., Sheu, G. R., and Giang, A.: Use of a global model to understand speciated atmospheric mercury observations at five high-elevation sites, Atmos. Chem. Phys., 15, 1161-1173, 10.5194/acp-15-1161-2015, 2015.

Winiger, P., Barrett, T. E., Sheesley, R. J., Huang, L., Sharma, S., Barrie, L. A., Yttri, K. E., Evangeliou, N., Eckhardt, S., Stohl, A., Klimont, Z., Heyes, C., Semiletov, I. P., Dudarev, O. V., Charkin, A., Shakhova, N., Holmstrand, H., Andersson, A., and Gustafsson, Ö.: Source apportionment of circum-Arctic atmospheric black carbon from isotopes and modeling, Science Advances, 5, eaau8052, 10.1126/sciadv.aau8052, 2019.

Yang, X., Cox, R. A., Warwick, N. J., Pyle, J. A., Carver, G. D., O'Connor, F. M., and Savage, N. H.: Tropospheric bromine chemistry and its impacts on ozone: A model study, Journal of Geophysical Research: Atmospheres, 110, 10.1029/2005jd006244, 2005.

Ye, Z., Mao, H., Lin, C. J., and Kim, S. Y.: Investigation of processes controlling summertime gaseous elemental mercury oxidation at midlatitudinal marine, coastal, and inland sites, Atmos. Chem. Phys., 16, 8461-8478, 10.5194/acp-16-8461-2016, 2016.

Zanatta, M., Laj, P., Gysel, M., Baltensperger, U., Vratolis, S., Eleftheriadis, K., Kondo, Y., Dubuisson, P., Winiarek, V., Kazadzis, S., Tunved, P., and Jacobi, H. W.: Effects of mixing state on optical and radiative properties of black carbon in the European Arctic, Atmos. Chem. Phys., 18, 14037-14057, 10.5194/acp-18-14037-2018, 2018.

Zheng, C., Wu, Y., Ting, M., Orbe, C., Wang, X., and Tilmes, S.: Summertime Transport Pathways From Different Northern Hemisphere Regions Into the Arctic, Journal of Geophysical Research: Atmospheres, 126, e2020JD033811, https://doi.org/10.1029/2020JD033811, 2021.